

國立交通大學

生物科技學系

碩士論文

據互補式金氧半導體晶片發展之
多功能調頻光學生物感測器

**Development of a Multifunctional Optical Biosensor
Based on Frequency Modulation CMOS Chip**

研究生：張文穎

指導教授：楊裕雄 教授

中華民國九十六年六月

據互補式金氧半導體晶片發展之

多功能調頻光學生物感測器

**Development of a Multifunctional Optical Biosensor
Based on Frequency Modulation CMOS Chip**

研究生：張文穎

Student : Wen-ying Chang

指導教授：楊裕雄

Advisor : Yuh-Shyong Yang



碩士論文

A Thesis Submitted to Department of Biological Science and Technology
National Chiao Tung University in partial Fulfillment of the Requirements
for the Degree of Master in Biochemical Engineering

June 2007

Hsinchu, Taiwan, Republic of China

中華民國九十六年六月

據互補式金氧半導體晶片發展之

多功能調頻光學生物感測器

學生：張文穎

指導教授：楊裕雄

摘要

此研究提出一個同時具有生物化學冷光訊號和發色物質偵測量能力的互補式金氧半導體(CMOS)晶片。此互補式金氧半導體晶片首創被指出可用於多樣式的光學反應偵測，可直接偵測冷光訊號，並於組裝市售發光二極體後，進行發色物質定量。晶片偵測面積為 1.28 毫米 × 1.28 毫米，經由 0.35 毫米半導體標準製程製成。在集成電路中設計的阻抗放大器可放大由化學冷光或發散光源所激發的訊號電流，並可藉調整晶片週期波頻率參數，針對不同強度光訊號設定最適應的掃描頻率。本實驗先以山葵過氧化氫酶（過氧化氫酶）- 胺基苯二醯井 - 過氧化氫和過氧化氫酶- 4-胺基安替琳-酚-過氧化氫系統為設立實用操作平台的範例，在待測物氧化反應生成過氧化氫後，連結上述系統而成不同的光學訊號。膽固醇 - 膽固醇氧化酵素(COD)和葡萄糖-葡萄糖氧化酵素(GOD)氧化反應皆各自與不同過氧化氫光學反應結合，證明其具備冷光物質及發色物質定量能力，極具應用於不同臨床分析的潛力。相較於早期晶片，此晶片具有多項優點，如高靈敏度、少量樣品體積需求、高度辨識範圍，同時也證實，此晶片相較於組裝式商用感光二極體設備，擁有較高單位靈敏度。總結之，創新之互補式金氧半導體集成電路與商用電子元件相結合，可建立起實用且有力的多功能生物光學感測器。

Development of a Multifunctional Optical Biosensor Based on Frequency Modulation CMOS Chip

Student: Wen-ying Chang

Advisor: Dr. Yuh-Shyong Yang

Abstract

This work presents a complementary metal oxide semiconductor (CMOS) chip with accompanied accessories as a system for the detections and quantifications of both biochemical luminescence and chromogens. The CMOS photosensing chip originality has been reported to detect multiple optical reactions, which detects not only chemiluminescence directly but also chromogen quantification while integrated with a commercial light emitting diode (LED), with a 1.28 mm× 1.28 mm detection area via a 0.35μm standard process. A transimpedance amplifier was designed in integrated circuit (IC) to amplify the signal current induced by luminescence or emitted light. By adjusting the frequency parameter setting of CMOS chip, the optimized scanning frequency can be set to fit different optical reactions. After the detected target is oxidized, hydrogen peroxide occurs. Horseradish peroxidase (HRP)–luminol–H₂O₂ and HRP-phenol-H₂O₂ systems were used as examples to constitute the platforms for coupling to produce different optical signals. Cholesterol–cholesterol oxidase (COD) and glucose-glucose oxidase(GOD) reactions were both coupled with different H₂O₂ production reactions to demonstrate the ability of biological luminescence and chromogen quantification and potential for diverse

clinical diagnosis.

Compared with the CMOS chip in the early stages, our chip has many advantages, such as high sensitivity, a less sample volume requirement, and high dynamic range. It even possesses higher unit sensitivity compared with the integrated commercial photodiode setup device. In conclusion, the combination of the specifically designed CMOS IC and available electronic devices establishes a useful and powerful multifunctional optical biosensor.



Acknowledgement

歷經兩年的碩士生涯，我學習到掌握分配自己的工作和生活。實驗室的生活，是碩士生最重要的經驗，很感謝指導我的楊裕雄老師，亦師亦友，是個可親的老闆，不吝給我幫助、指導和包容。我所研究的論文，希望可以讓未來有興趣研究 CMOS 晶片的同伴稍作參考，也歡迎大家一起討論研究。

實驗室的學長姐、同學、學弟妹，都親切友善且樂於討論。不論是 LEPE 實驗團隊或羽球隊，都是我的好夥伴、好哥兒們。在要離開的時刻，更細細發覺大家的可愛。我也感謝對我多加提攜的生物電子組學長姐、同伴們。政哲學長給我不少想法和知識，雖然他常有可能散播八卦；程允是電子組資深前輩，總不吝於給所有人幫助和建議，雖然跟政哲合併起來也可能散播八卦；淵仁會給我不同的生活啟發，他可能除了熱舞之外，其他運動都有一手。學長們都對我很好，可以忍受我的無厘頭和調皮，祝福大家順利畢業，paper 越發越上手。此外，Rich 學長總提供我生活經驗和做人處事道理，外加中醫把脈和養身之道；郁吟像個正氣凜然又慧點的大姐姐關心著大家，小米學姊總是溫柔地包容我的錯誤和不時提供食物；大晃學長會溫暖地關心我的實驗和生活；PuPu 是熱心又會修電腦的好人學長；陸宜會告訴我哪天老師請假還有考前整理；小志是陽光男孩，可以輕鬆呼吸上層空氣；Peggy 是我的閨中密友；美春、Jumping 和韋汝是我患難與共的同窗；小胖、家瑋、秀華、若芬，則是可愛又有趣的學弟妹。秉鈞、昆熹和明瑜也讓我有許多啟發和不同的思考方向。還有已畢業的學長姐們，其他實驗室合作的學長學弟，也跟我分享不少生活上分享和提供實驗協助，跟你們一起共事，真是幸運！謝謝大家的照顧！如果我不慎遺漏了誰，請大家來信通知我。

在心靈上和生活上支持我的，是我的家人。你們永遠是我的最愛，無論我迷惘、失意或是不安矛盾，你們總給我堅定的力量和鼓勵；如果我有能力去愛人，也是因為有你們的愛來充沛我的動機和意念。有你們的支持，讓我堅定我的生活和目標。感謝辛勞又英俊的爸爸、可愛又美麗的媽媽、堅毅又和煦的大姐、貼心又照顧我的二姐、永遠年輕的姐夫、帥氣的阿良和對我最好最好的葛格。你們都是讓我促使自己更好的動力。生活的需求趨動著工作和自我充實；而你們，驅動著我的生活。我也感謝上天，讓我有這麼可愛的家庭。

在新竹六年的生活，我也感謝一直陪伴著我的好朋友，最有默契的室友們，大學社團的好朋友，舞蹈教室的老師們，還有每天走出宿舍門口都可以看到的胖白，每天都羨慕牠悠閒的曬太陽，牠告訴我，生命是一種態度，不管是辛苦還是輕鬆的活著，都可以學習如何去享受生命。

| Contents | Page |
|---|-------------|
| Abstract (Chinese) | i |
| Abstract (English) | ii |
| Acknowledgement | iv |
| Contents | v |
| Contents of Tables | vii |
| Contents of Figures | viii |
| | |
| Chapter1. Introduction | 1-19 |
| 1.1 Main trend in biosensor..... | 1 |
| 1.2 CMOS Technology and why do we use CMOS | 2 |
| 1.3 A multifunctional optical biosensor for biological reaction..... | 3 |
| 1.4 Design of a CMOS based frequency modulation optical sensor..... | 4 |
| 1.5 CMOS photodiodes as chemiluminescence sensor..... | 6 |
| 1.6 CMOS photodiodes as chromogenic sensor..... | 8 |
| 1.7 Cholesterol chromogenic quantification..... | 10 |
| 1.8 Light emitting diodes (LEDs)..... | 16 |
| 1.9 Photodiode..... | 18 |
| Chapter2. Materials and Methods | 20-36 |
| 2.1 Materials..... | 21 |
| 2.2 Apparatus..... | 21 |
| 2.3 Photomultiplier tube (PMT) detection system..... | 22 |
| 2.4 Reaction 1. Luminescence Reaction of HRP-luminol-H ₂ O ₂ enzyme reaction..... | 22 |
| 2.5 Reaction 2. Colorimetric Reaction of HRP-Phenol-H ₂ O ₂ enzyme reaction..... | 29 |
| 2.6 Sample Volume Reduction..... | 36 |
| Chapter3. Results and Discussion | 37-59 |
| 3.1 Measured output voltage (V _{out}) with adjusted clock frequency..... | 37 |
| 3.2 Measured output voltage (V _{out}) versus illuminated intensity..... | 38 |
| 3.3 Different Frequency versus LED supplied voltage variation..... | 38 |
| 3.4 Chemiluminescence Method..... | 39 |
| 3.5 Chromogenic Method..... | 49 |
| Chapter4. Conclusions | 60-61 |

Chapter5. References 62-69
Chapter6. Tables..... 70-78
Chapter7. Pictures 79-118



| Contents of Tables | Page |
|---|-------------|
| Table 1 Biomedical Detection Target..... | 69 |
| Table 2 Cholesterol Desirable Level in Human Body | 70 |
| Table 3 The Comparison of the Two Generation Chips..... | 71 |
| Table 4 Optimized reaction conditions of HRP and CHOD | 72 |
| Table 5 Luminescence Assay: The comparison of sensitivity, detection limits, sensing area of four instruments: Luminescence spectrometer, commercial photodiode, novel CMOS chip and early stage CMOS chip..... | 73 |
| Table 6 The comparison of the enzyme amount required during measurement by different devices | 74 |
| Table 7 Chromogenic Assay: The comparison of sensitivity, detection limits, sensing area of three instruments | 75 |
| Table 8 Chromogenic Assay: The comparison of sensitivity, detection limits, sensing area of three instruments: UV-vis 3300 spectrometer, commercial photodiode, and novel CMOS chip. Under two conditions: (a.) H_2O_2 -4-AAP – Phenol HRP reaction (b.) CHOD-HRP coupled enzyme reaction | 76 |
| Table 9 The comparison of sensitivity and saturation concentration of different frequency parameters with luminescence assay..... | 77 |
| Table 10 The comparison of sensitivity and K_m value of different frequency parameters with chromogenic assay | 78 |

| Contents of Figures | Page |
|---|-------------|
| Figure 1 The concept of a biological sensor | 79 |
| Figure 2 Optical absorption for (a) $h\nu = E_g$, (b) $h\nu > E_g$, (c) $h\nu < E_g$ | 80 |
| Figure 3 Absorption coefficient α versus wavelength | 81 |
| Figure 4 N+/P well photodiodes side structure view | 82 |
| Figure 5 cholesterol conformation | 83 |
| Figure 6 Roadmap of the experiment scheme | 84 |
| Figure 7 The component instruments connection diagram of assembled semiconductor element setup included of instruments: power supply, multimeter, GPIB card, CMOS chip, and Pulse Generator | 85 |
| Figure 8 Die Photograph..... | 86 |
| Figure 9 The optimization of the absorbance wavelength | 87 |
| Figure 10 Experimental Procedure | 88 |
| Figure 11 Environmental setup of output voltage (V_{out}) versus illuminated intensity measurement | 89 |
| Figure 12 Frequency vs. Output Voltage Variation (Saturation/Blank ; Light/ Dark) . | 90 |
| Figure 13 (a) Frequency vs. Output Voltage Variation (20 to 150 Hz) | 91 |
| Figure 14 Measured output voltage (V_{out}) with clock frequency = 125 KHz | 92 |
| Figure 15 Measured output voltage (V_{out}) vs. illuminated intensity under 125kHz . | 93 |
| Figure 16 Measured output voltage (V_{out}) with clock frequency = 10 KHz | 94 |
| Figure 17 Measured output voltage (V_{out}) vs. illuminated intensity under 10kHz ... | 95 |
| Figure 18 Different Frequency versus LED supplied voltage variation | 96 |
| Figure 19 The variation of luminal concentration in HRP-luminol- H_2O_2 system determined by F-4500 fluorescence meter | 97 |
| Figure 20 Variation of glucose concentration in a GOD coupled HRP-luminol- H_2O_2 system determined by F-4500 fluorescence meter | 98 |
| Figure 21 Variation of glucose concentration in a GOD coupled HRP-luminol- H_2O_2 system determined by our CMOS chip | 99 |
| Figure 22 Michaelis-Menten kinetics graphs got from incubation test (left) and real time test (right) | 100 |
| Figure 23 The Michaelis-Menten graph obtained with incubation test | 101 |
| Figure 24 Frequency Adjusted in the Luminescence Reaction | 102 |
| Figure 25 HRP-luminol- H_2O_2 kinetic Graph detected with F4500 luminescence | |

| | |
|--|-----|
| spectrometer (upper graph) and the novel CMOS chip (lower graph) | 103 |
| Figure 26 HRP-luminol-H ₂ O ₂ luminescence assay kinetic graph detected by CMOS chip | 104 |
| Figure 27 Variation of H ₂ O ₂ concentration in an HRP-luminol- H ₂ O ₂ system determined by F4500 luminescence spectrometer (a) integrated commercial photodiode system (b) and the early stage CMOS chip | 105 |
| Figure 28 Optimization of pH value | 106 |
| Figure 29 Temperature Optimization | 107 |
| Figure 30 Incubation time optimization | 108 |
| Figure 31 The linear range of peroxidase (HRP) | 109 |
| Figure 32 The linear range of cholesterol oxidase | 110 |
| Figure 33 Phenol concentration optimization | 111 |
| Figure 34 Aminoantipyrine concentration optimization | 112 |
| Figure 35 The variation of initial rate by varying H ₂ O ₂ concentration via 2.5 volts supplied voltage. The measurements are detected CMOS chip (a) and UV-Vis-3300(b) as illustrations | 113 |
| Figure 36 The variation of initial rate by varying cholesterol concentration via supplied voltage 2.5 volts. The measurements are detected by CMOS chip (a) and UV-Vis-3300(b) as illustrations | 114 |
| Figure 37 The variation of initial rate by varying cholesterol concentration via supplied voltage 2.48 volts | 115 |
| Figure 38 The variation of initial rate by varying cholesterol concentration via supplied voltage 2.48 volts. The measurements are detected by CMOS chip (a) and uv/vis 3310 (b) | 116 |
| Figure 39 Glucose test with colorimetric assay. GOD-HRP colorimetric assay detect by uv/vis 3310 (a.) and GOD-HRP colorimetric assay detect by CMOS chip in 45 Hz (b.), 50 Hz (c.) and 60 Hz (d.) | 117 |
| Figure 40 Sensitivity variation with different frequency parameter (a.)Luminescence Assay (b.) Chromogenic Assay..... | 118 |

1. Introduction

1.1 Main trend in biosensor

According to the estimation of the report published by Takeda Pacific, the market size for global medicine biosensor-based products in 2004 reached \$ 7.1 billion and is growing at about 9.7% to 2008. Medical biosensors are utilized in key medical applications which include home blood glucose monitoring used for diabetes management and clinical biosensor applications including Point-of-Care-Testing devices, IV (Intravenous) diagnostics and related applications (1).

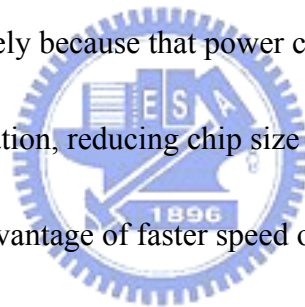
The modern concept of biosensors represents a rapidly expanding field of instruments to determine the concentration of substances and other parameters of biological interest since the inventions of Clark and Lyons in 1962, for example, created the availability of a rapid, accurate, and simple biosensor for glucose. (2) In recent years, there is a general trend toward more decentralized and immediate diagnostic (3-5). The concept of a biological sensor is shown in the figure 1.

Therefore, an accurate, inexpensive, portable, and easy-to-use biosensor becomes the most important issue in the healthcare industry (6-8). The tendency of the “ lab on a chip” , miniaturized analysis system, design is growing rapidly to meet the demand and the developing technology of semiconductor chips for biosensor may satisfy the destination today and in the future.

1.2 CMOS Technology and why do we use CMOS

CMOS has become the mainstream IC technology. Extending well into the sub-0.1- μm regime, its potential provides enormous chip complexities for integration of complete systems on one chip. A number of general trends in the development and manufacturing of CMOS technologies and ICs are discussed (9).

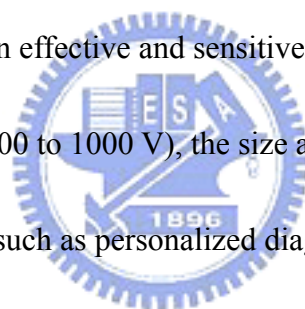
In a CMOS sensor, each pixel has its own charge-to-voltage conversion, and the sensor often also includes amplifiers, noise-correction, and digitization circuits, so that the chip outputs digital bits (10). According to Jim Plusquellic's theorem, CMOS technology is used progressively because that power consumption (heat) of bipolar circuits reduce level of integration, reducing chip size increases physical size of the system, multiple ICs offset advantage of faster speed of bipolar since intra-chip signal propagation is much smaller than inter-chip propagation and on-chip wires suffer capacitance and resistance. However, off-chip wires suffer from capacitance and inductance (ringing effects). The CMOS technology is employed with advantages such as, low power, low cost by standard fabrication, fully restored logic levels, rise and fall transition times are of the same order, very high levels of integration and high performance.



1.3 A multifunctional optical biosensor for biological reaction

Most optical biosensors are developed based on optical fiber technology, which is used as a waveguide medium to transmit light signals from the immobilized enzyme to the photomultiplier tube (11-15). The need for an expensive setup, involving a photomultiplier tube (PMT) and associated equipment, limits the application of the fiber-optic biosensors to the development of simple portable devices for fast screening and in-field/on-site monitoring (2).

Photomultiplier tube is the most common light sensor used in these spectrophotometers. PMT is an effective and sensitive light sensor. However, the needs for high power (about 500 to 1000 V), the size and the price of PMT limit its application in a variety fields such as personalized diagnosis kits.



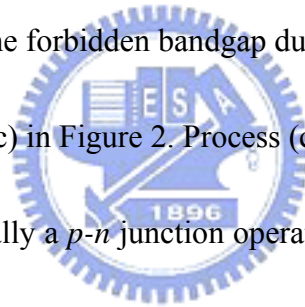
Contrary to PMT, Complementary Metal Oxide Semiconductor (CMOS) process is the most commonly used procedure in semiconductor industry with the advantages of low price, small size and low power consumption compares to that of PMT. CMOS photodiodes can be very useful as light sensor for a portable health care instrument. So we tried to construct some novel CMOS based instruments for the quantification of biological optical signals. For the attempt to replace the photomultiplier tube with a photodiode to detect different optical signals directly, we present a CMOS based multifunctional optical biosensor in this work.

1.4 Design of a CMOS based optical sensor

The basic design of a CMOS based optical sensor is illustrated in Figure 2 to 4.

When the semiconductor is illuminated, photons are absorbed to create electron-hole pairs as shown at (a) in Figure 2 if the photon energy equal to the bandgap energy, that is, $h\nu$ equals E_g . If $h\nu$ is greater than E_g , an electron-hole pair is generated and, in addition, the excess energy ($h\nu - E_g$) is dissipated as heat as shown at (b) in Figure 2. Both processes, (a) and (b), are called intrinsic transition (or band-to-band transition).

On the other hand, for $h\nu$ less than E_g , a photon will be absorbed only if there are available energy states E_t in the forbidden bandgap due to chemical impurities or physical defects as shown at (c) in Figure 2. Process (c) is called extrinsic transition.



A photodiode is basically a $p-n$ junction operated under reverse bias. When an optical signal impinges on the photodiode, the depletion region serves to separate photogenerated electron-hole pairs, and an electric current will flow in the external circuit. For high-frequency operation, the depletion region must be kept thin to reduce the transit time. On the other hand, to increase the quantum efficiency, the depletion layer must be sufficiently thick to allow a large fraction of the incident light to be absorbed. Thus there is a trade-off between the response speed and quantum efficiency (16). Fortunately, the response time of enzymatic reaction is in second's level for steady-state kinetics. It is quite slow compare to electric signal. So we only

need to focus on the problem of quantum efficiency.

The absorption coefficient α , which is dependent on the material used for the optical device, is a function of $h\nu$, shown in Figure 2. The absorption coefficient decrease rapidly at the cutoff wavelength λ_c ; that is,

$$\lambda_c = \frac{1.24}{E_g} \mu m \quad (1)$$

because the optical band-to-band absorption becomes negligible for $h\nu < E_g$, or $\lambda > \lambda_c$.

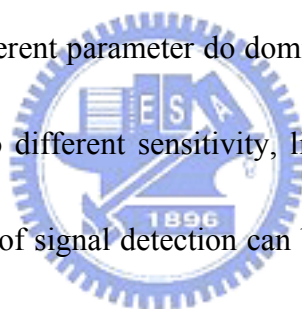
The quantum efficiency is defined as the number of electron-hole pairs generated for each incident photon, that is:

$$\eta = \left(\frac{I_p}{q} \right) \left(\frac{P_{opt}}{h\nu} \right)^{-1} \quad (2)$$

where I_p is the photogenerated current from the absorption of incident optical power P_{opt} at the wavelength λ (corresponding to a photon energy $h\nu$). One of the key factors that determine η is the absorption coefficient α . Since α is a strong function of the wavelength, the wavelength range in which appreciable photocurrent can be generated is limited. The long wavelength cutoff λ_c is established by the bandgap, Eq. 2, and is, for example $1.1\mu m$ for silicon. For wavelengths longer than λ_c the α values are too small to give appreciable band-to-band absorption. The short-wavelength cut-off of the photoresponse comes about because of short wavelengths the α values are very large ($\sim 10^5 \text{ cm}^{-1}$), and hence the radiation is mostly absorbed very near the surface where recombination time is short. Therefore, the

photocarriers can recombine before they can be collected in the p-n junction (16). The photodiodes utilized in this report is N⁺/P well structure as shown in Figure 3.

The novel CMOS is designed to detect the light signal variation and driven by a supplied 3.3 volts and a functional wave. The functional wave is offered by a pulse generator and the frequency of it will effect the detection ability of the CMOS chip. When a lower frequency parameter was supplied to the chip, the capacitance of the readout circuit integrates the electric current produced in a longer time period; on the contrary, the chip with a higher frequency scans in a higher speed and integrates a shorter time interval. The different parameter do dominates in different light intensity range and they are leading to different sensitivity, limit of detection and saturation value. The different demands of signal detection can be satisfied if the characteristics can be applied for clinical diagnosis.



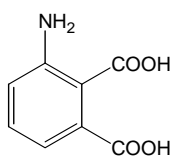
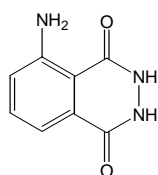
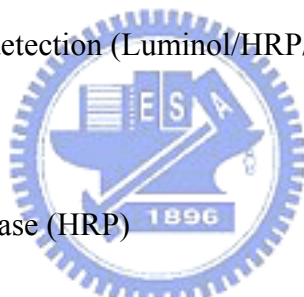
1.5 CMOS photodiodes as chemiluminescence sensor

Chemiluminescence is a powerful tool for a variety of biologically molecules assaying and modern instruments have made it possible to measure luminescence emission with great precision. Thus, chemical or enzyme-catalyzed reactions coupled to luminescence emitting reaction to be exercised to determine numerous biological molecules with high sensitivity (17). The Horseradish Peroxidase (HRP) with its

substrate luminol and perhydrogen oxidase (H_2O_2) reaction system is one of the most popular chemiluminescence enzyme assay system (18). It could be served as a H_2O_2 quantification platform and coupled with reactions that produce H_2O_2 at the same time (19). Here we design an integrated circuit (IC) with photodiodes array and establish an elaborate instrument for the luminescence quantification produced by HRP-luminol- H_2O_2 reaction. Firstly, we prove the reaction can be used as the platform light emitting reaction and the enzymatic activity can be observed and analyzed by a CMOS chip.

Chemical equation (1): H_2O_2 detection (Luminol/HRP/ H_2O_2) system

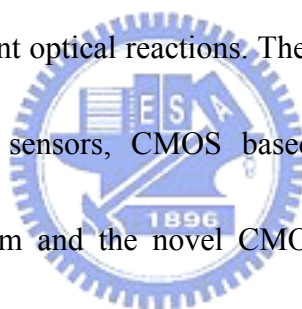
Horseradish peroxidase (HRP)



Equation one shows the luminescence emitting reaction catalyzed by horseradish peroxidase (HRP). HRP-luminol- H_2O_2 reaction could be competent for a platform by right of many enzymes in biological reactions produce reaction H_2O_2 (19). In our system, chemiluminescence generated from biochemical reaction produces current flow that corresponds to the rate of enzymatic catalyzed reaction. By using this

luminescent coupled enzyme assay, we can easily translate the concentration of specific compound to luminescence. The CMOS based sensor is proved to be a successful H₂O₂ sensor with potential to be coupled to detect many clinical biological molecules. There are many biomedical targets detected by the production of H₂O₂ and it produces substances for quantification. These applications are listed in the table1.

A CMOS based sensor used for luminescence assay was proved in use (18) and the multifunctional optical sensor we propose in the report attempts to make stride on sensitivity, less sample requirement, convenience, and multiple biological molecules detection coupled with different optical reactions. Therefore, the quantification ability of three kinds of designed sensors, CMOS based sensor published, integrated commercial photodiode system and the novel CMOS based sensor we present, is compared and analyzed in our report.



1.6 CMOS photodiodes as chromogenic sensor

UV-vis spectrophotometry, HPLC, chemiluminescence and electrochemical methods were used to determine the concentration of reagents (20). Nevertheless, spectrophotometry which performs kinetic assays and determines the organic or inorganic analytes concentration in solution is widely used in clinical tests. Beer's law describes that molecule absorption at the particular wavelength is related to the molecule concentration in solution.

Beer's Law $A = \epsilon c l$ (1)

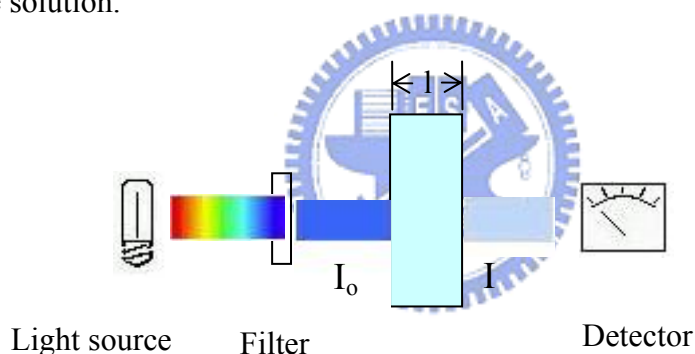
A is the absorbance of the sample at some wavelength ,

c is the concentration of sample in molarity units,

l is the path length of sample the light beam traverses (in centimeters),

and ϵ is an intrinsic constant of the molecule (extinction coefficient).

The following figure explains how a spectrophotometer works, as monochromatic radiation passes through the homogeneous solution in a cell, the intensity of the emitted radiation depends upon the thickness (l) and the concentration (c) of the solution.



I_0 is the intensity of the incident radiation and I is the intensity of the transmitted radiation. The ratio I/I_0 is called transmittance (T). This is sometimes expressed as a percentage and referred to as % transmittance. Mathematically, absorbance is related to percentage transmittance T by the expression:

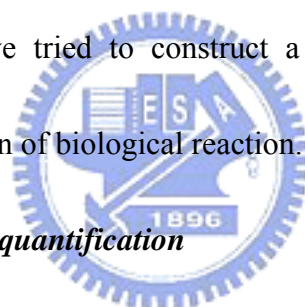
$$A = \log (I_0 / I) = \log (100/T) = \epsilon c l \quad (2)$$

Absorbance is sometimes referred to as ‘extinction’ or ‘optical density’ (OD).

However, a common error associated with absorption measurements is deviation from

Beer's law. The form of Beer's law only suggests that the absorption of a sample will increase linearly with the concentration of the molecule being analyzed (21, 22).

Indeed, optical instruments, such as UV-vis absorption spectrophotometer, fluorescence meters, and luminescence meters are commonly used to measure biochemical reactions. Moreover, photomultiplier tube (PMT) is the most common light sensor used in these spectrophotometers. PMT is an effective and sensitive light sensor. Nevertheless, the needs for high power (about 500 to 1000 V), the size and the price of PMT limit its application in a variety fields such as personalized diagnosis kits. Thus, in this report, we tried to construct a semiconductor multifunctional biosensor for the quantification of biological reaction.



1.7 Cholesterol chromogenic quantification

Cholesterol is found almost exclusively in animals used for the manufacture and repair of cell membranes, for synthesis of bile acids and vitamin D, and is the precursor of five major classes of steroid hormones: progestins, glucocorticoids, mineralocorticoids, androgens, and estrogens (23). Cholesterol is an unsaturated steroid alcohol of high molecular weight, consisting of a perhydrocyclopentanthaline ring and a side chain of eight carbon atoms. In its esterified form, it contains one fatty acid molecule. The conformation of cholesterol is shown in figure 5.

There are different kinds of lipoproteins in the body but the two kinds which

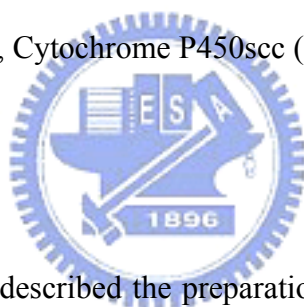
indicate the risk of heart attack are “Low Density Lipoproteins” or LDL and “High Density Lipoprotein” or HDL. Low Density Lipoprotein is the major cholesterol carrier in the blood. It is also known as the “bad” cholesterol. HDL cholesterol also known as the “good” cholesterol carries the cholesterol from other parts of the body back to the liver. The liver removes cholesterol from the body (24).

Cardiovascular diseases in people are increasing day by day and cardiac arrest is a major cause of death world over. There are several causes for this but one of the most important reasons is hypercholesterolemia i.e. the increased concentration of cholesterol in the blood (25). Cholesterol is usually measured in milligrams (mg) of cholesterol per deciliter (dl) of blood. The range of total cholesterol level recommended by National Cholesterol Educational Program (NCEP) is: Desirable, 200mg/dL or less; Borderline-high, 200 to 239mg/dL and High, 240mg/dL, of which two third is esterified with fatty acids and one third is present as sterol (26). The cholesterol standard in human body is listed in the table 2. There is a strong positive correlation between high serum cholesterol level and arteriosclerosis, hypertension and myocardial infarction. So, the determination of cholesterol is important in clinical diagnosis.

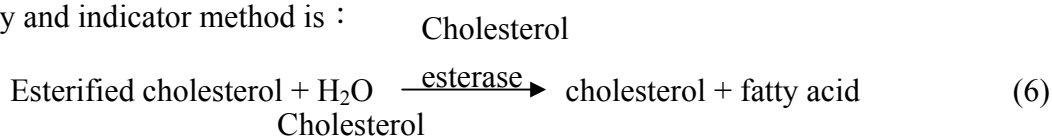
As awareness of the importance of total cholesterol levels has increased, numerous methods for human blood cholesterol assays have been developed (27, 28, 29),

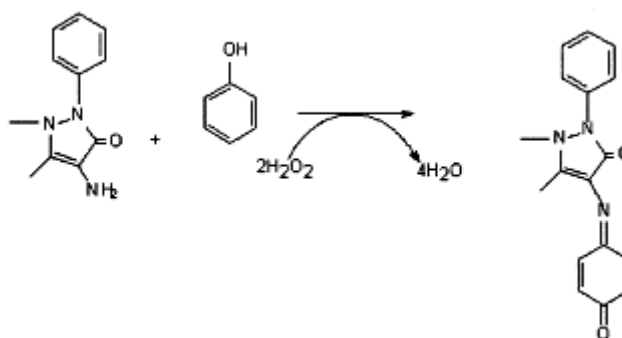
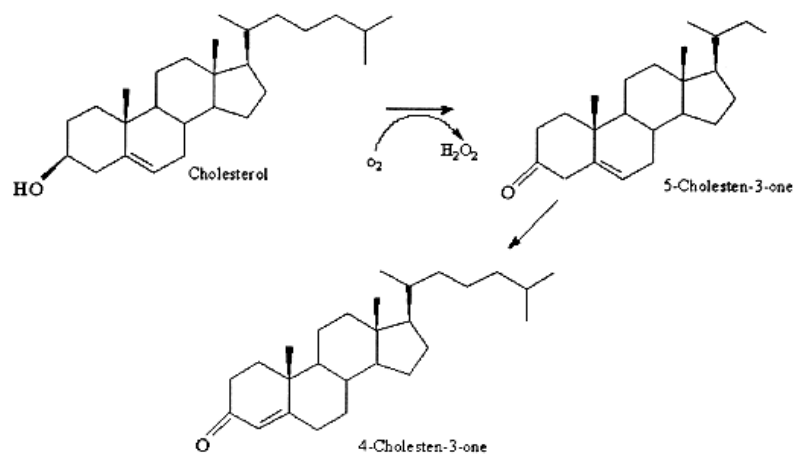
including colorimetric spectrometric and electrochemical methods. Mainly enzymatic procedures are employed in clinical diagnosis due to their rapid, selective, sensitive nature and the great accuracy.

Enzymatic procedures have practically replaced the chemical methods based on the classical Libermann – Burchard reaction, used traditionally for free and total cholesterol determination (30). Owing to the advantages of simplicity, rapidness and cost efficiency, a few cholesterol biosensors have been developed which are based on cholesterol oxidase (ChOX) and cholesterol esterase (ChEt)(31,32), cholesterol oxidase (33,34,35), Cytochrome P450_{scc} (36), fiber-optic biosensor (30), acoustic wave (28).



Richmond (1973) firstly described the preparation of an oxidase from *Nocardia* and its application to the enzymatic assay of cholesterol in saponified serum extracts (37). The product of this enzymatic assay could be detected by direct UV measurement at 240nm. This work was extended by Allain et al. (1974) to include the enzymatic hydrolysis of cholesterol esters and the coupled reaction with 4-aminoantipyrine and phenol (38-43). The reaction followed by the three-enzyme assay and indicator method is :

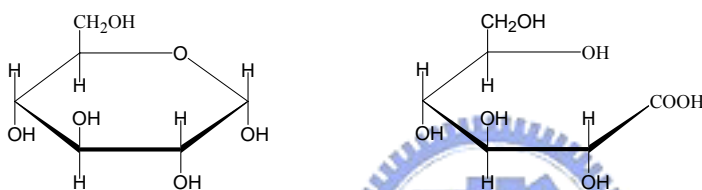
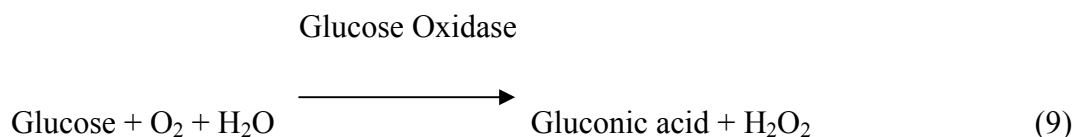




In the blood circulation, two thirds of the cholesterol is esterified, and one third is in free form, so we should use cholesterol esterase (EC 3.1.1.13) to catalyze cholesterol ester to free cholesterol first. And then cholesterol oxidase (EC 1.1.3.6) catalyzes the oxidation and isomerization of 3β -hydroxy steroids with the concomitant formation of H_2O_2 . Hydrogen peroxide oxidoreductase (EC 1.11.1.7), also known as peroxidase, catalyzes the oxidation of aqueous aromatic compound by

hydrogen peroxide.

In this report, we also choose glucose/glucose oxidase system (chemical equation 9) to demonstrate a CMOS chip can measure glucose frequently used clinical coupled assay.



High cost and inconvenient health instruments lead people not to make the periodic health examination, so the development of an accurate, portable, relatively inexpensive and easy-to-use biosensor will become the most important issue in the healthcare industry. Hence LED (light emitting diode) was used as light source, photodiode was the light detector plus biological reaction to develop the diagnostic setup which meets all demands.

1.8 Light emitting diodes (LEDs)

Light can be produced and/or controlled electronically in a number of ways. In light emitting diodes (LEDs), light is produced by a solid state process called electroluminescence. LEDs are the ultimate light source in the light technology. The

LED technology has flourished for the past few decades. High efficiency, reliability, rugged construction, low power consumption, and durability are among the key factors for rapid development of solid-state lighting based on high-brightness visible LEDs while compared with conventional light sources, such as filament light bulbs and fluorescent lamps which depend on either incandescence or discharge in gases and accompanied by large energy losses, which are attributed to the high temperatures and large Stokes shift characteristics.

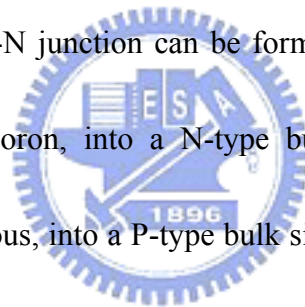
Semiconductors allow an efficient way of light generation and LEDs made of semiconductor materials have the potential of converting electricity to light with near unity efficiency (44). Conventional LEDs includes GaAsP (yellow to red) and GaP (green to red) devices while a new development is directed to various materials used for high brightness (HB) LEDs based on AlGaAs (red), AlInGaP (yellow-green to red) and InGaN (blue, green and white) devices. The basic LED consists of a p-n junction. Under forward bias condition, electrons are injected into p-type region, and holes are injected into the n-type region. Recombination of these minority carriers with the majority carriers at the p-n junction leads to light generation. The wavelength and color of the light is determined by the difference in the energy levels of the electrons and holes (44-46). The output from an LED can range from red (at a wavelength of approximately 700 nanometers) to blue-violet (about 400 nanometers). Some LEDs

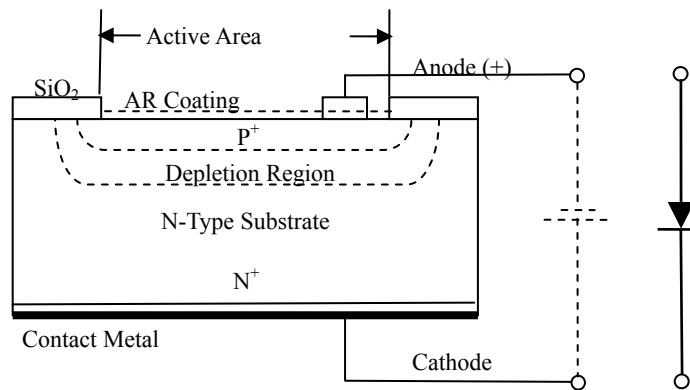


emit infrared ([IR](#)) energy (830 nanometers or longer); such a device is known as an *infrared-emitting diode* (IRED).

1.9 Photodiode

Photodiodes are semiconducting devices that convert light into electrical signals, responsive to high energy particles and photons. There are several kinds of semiconductor photodiodes. They all work on the same principle which is based on [photoconductivity](#) summarized in Table 3. Photodiodes operate by photons or charged particles absorption and generate a current flow in an external circuit, proportional to the incident power (47). A P-N junction can be formed by diffusing either a P-type impurity (anode), such as Boron, into a N-type bulk silicon wafer, or a N-type impurity, such as phosphorous, into a P-type bulk silicon wafer. However, the top p layer is very thin and the thickness is determined by wavelength of radiation to be detected. Near the p-n junction, the silicon becomes depleted of electrical charges and is known as the “depletion region”. The depletion region depth can be varied by applying a reverse bias voltage across the junction, and it is important to photodiode performance since most of the sensitivity to radiation emanates there. Below is a figure of a planar diffused silicon photodiode under reverse bias voltage.





The responsivity (R_λ , A/W) of a silicon photodiode is a measure of the effectiveness of the conversion of the light power into electrical current, or of the sensitivity to light. It is defined as the ratio of the photocurrent I_p (A/cm²) to the incident light power P (W/cm²) at a given wavelength:

$$R_\lambda = I_p / P \quad (3)$$

Responsivity (R_λ) increases slightly with applied reverse bias by dint of improved charged collection efficiency in the photodiode, and the increase of temperature also causes responsivity variations due to band gap decrease. The spectral responsivity of a specific photodiode is known by measuring the responsivity of a photodiode.

When a photodiode is exposed to light, the current-voltage characteristic of a photodiode is:

$$I_{Total} = I_{SAT} (e^{qV_A/k_B T} - 1) - I_p \quad (4)$$

where the I_{SAT} is the reverse saturation current, q is the electron charge, V_A is the applied bias voltage, $k_B = 1.38 \times 10^{-23}$ J/K, is Boltzmann Constant, T is the absolute temperature and I_P is the photocurrent.

A photodiode's capability to convert light energy to electrical energy, expressed as percentage, is its Quantum Efficiency (Q.E.). It is defined as the fraction of the incident photons that contribute to photocurrent. It is related to responsivity by:

$$\begin{aligned} \text{Q.E.} &= R_{\lambda \text{ Observed}} / R_{\lambda \text{ Ideal}} \\ &= R_{\lambda} hc / \lambda q = 1240 R_{\lambda} / \lambda \end{aligned} \quad (5)$$

where $h = 6.63 \times 10^{-34}$ J/s, is the Planck constant, $c = 3 \times 10^8$ m/s, is the speed of light, $q = 1.6 \times 10^{-19}$ C, is the electron charge, R_{λ} is the responsivity in A/W and λ is the wavelength in nm. A high quality silicon photodiode of optimum design should be capable of approaching a Q.E. of 80% under ideal operation conditions of reflectance, crystal structure and internal resistance (46).

1.10 Assembled commercial semiconductor devices setup

There are electronic devices available in the market to be an alternative choice. To integrate semiconductor elements sold in the market can save time waiting for self-design semiconductor element manufacturing. We can depend on what results we discover to design the more suitable semiconductor elements for biochemical reactions. Thus, we use LED (light emitting diode) as light source and photodiode as

light detector plus biological reaction to develop a portable, easy-to-use and accurate diagnostic setup.



2. Material and methods

Sub Abstract

A light sensitive complementary metal oxide semiconductor (CMOS) chip is designed for measuring biochemical reactions. This CMOS chip is processed through a standard $0.35\ \mu\text{M}$ CMOS process. A light producing enzymatic reaction catalyzed by horseradish peroxidase (HRP) is designed as platform reaction to determine the concentration of hydrogen peroxide by the CMOS chip. We have already proved that there are two enzyme reactions both catalyzed by HRP to react with H_2O_2 to produce the products for light sensing. The kinetics of enzymatic reactions are determined and compared by the standard and sophisticated fluorescence spectrometer (Hitachi F-4500) and UV-vis spectrophotometer (UV-3300, Hitachi) in a biochemical laboratory. Our data shows that enzymatic reactions determined by both methods are the same. Using cholesterol oxidase as an example, we further demonstrate that the HRP platform can be used to determine other hydrogen peroxide producing reaction with the CMOS system. The result points to an important application of the CMOS chip in many biological measurements and in diagnosis of many health factors. Figure 6 is the flowchart of experimental design and process.

2.1 Materials

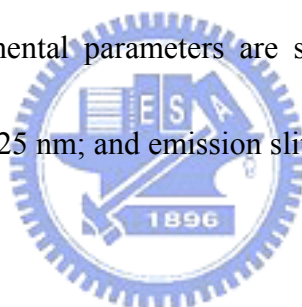
Cholesterol, Horseradish peroxidase (HRP), cholesterol oxidase (from *Pseudomonas fluorescens*), cholesterol oxidase (from *Streptomyces* sp.), 4-aminoantipyrine, pyrogallol, H₂O₂ (30%, w/w), Triton[®] X-100, luminol and O-dianisidine (ODA) are purchased from Sigma. Phenol (90%), H₂KPO₄ are obtained from Riedel-deHaën. K₂HPO₄ and 2-propanol are supplied by J. T. Baker. Tris-HCl buffer is purchased from Pharmacia Biotech.

2.2 Apparatus

Figure 7 displays the complete experimental setup of the CMOS optical biosensing system. Blue light emitting diode (LED) is needed to semiconductor biomedical sensing device which is composed of all commercially available elements. E3646A power supply (Agilent), 4401A multimeter (Agilent), General Purpose Interface Bus (GPIB) card, connection wire (National Instruments), 8110A pulse generator (Hp) and a common personal computer (PC) are used to collect the data output from photodiode. And a traditional UV/vis spectrophotometer (UV-3300, Hitachi) and the luminescence spectrometer (F4500, Hitachi) are used to confirm the validity of the data of our semiconductor biomedical sensing device.

2.3 Photomultiplier tube (PMT) detection system

PMT is the most commonly used sensor in spectrophotometer (e.g. luminescence, fluorescence, and UV-vis absorption spectrophotometer in many biochemical laboratories). It has the advantage of high quantum efficiency that approximately one photon could induce 10^6 electrons in photomultiplier tube. Hitachi F-4500 Fluorescence Spectrometer and UV/vis 3310 are used in this report. The values of chemiluminescence and absorbance responded by F-4500 and uv/vis 3310 are proportion to the reaction rate of enzymatic reaction. To obtain comparable luminescent data, the instrumental parameters are set as following: PMT voltage, 700V; emission wavelength, 425 nm; and emission slit, 1 nm.



2.4 Method

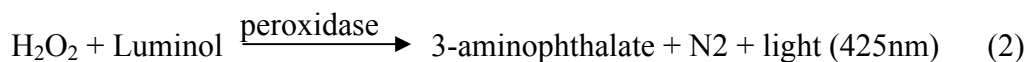
Reaction 1. Luminescence Reaction of HRP-luminol-H₂O₂ enzyme reaction

2.4.1 Scheme

There are two parts in our experiment. One is the design of new generation semiconductor setup (provided by Prof. Wu's lab, departments of electro engineering), and the other is biochemical reaction design.

We choose HRP-luminol-H₂O₂ luminescence system as platform to couple with cholesterol oxidase to determine the amount of free cholesterol. Below is the chemical

equation:



Before the kinetics of cholesterol oxidase was measured, HRP-luminol-H₂O₂ luminescence studies were performed by traditional fluorescence spectrophotometer (F-4500, Hitachi). Secondly, compare the data of kinetics got from F-4500 to the data kinetics from our semiconductor setup in order to confirm the usability of our setup.

2.4.2 *Semiconductor setup*

CMOS with Agilent 34401A Multimeter Detection System

A 3.3V reverse bias is given to CMOS photodiodes chip by HP 4145. The reaction condition is the same as that used by PMT detection system (Hitachi F4500) described above. Our light sensing CMOS photodiodes is N⁺/P well structure, which is manufactured with standard 0.35μm CMOS process. The CMOS photodiode and layout diagram of N⁺/P well photodiodes array is a 128×128 photodiodes array with single pixel size 10μm×10μm, as figure 8(a.) shows and the circuit design is displayed in Figure 8 (b.). The photodiodes chip has no color filter, so it absorbs the full luminescence spectrum of chemical reaction (from 400nm to 800nm). The characteristics of the CMOS chip are listed in the table 3 and compared with the early stage CMOS chip reported in 2004 (48).

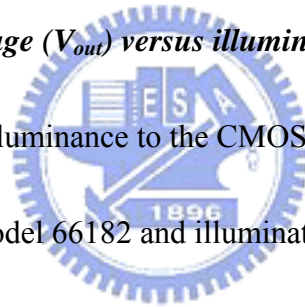
2.4.3.1 Measured output voltage (V_{out}) with adjusted clock frequency

A functional wave needs to be supplied to drive the CMOS chip system. In our work, the range of the pulse produced by 8110A pulse generator (Hp) is from 0 to 3.3 Volts with a clock frequency. The output voltage under identical light stimulus varies with different frequency and so does the available **discriminable signal output range**.

The test of frequency parameter ranges from 20 to 250 kHz, and the output voltage is recorded under dark and light. Regardless of operation in dark or light, the dark current and the saturated current both differ with frequency.

2.4.3.2 Measured output voltage (V_{out}) versus illuminated intensity

Supplying the adjusted illuminance to the CMOS photodiode by oriel constant current lamp power supply model 66182 and illuminator model 66033, the output voltage can be read under different luminosity. The setup needed for the experiment is displayed in figure 11.



2.4.4 Different Frequency versus LED supplied voltage variation

LED supplied voltage will affect the light intensity of the LED emitting, and the supplied voltage is proportional to in the light intensity in certain range. Frequency parameter could be modulated in different optical reactions, so the output voltage from the sensor varies not only by the LED supplied voltage but also the frequency parameter setting. The relationship between frequency and LED supplied voltage

could be studied in our test. The supplied voltage range was selected from 2.3 volts to 2.6 volts. The illuminated intensity of the LED driven by the supplied voltage was measured as well to observe the output characteristics with the quantified light signal variation.

2.4.5 Biochemical reaction

2.4.5.1 Reagents preparation

Hydrogen peroxide (H₂O₂) (1M stock solution)

Add 102 μ l 30% hydrogen peroxide in ddH₂O and make up to 1 ml. Hydrogen peroxide is light sensitive, and it should be stored in a brown bottle.

Luminol (100 mM stock solution)

Dissolve 199.1 mg luminol in ddH₂O and make up to 10 ml. Luminol is light sensitive; it should be stored in a brown eppendoff.

Tris- HCl buffer (50 mM stock solution , 500ml, pH=8.6)

Dissolve 30.285g tris powder in ddH₂O and make up to 500 ml.

Glucose (1M stock solution)


The powder of Glucose, 180mg is dissolved in ddH₂O and to made up to 1ml.

2.4.5.2 Enzymes preparation

HRP powder (1 mg or 80 units) is dissolved in 1ml Tris-HCl buffer (0.1 M at pH 8.6). The enzyme solutions are melted in ice bath just before use and are diluted with

specified dissolved buffer. Aliquot amount of enzyme is added into the cuvette following by the injection of all other necessary reagents and sample. These processes are going to make sure that the whole compounds are well mixed in the cuvette without extra shaking and the data can be collected in a short period of time. One unit of HRP means 1.0 mg of purpurogallin is formed from pyrogallol in 20 seconds at pH 6.0 at 20°C as described by Sigma. Else, Glucose oxidase (20mg or 3000 units) is dissolved in 1ml phosphate buffer (0.2 M at pH7.0). The enzyme solution is stored in -80°C. The HRP and GOD solutions are melted in ice bath just before use and are diluted with specified dissolved buffer.

2.4.5.3 Reaction condition of HRP-luminol-H₂O₂ system



The optimal condition for HRP-luminol-H₂O₂ system is determined as shown in Figures. Unless otherwise specified, the standard condition involved HRP-luminol-H₂O₂ system includes luminol (1 mM), H₂O₂ (3 mM), Tris-HCl (100 mM at pH 8.6) and HRP (0.02 units) at 25°C. For the coupled enzyme assay, H₂O₂ is omitted. Each data point is the average of three measurements. Luminescence of each measurement is obtained from the average of first ten seconds in each reaction.

2.4.5.4 Glucose oxidase coupled HRP-luminol-H₂O₂ system

HRP-luminol-H₂O₂ system couple to GOD catalyzed reaction can determine the concentration of glucose. The standard condition for this coupled enzymes system

includes 150 units GOD, 0.32 units HRP, 1mM luminol, 0.1M Tris-HCl buffer (pH 8.6) in a final volume of 1 ml at room temperature. To start the measurement, the mixture of luminol, Tris-HCl buffer, glucose and GOD that has been incubated for 10 min at room temperature is mixed with HRP. Each data point is the average of three measurements. Luminescence of each measurement is obtained from the average of first three seconds in each reaction.

2.4.5.5 Optimization

2.4.5.5.1 Luminol concentration variation vs. reaction initial rate

To see the relation between luminol concentration and reaction initial rate, the amount of enzyme HRP and the other substrate, H_2O_2 , are both fixed. We work the coupled enzyme reaction under the standard condition and find out the optimum luminol added concentration where initial rate achieves the maximum.

2.4.5.5.2 Cholesterol oxidase coupled HRP-luminol- H_2O_2 system

Incubation time optimization of HRP-CHOD coupled enzyme reaction

Studying with two different experimental methods, incubation and real time test, under the standard condition, we try to find out the proper method for luminescence assay.

(1.) Incubation test

To prevent the insufficiency of reaction products, all the reagents for cholesterol oxidation mixed before enzyme treatment and incubate for 10 minutes to complete the cholesterol oxidation. After 10 minutes incubation, enzyme HRP is added into the

working well to start the coupled enzyme reaction and use H_2O_2 produced from the first equation, cholesterol oxidation, for the luminescence reaction.

(2.) Real time test

To save the total detection time, the user starts the coupled enzyme reaction by adding enzyme HRP as soon as we have added all necessary reagents into the cell. After the measurements of two methods, the comparison of them will help us to choose the better way to work our luminescence.

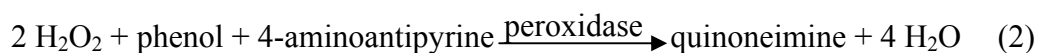


2.5 Reaction 2. Colorimetric Reaction of HRP-Phenol-H₂O₂ enzyme reaction

2.5.1 Scheme

Cholesterol oxidase coupled HRP-phenol-H₂O₂ system

In this part, we use phenol/4-aminoantipyrine/H₂O₂ system as the colorimetric platform to couple with cholesterol oxidase to determine the amount of free cholesterol. The chemical equation is shown as following:



Except cholesterol oxidase, phenol/4-aminoantipyrine/H₂O₂ chromogenic system could couple with various enzymes to assay different kinds of substrates. Optimization studies were performed for each of the components of cholesterol assay on traditional UV-vis spectrophotometer (UV-3300, Hitachi) before the kinetics of cholesterol oxidase was measured. Afterwards, the data of kinetics of cholesterol oxidase got from UV-3300 was compared to the data kinetics of cholesterol oxidase got from the semiconductor setup to make sure the usability of our device. The overall biological experimental procedure is shown in the figure 10.

2.5.2 Glucose oxidase coupled HRP-phenol-H₂O₂ system

HRP-phenol-H₂O₂ system couple to GOD catalyzed reaction can also determine the concentration of glucose. The standard condition for this coupled enzymes system

includes 150 units GOD, 0.32 units HRP, 1mM luminol, 0.1M Tris-HCl buffer (pH 8.6) in a final volume of 1 ml at room temperature. To start the measurement, the mixture of luminol, Tris-HCl buffer, glucose and GOD that has been incubated for 10 minutes at room temperature is mixed with HRP. Each data point is the average of three measurements. Initial rate of each measurement is obtained from the average of ten seconds in each reaction.

2.5.3 Semiconductor setup

2.5.3.1 The design of assembled semiconductor setup




Figure 7 is the component instruments connection diagram of assembled semiconductor element setup. We use LED as an illuminant, when photodiode absorbs photons, it will generate a flow of current in an external circuit, proportional to the incident light, and we could know the corresponding concentration of reagents by measuring the voltage value. E3646A power supply provides 3.3 V bias voltage, and 34401A multimeter collects the voltage data and transfers it to a personal computer (PC) through GPIB connection. There is another need of the supply of some function wave to drive the semiconductor device. Besides, we choose a blue LED as a light source because the product of phenol/4-aminoantipyrine/H₂O₂ chromogenic system has a maximal absorbance of quinoneimine at 495 nm. Seeing figure 9 would provide

specific illustration.

2.5.3.2 Commercial photodiode

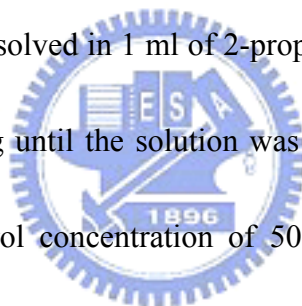
The commercial photodiode has a light range from 320 nm and 1100 nm, and has a maximum absorption peak at 960 nm.

2.5.4 Biochemical reaction

2.5.4.1 Reagents preparation

Cholesterol :

Cholesterol solution was prepared according to the following procedure: 50 mg of cholesterol powder was dissolved in 1 ml of 2-propanol and 1 ml of Triton[®] X-100 by slowly heating and stirring until the solution was clear, 8 ml of ddH₂O was then added. This gave a cholesterol concentration of 500 mg/dl. Solutions of different concentrations were similarly prepared.



4-aminoantipyrine (9.6 mM stock solution)

Dissolve 195.07 mg 4-aminoantipyrine in ddH₂O and make up to 100 ml. 4-aminoantipyrine is light sensitive; it should be stored in a bottle wrapped in aluminum foil.

Phenol (100 mM stock solution)

Add 0.98 ml 90% Phenol in ddH₂O and make up to 100 ml. Phenol is light sensitive, it should be stored in a brown bottle.

Phosphate buffer (0.2 M stock solution)

To make a 0.2 M dibasic phosphate solution, add ddH₂O to 5.68 g Na₂HPO₄ until final volume 200 ml is obtained. 0.2 M monobasic phosphate solution is prepared by add ddH₂O to 5.52 g NaH₂PO₄ • H₂O until final volume 200 ml is obtained. And then add NaH₂PO₄ solution to Na₂HPO₄ solution to bring desired pH. Phosphate buffer is stored at room temperature.

2.5.4.2 Enzymes preparation

Horseradish peroxidase (HRP, EC 1.11.1.7)

HRP stock is made by dissolving 1.0 mg HRP in 1 ml potassium phosphate buffer (0.1 M at pH 6.0), and the stock is stored at 4°C. One unit of HRP is defined as 1.0 mg of purpurogallin from pyrogallol in 20 sec at pH 6.0 at 20°C.

Cholesterol oxidase (CO, EC 1.1.3.6)

Cholesterol oxidase purchased from Sigma is sold by 25 units per bottle. We add 2.5 ml potassium phosphate buffer (50 mM at pH 7.5) in the bottle; stir gently until all powder is completely dissolved. Aliquot 0.5 ml enzyme solution to 1.5 ml eppendorf tubes and stored at 4°C. One unit cholesterol oxidase will convert 1.0 μ mole of cholesterol to 4-cholesten- 3-one per min at pH 7.5 at 25°C.

2.5.4.3 Optimal condition for enzyme assay

2.5.4.3.1 Absorption wavelength of product

We use the “wavelength scan” function of UV-3310 to measure the range of absorption wavelength of reaction product. The scan parameters of UV-3300 are: start wavelength is 600 nm, end wavelength is 400 nm, delay time is 180 sec, scan speed is 300nm/min and slit is 2 nm. Reaction condition is: 25°C, pH 6, 50 mM phosphate buffer, 10 mM phenol, 2.4 mM 4-aminoantipyrine, 0.2 mM H₂O₂ and HRP 1 μg/ml.

2.5.4.3.2 Optimal concentration of reagents

Optimization studies were performed for each of the components of cholesterol assay. We use the “time scan” function of UV-3310 to find out the optimal concentration of reagents. The scan parameters of UV-3100 are: wavelength is 505 nm, sampling interval is 0.1 sec, total time is 300 sec, and delay time is zero. Constant reaction condition is: 25°C, pH 7.4, 50 mM phosphate buffer, 9 mM H₂O₂ and 50 mg/dl cholesterol.

We start the optimization studies with phenol/4-aminoantipyrine/H₂O₂ chromogenic system to find out the linear range of HRP, and then we add appropriate amount of HRP, excess phenol or 4-aminoantipyrine to figure out the optimal concentration of reagents.

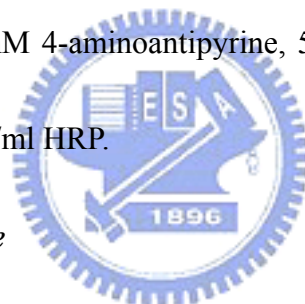
After knowing the suitable amount of other reagents, we couple

phenol/4-aminoantipyrine/H₂O₂ chromogenic system with cholesterol oxidation reaction to find out the linear range of cholesterol oxidase.

2.5.4.3.3 Optimal pH value and concentration of buffer

The “time scan” function of UV-3310 is used to find out the optimal pH value and concentration of phosphate buffer. Value of pH range from 6 to 8.5 with an interval of 0.5; concentrations of phosphate buffer are 0.05 M, 0.1 M and 0.2 M.

The scan parameters of UV-3310 are: wavelength is 495 nm, sampling interval is 0.2 sec, total time is 120 sec, and delay time is zero. Constant reaction condition is: 25°C, 14 mM phenol, 0.82 mM 4-aminoantipyrine, 50 mg/dl cholesterol, 0.02 U/ml cholesterol oxidase and 2 μ g/ml HRP.



2.5.4.3.3 Optimal temperature

We use the “time scan” function of UV-3310 to find out the optimal temperature for the coupled enzyme assay. Temperature ranges from 15°C to 40°C. All reagents except enzymes are mixed and incubated at appropriate temperature for at least 5 min, and then enzymes are added into mixed reagents immediately before we start to measure the process of time scan. The scan parameters of UV-3310 are: wavelength is 505 nm, sampling interval is 0.5 sec, total time is 300 sec, and delay time is zero. Constant reaction condition is: pH 7.4, 14 mM phenol, 0.82 mM 4-aminoantipyrine, 50 mg/dl cholesterol, 0.02 U/ml cholesterol oxidase and 1 μ g/ml HRP.

2.5.4.3.4 Optimal incubation time

To see how different incubation time acts on the enzyme reaction, the incubation time altered before the experimenter add the second enzyme cholesterol oxidase to start the coupled enzyme reaction. There are five different incubation time condition (0 min, 2 min, 3 min, 5 min, and 8 min) tested before the coupled enzyme reaction start.

2.5.4.4 Coupled enzyme assay to determine concentration of cholesterol

Phenol/4-aminoantipyrine/H₂O₂ chromogenic system couple to CO catalyzed reaction can determine the concentration of cholesterol. The reaction condition for this coupled enzymes system includes 0.02 U/ml COD, 0.16 U/ml HRP, 4-aminoantipyrine (0.82 mM), phenol (14 mM) and phosphate buffer (50 mM, pH 7.4) in a final volume of 1 ml at room temperature.

To start the measurement, all reagents except COD were added into cuvette orderly, upon addition of the cholesterol oxidase to the cuvette, the cuvette was capped and inverted three times prior to being placed in the spectrophotometer or our semiconductor setup. Each data point is calculated from the mean value of triplicate assay which has standard deviations less than 3%. The curve and K_m value are obtained with Michaelis-Menten equation in enzyme kinetics analysis of Sigma Plot

2001.

2.6 Sample Volume Reduction

The quartz cuvette was used while operator manipulates experiments by spectrophotometer and the capacity of the transparent quartz reactor is fixed. The sample volume must be more than 0.7 milliliter to reach the height requirement for detection. Customarily in the past the sample volume is fixed in 1 milliliter and all reagents should be added together to reach the sum. While the new generation CMOS chip works, we use a handmade vessel instead of quartz cuvette. The container is composed of the wider part of plastic tip and the thin glass slide. The gauge of 1 milliliter plastic tip fits the sensing area with adequate radius and the tip constitutes the vessel wall. The thin glass slide (0.17mm) serves as the handmade vessel bottom with good light transmittance. The handmade vessel requires 500 micro liter sample volume which is half the original requirement. After used repetitively, the new container is found with several advantages such as low cost, light, available and handy. Such characteristics help to develop the disposable sample container which makes the diagnostic test more convenient and accuracy.

3. Results and discussion

3.1 Measured output voltage (V_{out}) with adjusted clock frequency

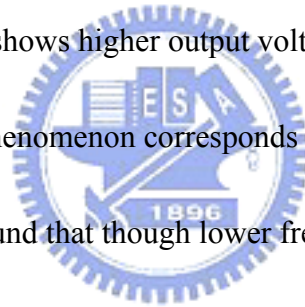
According to the trend of the curve (Figure 12), the saturated output voltage in light remains stable (around 0.7 volts) before 40 kHz but begins to decline after 40 kHz and it decreases from 0.7 volts to 0.3 volts to where the frequency goes to 250 kHz. As for the dark situation, low frequency on the contrary leads to fluctuant output voltage. From 20 to 60 Hz (Figure 13), the output voltage decreases from 0.7 volts to 0.15 volts. As frequency increases, the output voltage slight goes down.

These results tell that higher output voltage is recorded in dark or with little light with lower frequency. On the other hand, CMOS chip output signal gradually decays with higher frequency over 40 kHz even in intensive light or saturated state.

Generalizing the events, an suitable frequency need to be chosen to operate in harmony with different light intensity and the detector can adjust the frequency parameter to fit the requirement of each optical assay.

3.2 Measured output voltage (V_{out}) versus illuminated intensity

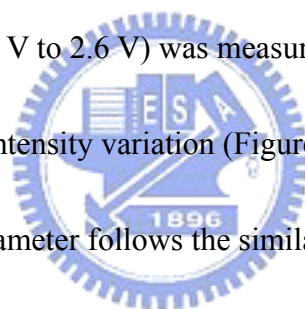
As presented in Figure 11, the apparatus of illumination test, the signal from CMOS chip can be displayed in Agilent 81110A pulse/ pattern generator. The measured output voltages with clock frequency 125 kHz and 10 kHz are present in Figure 14 and 16, the linearity of illuminated intensity to output voltage achieves 98.3% in 125 kHz and 99.3% in 10 kHz, shown in Figure 15 and 17. The high linearity demonstrates that the CMOS chip actually serves as a reliable optical sensor. Besides, comparing the identical illuminated intensity supplied to chip with diverse frequency, the output voltages differs. It shows higher output voltage under feeble light intensity in lower frequency and this phenomenon corresponds to the test result in dark. From the measurements, we also found that though lower frequency responses to weak light resource more effectively, it attains saturation more easily as well. Thus, the adjusted frequency parameter takes part in different luminosity zone.



3.3 Different Frequency versus LED supplied voltage variation

According to Figure 18 (a), LED supplied voltage effected the intensity of the LED emitting, and led to different sensor output voltage. The output voltage varies obviously when LED supplied voltage surpass 2.3 volts. The rising of output voltage becomes earlier while the frequency parameter becomes smaller. The saturated voltage showed up earlier with smaller frequency parameter as well. Figure 18 (a)

shows that the different frequency setting would lead to different LODs (limit of detection) of chip. For example, when the LED supplied voltage is 2.3 Volts, chip with small frequency setting would have a rising output voltage but it didn't if it is with a higher frequency. In another hand, different frequency parameters not only lead to different LODs, but also the different sensitivity. Different slope occurs while the frequency parameter changes. The characteristics of modulation with different frequency setting would be more flexible for users to select the optimal sensitivity and sensing range for different detections. The quantified light intensity of the LED with different supplied voltage (2.3 V to 2.6 V) was measured to display relationship of the output voltage and unit light intensity variation (Figure 18 (b)). In Figure 18(b.), the variation of the frequency parameter follows the similar tendency as Figure 18(a.) reflected by the variation of light intensity. It also shows that the frequency parameter indeed changes the sensitivity of the CMOS chip of different light intensity range.



3.4 Chemiluminescence Method

The HRP-luminol-H₂O₂ reaction system emits chemiluminescence in the initial steady state of the reaction most brightly, and decays quickly. The optimization experiment condition is important for users to measure chemiluminescence.

3.4.1 Optimization of enzymatic assay condition

3.4.1.1 HRP activity standard curve

According to the data of HRP activity standard curve, the linear range of HRP sits between 0.008~ 0.72 unit. To select an appropriate temperature to manipulate our experiments, we observed the temperature dependent curve which and it indicates that the HRP-luminol-H₂O₂ system gives similar luminescence around 15°C~40°C (Table 3). Nevertheless, data shows that change of pH significantly affects the activity of HRP-luminol-H₂O₂ system (49). The standard condition for HRP-luminol-H₂O₂ system described in experiments is determined based on these results.

3.4.1.2 Optimal concentration of reagents

Luminol concentration variation vs. reaction initial rate

The optimized concentration of luminol is near 8 mM. By observing the pattern of the graph, it shows that the reaction initial velocity gradually decays after arriving the V_{max}, and tends toward saturate state. The initial rate value of it is similar to that when the luminal concentration is 5 mM.

3.4.2 HRP-luminol-H₂O₂ kinetic Graph

After the adequate concentration of reagents in HRP-luminol-H₂O₂ reaction are found out, we fix the enzyme amount as well and then drive the coupled enzyme reaction in the uniform condition. By varying the concentration of H₂O₂, the initial rates differ and lead to a kinetics curve fluctuated by H₂O₂ variation.

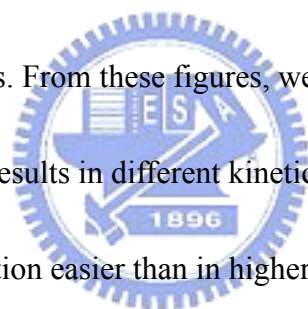
Under uniform reaction condition, we operate the coupled enzyme reactions and detect it with the three different setups, traditional chemiluminescence detector, F4500, integrated commercial photodiode system and the novel CMOS based sensor we

present here. The experiment results are compared to each other and the data of the early stage CMOS chip is also discussed in our report later.

3.4.3 Frequency Adjusted in the Luminescence Reaction

Frequency is one of the instrument parameters experimenters need to set properly before we start our optical reaction. According to data of the above-mentioned experiments, different frequency setting may lead to different detected output voltage and that may lead to distinct data analysis.

The following figures display the experiments under the standard condition with different frequency parameters. From these figures, we know that diverse frequency of 35, 45, 50, 65, and 80 Hz, results in different kinetic curves and in lower frequency the initial rate achieves saturation easier than in higher one. The conclusion can be told from the k_m values of these results with different frequency. In another hand, the V_{max} of the initial rate altered as well while we set different frequency parameters.



The results of experiments with different frequency setting are displayed in Figure 24.

Seeing Figure 40(a.), the chip with different frequency parameters would result in different sensitivities even in the same substrate concentration range. Figure 40(a.) showed the different slopes from different frequency parameters. When frequency parameter was set in 45Hz, the slope (Δ Initial Rate/ Δ mM) of the recognizable range of H_2O_2 is 1.6984. The slopes of 50, 65 and 80 Hz are 1.077, 0.307 and 0.0303. The

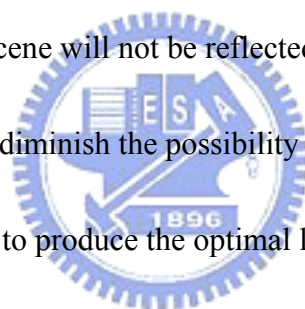
slope decreased when frequency parameter increases. In another hand, seeing table the saturation concentration shows up earlier when the frequency parameter is lower. The comparison of the slope and saturation concentration of different frequency parameters is shown in Table 9. That is, the lower frequency parameter leads to a higher slope and sensitivity and there comes with a lower limit of detection (seeing Table 9) but saturates earlier than the higher frequency parameter. The chip detection ability changes with the variation of frequency parameter. This characteristic helps users to find the optimal condition for specific target detection. For example, when the chip measures a wider light signal variation, the higher frequency parameter is necessary to detect the lighter signal where the output voltage may achieves saturation in lower frequency parameter. Else, if there is a dim light signal interval produced by our interested target variation, a smaller frequency parameter could be chosen for detection with its high sensitivity.

3.4.4 Enzyme amount Adjusted in Luminescence Reaction (HRP : 0.16 unit)

The enzymatic reactions designed for PMT measurement system (by Hitachi F-4500) are to be compared with those obtained with CMOS detection system described later. For this purposes, the parameters of the PMT measurement system as described in experimental section are adjusted so that comparable data can be obtained from both instrumentation in similar reaction conditions.

Comparing the luminescence reaction measured by the CMOS chip with the one by the F-4500 fluorescence detector, seeing figure 25, the K_m value of the former is 0.889 and the latter is 1.8. The difference between them is notable and we need to return back to discuss our condition setting to correct and lessen the error.

By observing the figure of the kinetics graph, the initial rate inclines to approach saturation rate value as the H_2O_2 nears 1 mM. Analyzing this graph, the point where the curve bends to near saturation appears earlier. The phenomenon might occur because the luminescence intensity has already over the CMOS chip voltage output range. The overmuch luminescence will not be reflected through the voltage output and that will lead to the errors. To diminish the possibility of overrun, the adequate amount of enzyme is adjusted to produce the optimal luminescence for detection.



3.4.5 Enzyme amount Adjusted in Luminescence Reaction (HRP :0. 02 unit)

To control the luminescence intensity, the HRP amount is decreased to 0.02 units in figure 26. Under the standard condition as before expects enzyme amount, we experiment the luminescence again and work out the enzyme kinetics graph.

Observing the curve in figure, the point which tends to saturation shows up while H_2O_2 nears 5 mM and the outcome is more similar to the one detected by F4500 luminescence detector. The K_m value resulted from CMOS sensor is 1.4 mM which approaches the K_m value of the first generation CMOS chip study published in 2004

(56).

The variation of H_2O_2 can be identified by the CMOS chip reliably and it indicates that CMOS chip is able to detect luminescence and with a capacity for multi-function biological sensing while the H_2O_2 oxidation equation is coupled with other biological molecules oxidation reactions capable of H_2O_2 production.

3.4.6 Comparison of Luminescence Reaction Detection Limitation

Figure 27 displays the HRP-luminol- H_2O_2 luminescence assay kinetic graph detected with other instruments: F-4500 luminescence spectrometer, integrated commercial photodiode system and the early stage CMOS chip(49). They are all with the similar K_m to show the reliability but with the different sensitivity.

The organization of these devices characteristics is shown in table5. It shows the detection limits of luminescence reaction of four detectors, F-4500 luminescence spectrometer, commercial photodiode, early stage CMOS chip and the novel CMOS chip. The data of their sensing area and sensitivity is listed in table5.

Detecting the chemiluminescence by the traditional luminescence detector (F4500), the calibration curve required and the recognizable range starts from $10 \mu M$ and ends in 10 mM. The minimum detection limitation is $10 \mu M$ so the variation of H_2O_2 between the interval can be detected unerringly. By the integrated semiconductor photodiode, the recognizable range appears between 0.1 mM to 10

mM and the detection limitation approaches $100 \mu\text{M}$ which performs in the same level as the early stage CMOS chip. Comparatively, the new generation CMOS chip has the sensitivity of $50 \mu\text{M}$, and it is double sensitive than the early stage CMOS chip and the commercial photodiode system.

Concerning the amount of the enzyme in luminescence method, the quantity required in tests by novel CMOS chip is 0.02 U/ml . The requirement of HRP amount is much less than the early stage chip (49) and also with the better sensitivity than report published in 2007 (50). The comparison of HRP quantity is listed in Table 6.

The HRP-luminol- H_2O_2 system used as a platform system can be served to quantify enzymatic reactions that produce H_2O . Many biochemical measurements can be done by the HRP-luminol- H_2O_2 system with suitable design of biochemical reactions.

3.4.7 Results of the optimized method for HRP-CHOD coupled enzyme reaction

Comparing these graphs got from two methods, incubation test and real time test, the graph of incubation test outputs the higher initial rate than real time test ($V_{\text{max}} = 884.6 \text{ CL/ sec}$ in incubation test and the one is 104.3 CL/ sec in the real time test.)

The two graphs of tests are displayed in figure 22.

It is thus evident that the result under incubation test presents more sufficient signals for analysis. Because the reaction conditions of both reactions coupled

together is hard to coordinate, the optimization is not easy to carry out. To solve the problem, pretreatment is proceeded to incubate more products for the next reaction going on later.

3.4.8.1 Real time test analysis

Real time test is the most direct way to work our reaction with. The possible variability occurred during incubation can be removed but we need to considerate the rate chemicals emits luminescence with coupled enzyme reaction is not as fast as with single HRP reaction. Thus, we need to adjust ratio of the second reaction enzyme amount to first one. While the initial rate of the second equation is faster than that of the first, the real amount of H_2O_2 can be detected actually right away and that can be reflected. (The enzyme amount of the second equation needs not to be excess, but the reaction rate of the second one need to be verified to be faster.)

3.4.8.2 Incubation test analysis

The principle of the incubation method is based on the transference of products from the first equation that passes to the next reaction actually to complete the coupled enzyme reaction. Thus, the condition during incubation needs to be identical to acquire the products with equal rate each time. The trusty data output under same

condition hence could be compared with each other exactly.

After samples are incubated, further, the enzyme amount is fixed to carry out the coupled enzyme reactions (Incubation test). The reaction curve obtained with incubation test is displayed in figure 23.

Being effected by the low K_m value of the first equation(cholesterol oxidation) (cholesterol oxidation) and substrate inhibition , the K_m value of coupled enzyme reaction nears 1.4 mM and the initial rate tends to maximum while cholesterol concentration nears 0.2 mM. Therefore, the recognizable cholesterol range falls between 0.01 mM and 0.2 mM.

Human desired cholesterol concentration is below 3.85 mM, and that means we can test human blood with few sample then dilute it to the recognizable range for analyze. Contrasting the human desired cholesterol concentration to the detectable range of the chip. (The recognizable range of H_2O_2 concentration falls between 0.1mM to 0.2mM)

It is believed that the cholesterol recognizable range is at least between 0.1 to 0.2mM. The transformation percentage between cholesterol and H_2O_2 does not reach 100 %, thus, if cholesterol transfers into luminescence more efficiently, the detectable cholesterol range could be amplified and larger than 0.2mM with a wider recognizable range. That would be more flexible for users to quantify the sample concentration

with a wider recognizable range (0.1 to 0.2 mM). Furthermore, following the pathway before, the coupled enzyme reactions can be realized with the photodiode system and the CMOS chip system to verify the better condition for cholesterol detection. Hence, the next step is to enlarge the detectable range and widen it to except a more sensitive and realizable interval for cholesterol analysis.

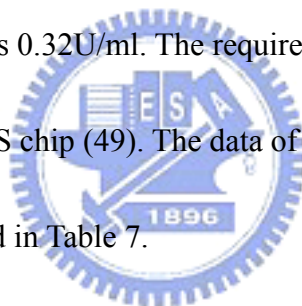
From the experimental results required by F-4500 luminescence spectrometer detection, we know that cholesterol oxidation could be coupled with the HRP-luminol-H₂O₂ system to quantify the amount of cholesterol by luminescence detection. Following the conditions got from the former experiments, the coupled enzyme reaction for cholesterol measurement detected by CMOS chip requires excess enzyme amount, 0.64 U/ml, to produce the detectable light source for CMOS chip detection. The enzyme amount does not fit the bill and is cost consuming. Thus, the HRP-luminol-H₂O₂ system is established but the method of coupled to cholesterol quantification still needs to be improved to fit the practical application. The co-ordination of the two reactions, cholesterol oxidation and HRP-luminol-H₂O₂ reaction, is not easy to be achieved. To test the feasibility of cholesterol diagnosis, we have tried to detect the cholesterol signals with the chromogenic method in addition. The chromogenic assay will be discussed later and it shows that CMOS chip can be integrated with available devices to detect different optical signals, chemiluminescence or absorbance.

3.4.9 Results of the method for HRP-GOD coupled enzyme reaction

To prove the ability for new generation CMOS chip for target detection with luminescence method. We use glucose and GOD to demonstrate that CMOS

photodiode and HRP-luminol-H₂O₂ system can be used as diagnostic kit. Figure 20 (from Ude LU's master thesis) shows the activity of HRP-luminol-H₂O₂ system is dependent on the concentration of glucose. The K_m of glucose is determined to be 3.4 mM ± 0.28 mM with PMT instrument (Hitachi F-4500). The same reactions observed by CMOS photodiodes give similar result as shown in Figure 21. Comparing the results with early stage CMOS chip(49), the sensitivity achieves 0.04mM which is 5 folds higher than the sensitivity of CMOS chip, 0.2mM, published in 2004.

Comparing the HRP enzyme amount used in both devices, the quantity required in tests by novel CMOS chip is 0.32U/ml. The requirement of HRP amount is much less than the early stage CMOS chip (49). The data of the comparisons of enzyme amount and sensitivity is listed in Table 7.



3.5 Chromogenic Method

3.5.1 Optimization of enzymatic assay condition

3.5.1.1 Optimal wavelength for product absorbance

Figure9, the result of wavelength scan from 400 nm to 700 nm, shows that reaction product, quinoneimine, has absorption peak at 495 nm and this wavelength was set to be used in the following experiments.

3.5.1.2 Optimal pH value of phosphate buffer

Figure 28 shows the effect of different and pH value (6.0, 6.5, 7.0, 7.4, 7.5, 8.0,

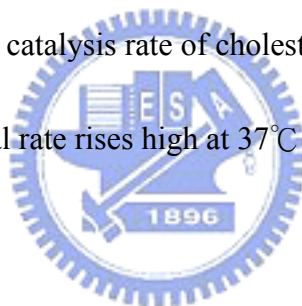
and 8.5) working on assay efficiency. This experiment is under the standard condition that contains HRP 0.16Unit, phenol 14mM, 4-AAP 0.82mM, and PBS 0.2M.

According to the result of this experiment, we realize that initial rate in lower pH value performs better than higher pH value in this closed interval (from 6.0 to 8.0).

Therefore, we choose a pH 6.0 phosphate buffer for coupled enzyme assay.

3.5.1.3 Optimization of temperature

The relationship between different temperatures (from 20°C to 40°C) and their initial rates of cholesterol assay is shown in figure 29 which tells that higher temperature tends to speed the catalysis rate of cholesterol oxidase more efficiency. It is able to discern that the initial rate rises high at 37°C and then returns to the original pattern that ascends gently.



Since there is no temperature controller integrated to our CMOS chip device, we do any experiment on traditional UV/Vis spectrometer in 25°C, which is selected to be the condition temperature that closes room temperature and thus we could compare the experimental results of our CMOS chip device and traditional UV/Vis spectrometer.

3.5.1.4 Optimization of incubation time

From Figure 30 of different incubation time (0 min, 2 min, 3 min, 5 min, and 8 min) observers can see that while it takes longer time for incubation, the initial rate

value goes higher. To short the total reaction time and to find a proper time point to start a better condition simultaneously, we experiment enzyme assay after 3 minute for incubation and compare it with the one with no incubation time (0 min) later.

3.5.1.5 Optimal concentration of reagents

3.5.1.5.1 HRP activity standard curve

The linear range of HRP falling between 0.016~1.2 unit/ml was found in figure 31, thus appropriate amount of HRP is chosen to catalyze phenol/4-aminoantipyrine/H₂O₂ chromogenic system.

3.5.1.5.2 Cholesterol oxidase activity standard curve

The cholesterol oxidase activity standard curve is shown in Figure 32. Studying the graph, we find out the linear range of cholesterol oxidase. The linear range falls between 0.0025~0.25 unit/ml, and then we choose the concentration falling in this interval to catalyze phenol/4-aminoantipyrine/H₂O₂ system. The concentration of CHOD is selected with 0.02 unit per milliliter.

3.5.1.5.3 Optimization of phenol concentration

Enough 4-aminoantipyrine is added in 4-aminoantipyrine/ phenol/H₂O₂ chromogenic system, the phenol concentration differs to ascertain the optimal concentration of phenol. By varying the concentration of phenol, we investigate the

optimal concentration of phenol in phenol/4-aminoantipyrine/H₂O₂ chromogenic system. Observing the kinetic graph, figure33, overmuch amount of phenol will inhibit the activity of HRP and decrease the initial rate of whole assay. The initial rate of absorbance accumulation tends to maximum and turns to decay gradually near 10 mM. Otherwise, to compare the result detected by CMOS chip with the former one by integrated photodiode system, we follow the phenol concentration used before which lies in the rational range of the kinetic graph. For this reason, we pick up 14 mM phenol for the following tests.

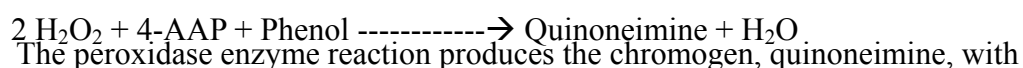
3.5.1.5.4 Optimization of 4-aminoantipyrine concentration

By the same way, we try to find out the adequate concentration for 4-aminoantipyrine. Figure34 displays that the initial rate of 4-aminoantipyrine tends to decrease as 4-AAP concentration increases in our detection range. In lower concentration, the initial rate of whole assay is higher than it in higher 4-AAP concentration. Considering that the stability of reaction and to compare our data with the experiment result from former tests, therefore we choose a concentration of 0.82 mM to be the fixed concentration of 4-aminoantipyrine. The 4-AAP concentration of 0.82 mM falls in the efficient zone of the kinetic graph as well. Besides, the delay in attained color for higher 4-AAP concentrations could be due to competition between phenol and 4-AAP in reaction with the oxidized enzyme (51).

After the amount of reagents is fixed, we couple the phenol/4-aminoantipyrine/H₂O₂ system with cholesterol oxidation reaction to find out the linear range of cholesterol oxidase.

3.5.2 Chromogenic peroxidase enzyme reaction

Peroxidase



the detectable absorbance in 495 nm (concluded in the former experiment). Steps by steps, before we test the coupled enzyme reaction, the single equation responded to chromogen production also needs to be worked under the standard condition we set.

Summing up the total experiments of assay optimization, we select the adequate reagent concentrations, instrument parameters and experimental conditions to be the standard condition. Under the standard condition, the phenol/4-aminoantipyrine/H₂O₂ chromogenic system is established to get the enzyme kinetic graph as standard curve for analysis. All of the curves and K_m value are obtained with Michaelis-Menten equation in enzyme kinetics analysis of Sigma Plot 2001.

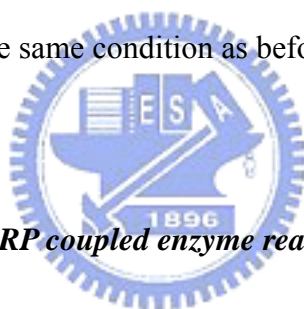
After testing peroxidase catalysis reaction by CMOS chip and UV/Vis spectrometer, the kinetic graphs are compared with each other and result in similar K_m values. They both display a typical enzyme kinetic curve with the variation of H₂O₂. As we see in Figure 35, the K_m value of peroxidase is 1.61×10^{-1} mM detected by the

CMOS sensor chip and the one detected by UV/Vis spectrometer is 1.91×10^{-1} mM.

The data means that the CMOS chip is able to detect chromogenic signal with the variation of H_2O_2 . The similar K_m values of HRP can also be the reference to support CMOS chip as a multifunctional CMOS chip since the ability of chemiluminescence reorganization has already been proved in the former part of the report.

3.5.3 Cholesterol Coupled Enzyme Reaction

After the half part of the coupled enzyme reaction is proved working solidly, the test of the whole coupled enzyme reaction is performed in sequence. Coupled enzyme reaction is performed under the same condition as before with the variation of cholesterol concentration.



3.5.3.1 Cholesterol oxidase-HRP coupled enzyme reaction with 2.5 Volts LED supplied voltage

As cholesterol coupled enzyme reaction works, an external light resource is necessary to be set to offer the incident radiation source for absorption. Since the product shows a peak of absorption at 495 nm (figure9), a blue light emitting device is chosen to be coupled with the CMOS sensor.

A blue LED is assembled to our CMOS system served as light source plus 2.5 volts to drive it. Under this standard condition, we operate the cholesterol coupled enzyme reaction to compare the result with the one detected by traditional UV/Vis

spectrometer.

Figure 36 displays the kinetic curve of CHOD-HRP coupled enzyme reaction. The K_m value of cholesterol oxidase is 3.746×10^{-1} mM detected by CMOS chip, which did not approaches the $K_m = 1.067 \times 10^{-1}$ mM obtained with traditional UV-vis spectrophotometer (UV-3310). To discuss the possible reason which causes the error between these two systems, the supplied voltage of LED is brought into discussion. A supplied voltage of 2.5 Volts added to LED leads to strong light source that may cause the saturation of the CMOS sensor and thus output voltage couldn't respond the difference over the saturation threshold. To verify this point, a suitable supplied voltage is tested to get the optimal experimental parameter. We adjusted the supplied voltage of LED around 2.5 volts and found that the output voltage of CMOS chip keeps saturation till the LED supplied voltage is lower than 2.48 volts. Hence, the threshold of LED supplied voltage adaptable to the CMOS chip output voltage limitation is 2.48 volts and that is the reason why the variation of light intensity between 2.48 volts and 2.5 volts can not be distinguished and this phenomenon may causes errors.

3.5.3.2 Cholesterol Coupled Enzyme Reaction by LED supplied voltage adjusted to 2.48 Volts with incubation = 0 minute and 3 minutes

To demonstrate the points of above, we set the supplied voltage of LED to 2.48 volts and record the output data under the same condition. According to the figures of

the experiments under standard condition, we found that the adjustment of supplied voltage instead of 2.48 volts works out. Enzyme kinetic analysis of figure 37,38 illustrates that the K_m value of cholesterol oxidase with 2.48 volts supplied voltage is approaches the K_m value obtained with traditional UV-vis 3310 spectrophotometer (UV-3310). The outcome proved that the setting of appropriate voltage influence the accuracy of the sensor and that need to be concerned.

Incubation time alters while the experiment goes and we set two different incubation time while we performs our coupled enzyme reaction to find out the relation between incubation time and initial rate.

The two different incubation time conditions before reaction begins are 0 minute and 3 minutes. The figure in the first panel shows the result of the 0 minute incubation time and reveals that the K_m value of cholesterol oxidase is 1.19×10^{-1} mM by this method, which approaches the $K_m = 1.067 \times 10^{-1}$ mM obtained with traditional UV-vis spectrophotometer (UV-3300) (as figure 37 displayed).

After 3 minutes incubation, comparing the result operated under spectrophotometer with the one resulted from CMOS chip detection as figure 38 shows. The comparison exhibits that the K_m value with the longer incubation time did altered ($K_m = 6.7 \times 10^{-1}$ mM obtained by the CMOS chip and $K_m = 6.68 \times 10^{-1}$ mM while detected by the UV-vis spectrophotometer), but these two parallel experiments

both results in similar K_m with reability.

Besides, the V_{max} of the initial rate with 3 minutes incubation time increases obviously from 0.06 delta A/ min to 0.37 delta A/ min detected by CMOS chip. That illustrates that longer experiment incubation time produce more products for the next going equation to cause reaction product, quinoneimine. The accumulation of products during incubation time leads to the appearance of higher initial rate.

3.5.4 Comparison of Chromogenic Reaction Detection Limitation

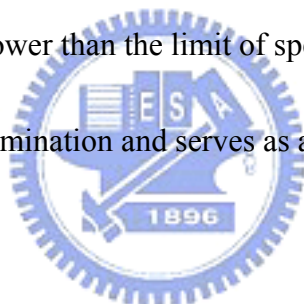
Table 7 shows the detection limitations of chromogenic reaction of three devices used for detectors, UV/ vis 3300 spectrophotometer, commercial photodiode, and the improved CMOS chip. The results are listed in the following table.

There are two tables of sensitivity about chromogenic assay. While table7 (a) displays the detection limit of the H_2O_2 -4-AAP – Phenol HRP reaction, table7 (b) shows the detection limit of the coupled enzyme reaction (cholesterol oxidation coupled with H_2O_2 -4-AAP – Phenol HRP reaction. Reading these tables, we realize that the detection limitations differs under two condition detected by different sensors.

In Table 8(a), the sensitivity of both UV-vis 3300 spectrometer and CMOS chip achieved are in the level of micro molar. Where the spectrometer has a minimum H_2O_2 concentration detected, **2 μ M**; the CMOS chip is also with the minimum concentration in the same level, **5 μ M**. While detecting the absorbance of chromogen,

CMOS chip performs well even if it is compared with the large instrument.

Coupled with cholesterol oxidation for cholesterol examination, the sensitivities of all devices decrease. The efficiency of the conversion from cholesterol to H_2O_2 isn't completed, so H_2O_2 provided to produce chromogen isn't as much as singular reaction operated before. It is approximately 1 order of magnitude lower than the limit reported in the singular reaction. The detection limit of assembled semiconductor device is **0.02 mM** while the cholesterol detection limit of UV-vis spectrophotometer is **0.01 mM**. The performance of novel CMOS chip sensitivity is **0.1mM** and it is almost 1 order of magnitude lower than the limit of spectrophotometer. But it works successfully in cholesterol examination and serves as a useful biosensor to measure the product absorbance.



The sensitivity got from chromogenic assay is relative to luminescence assay. Although the CMOS chip performs less sensitively than the commercial photodiode S2387, the comparison of the sensing areas of devices indicates that the CMOS chip did have better unit sensitivity. If the sensor size is restricted for being easy to carry and use, the CMOS chip will be more suitable for scale diminution.

3.5.5 Results of the method for HRP-GOD coupled enzyme reaction

In the same way, glucose oxidation reaction could also be coupled to HRP-phenol- H_2O_2 reaction for glucose detection. The glucose oxidation condition is

same as luminescence method. The standard condition is detected by UV/vis 3310 and the result is shown in Figure 39 (a.). The K_m of glucose is determined to be 0.05mM with PMT instrument (uv/vis 3310). The same reaction detected by CMOS photodiodes gives similar result as shown in Figure 39 (b.), (c.), and (d.) (Frequency parameters: 45hz, 50 hz, and 60 hz). Otherwise, among these detections under diverse frequency parameters, they both got a similar K_m value as uv/vis 3310 but the graph with 45 Hz frequency setting displays a more similar K_m with the one set in the same frequency parameter used for cholesterol detection (50 Hz). The kinetics of different frequency parameter are displayed in Figure 40(b.).

The result told that the quantification ability of our CMOS chip can be more accurate by modulate the frequency parameter. Like the luminescence test, Figure 40(a.), different frequency parameter resulted in different sensitivity. Notability, unlike luminescence test, lower frequency parameter inversely led into lower sensitivity. There is an opposite point against luminescence test and the difference could be explained by Figure 18. As Figure 18 illustrated, a higher frequency setting offered a higher sensitivity when a stronger light signal is being detected. The slope is steeper than that of a lower frequency parameter. Contrarily, a lower frequency setting gave a better sensitivity to detect dim signal. The results of the sensitivity, K_m value, and saturated concentration of different frequency parameter are displayed in Table 10.

The characteristic is useful for us to quantify the light signals in different intensity level. Thus, the detections of different optical reactions might be more reliable under specific parameter setting.

4. Conclusion

This work reveals that the CMOS-based photodiode chip can be served as an optical biosensor applied to multiple bio-molecule recognition. Integrated with commercial LED device, the application of CMOS chips could be more flexible and broad and it is also tested in distinct optical assays such as luminescence and colorimetric method. The new generation CMOS- based chips are also compared with the traditional large sized instrument, Hitachi UV/vis 3300 spectrometer and Hitachi F4500 luminescence spectrometer, and the commercial photodiode device.

The characteristics of frequency modulation of the CMOS chip helps users to detect diverse medical targets via different optical reactions. Since the different scanning rates of the function wave supplied to the CMOS chip are dominant in different light intensity level and lead into different sensitivity, the specific parameter setting optimized to different assays is helpful to make a multifunctional biosensor more precise and accurate.

The novel CMOS chip has been proved to detect at least two different optical signal: chemiluminescence and absorbance. Else, it has also been tested two kinds of biomedical targets: glucose and cholesterol. The tests of the novel chip confirm the potential to develop the novel CMOS chip into a multifunctional optical CMOS sensor. The less sample volume requirement, low cost, miniature, flexibility and the

disposable plastic cuvette used for CMOS chip are more benefit for a potable biosensor applied not only to clinical diagnosis but also blood composition analysis, environment monitoring and food quality control. (52-57).

In another hand, while the sensitivity of new generation CMOS chip is contrasted with the commercial photodiode device, though the commercial photodiode contributes to higher sensitivity with its large sensing area. Comparatively, via conversion, the sensitivity of unit sensing area of both CMOS chip and commercial photodiode is equal. It exhibits that the light transferring efficiency of integral CMOS chip performs as good as commercial photodiode device. Concerning the enzyme amount used for detection, our CMOS chip even take less enzyme amount than other silicon photodiode such as amorphorous photodiode (50). Besides, the characteristics of CMOS chips such as mass product, low cost, and integration are advantaged in practical application.



Else, the CMOS chip with multiple reaction detection ability will be designed to collect data of array composed of divided cells. These individual cells will set up a multifunctional diagnostic chip sensing different signals simultaneously.

In conclusion, by industrial fabrication, a more useful, sophisticated, powerful, and flexible optical sensor could be manufactured by combining both photodiodes and particular integrated circuits, for next generation biosensor market and study (58).

5. Reference

1. http://www.piribo.com/publications/medical_devices/biosensor_report.html
2. Mehrab Mehrvar, Mustafe ABDI, 2004. Recent developments, characteristics, and potential applications of electrochemical biosensors. *Analytical sciences*. 20, 1113-1127.
3. Hofmann, O., Voirin, G., Niedermann, P., Manz, A., 2002. Three dimensional microfluidic confinement for efficient sample delivery to biosensor surfaces: application to immunoassays on planar optical waveguides. *Anal. Chem.* 74, 5243–5250.
4. Kwakye, S., Baeumner, A., 2003. A microfluidic biosensor based on nucleic acid sequence recognition. *Anal. Bioanal. Chem.* 376, 1062–1068.
5. Askari, M., Alarie, J.P., Moreno-Bondi, M., Vo-Dinh, T., 2001. Application of an antibody biochip for p53 detection and cancer diagnosis. *Biotechnol. Prog.* 17, 543–552.
6. Baeumner, A.J., Cohen, R.N., Miksic, V., Min, J., 2003. RNA biosensor for the rapid detection of viable *Escherichia coli* in drinking water. *Biosens. Bioelectron.* 18, 405–413.
7. Choi, S.H., Gu, M.B., 2002. A portable toxicity biosensor using



- freeze-dried recombinant bioluminescent bacteria. *Biosens. Bioelectron.* 17, 433–440.
8. DeBusschere, B.D., Kovacs, G.T., 2001. Portable cell-based biosensor system using integrated CMOS cell-cartridges. *Biosens. Bioelectron.* 16, 543–556.
9. Armin W. Wieder Franz Nepl, 1992. CMOS Technology Trends and Economics . *IEEE micro.* 12, 10-19.
<http://ieeexplore.ieee.org/search/wrapper.jsp?arnumber=149732>
10. http://www.dalsa.com/markets/ccd_vs_cmos.asp
11. Blum LJ, Gautier SM. Bioluminescence- and chemiluminescence-based fiberoptic sensors. In: Blum LJ, Coulet PR, editors, *Biosensor principles and applications*. New York: Marcel Dekker, 1991:213–247.
12. Golden, J.P., Anderson, G.P., Rabbany, S.Y., Ligler, F.S., 1994. *IEEE Trans. Biomed. Eng.* 41, 585–591.
13. Chen, Z., Kaplan, D.L., Gao, H., Kumar, J., Marx, K.A., Tripathy, S.K., 1996. *Mater. Sci. Eng. C* 4, 155–159.
14. Marquette, C.A., Blum, L.J., 1999. *Anal. Chim. Acta* 381, 1–6.
15. Tsafack, V.C., Marquette, C.A., Pizzolato, F., Blum, L., 2000. *Biosens. Bioelectron.* 15, 125–133.

16. S.M.Sze (1985) *Semiconductor Devices (physics and technology)*, 1st Ed., John Wiley & Sons, New York.
17. Marlene A.Deluca (1978) Preface. In Marlene A.Deluca, editor. *Methods in Enzymology: Bioluminescence and Chemiluminescence*, Academic Press.
18. Larry J.Kricka and Gary H.G.Thorpe (1990) Bioluminescent and Chemiluminescent Detection of Horseradish Peroxidase Labels in Ligand Binder Assay. In Knox Van Dyke and Richard Van Dyke, editors. *Luminescence Immunoassay and Molecular Applications*, CRC press.
19. Larry J.Kricka, Irena Bronstein, and Jhon C.Voyta (2000) Chemiluminescence Methods for Detecting and Quantitating Enzyme Activity. In Mirian M.Ziegler and Thomas O.Baldwin, editors. *Methods in Enzymology: Bioluminescence and Chemiluminescence*, Academic Press.
20. Tan,A., Xiao,C., 1997. An automatic photometric method with high precision by gradually diluting a sample. *Talanta*. 44, 2081-2086.
21. Copeland, R.A., *ENZYMES A Practical Introduction to Structure, Mechanism, and Data Analysis 2nd*, Wiley-Vch, New York, 2000 .
22. He,M.F., *Clinical Biochemistry*, He-Ji, Taipei, 1992.
23. Gaw,A., Murphy,M.J., Cowan,R.A., O'Reilly,D.St.J., Stewart,M.J.,

- Shepherd, J., *Clinical Biochemistry* 3rd, Churchill Livingstone, London, 1995.
24. Nelson, D.L. and Cox, M.M., *Lehninger Principles of Biochemistry* 3rd, Worth, New York, 2000.
25. J. Zicha, J. Kunes, M.A. Devynek, 1999. Abnormalities of membrane function and lipid metabolism in hypertension. *Am. J. Hypertens.* 12, 315–331.
26. R. G. Bowden et al., 2006. A Cholesterol Primer for Health Professionals. *Californian Journal of Health Promotion* 2006, 4, 12-21.
27. Charpentier, L., Murr, I.E., 1995. Amperometric determination of cholesterol in serum with use of a renewable surface peroxidase electrode. *Anal. Chim. Acta* 318, 89–93.
28. Martin, S.P., Lamb, D.J., Lynch, J.M., Reddy, S.M., 2003. Enzyme-based determination of cholesterol using the quartz crystal acoustic wave sensor. *Anal. Chim. Acta* 487, 91–100.
29. Situmorang, M., Alexander, P.W., Hibbert, D.B., 1999. Flow injection potentiometry for enzymatic assay of cholesterol with a tungsten electrode sensor. *Talanta*. 49, 639–649.
30. M.D. Marazuela, B. Cuesta, M.C. Moreno-Bondi, 1997. A. Quejido, Free Cholesterol fiber-optic biosensor for serum samples with simplex optimization. *Biosens. Bioelectron.* 12, 233–240.

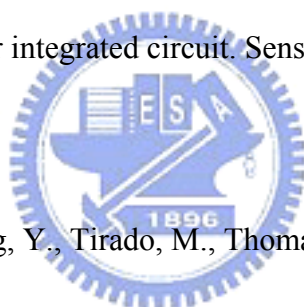
31. G. Li, J.M Lia, G.Q. Hu, N.Z. Ma, P.J. Wu, 2005. Study of carbon nanotubes modified biosensor for monitoring total cholesterol in blood. *Biosens. Bioelectron.* 20, 2140–2144.
32. S. Singh, A. Chaubey, B.D. Malhotra, 2004. Amperometric cholesterol biosenor based on immobilized cholesterol esterase and cholesterol oxidase on conducting polypyrrole film. *Anal. Chim. Acta.* 502, 229–234.
33. X. Tan, M. Li, P. Cai, L. Luo, X. Zou, 2005. An amperometric cholesterol Biosensor based on multiwalled carbon nanotubes and organically modified sol–gel/chitosan hybrid composite film. *Anal. Biochem.* 337, 111–120.
34. J.-C. Vidal, J. Espuelas, E. Garcia_Ruiz, J.-R. Castillo, 2004. Amperometric cholesterol biosensors based on the electropolymerization of pyrrole and the electrocatalytic effect of Prussian-blue layers helps with self-assembled monolayers. *Talanta.* 64, 655–664.
35. S. Brahim, D. Nariresingh, A. Guiseppi_Elie, 2001. Amperometric determination of cholesterol in serum using a biosensor of cholesterol oxidase contained within a polypyrrole–hydrogel membrane. *Anal. Chim. Acta.* 448, 27–36.
36. V. Shumyantseva, G. Deluca, T. Bulko, S. Carrara, C. Nicolini, S.A. Usanov, A. Archakov, 2004. Cholesterol amperometric biosensor based on cytochrome P450sc. *Biosens. Bioelectron.* 19, 971–976.

37. D. Reichl, T. M. Forte, t J-L. Hong, D. N. Rudra, J. Pflug, 1985. Human lymphedema fluid lipoproteins: particle size, cholesterol and apolipoprotein distributions, and electron microscopic structure. *Journal of Lipid Research*. 26, 1399-1411.
38. Allain, C.C., Poon, L.S., Chan, C.G.S., Richmond, W., 1974. Enzymatic Determination of Total Serum Cholesterol. *Chin. Chem.* 20, 470-475.
39. Loredano Pollegioni, Gaby Wels, Mirella S. Pilone¹, 1999. Kinetic mechanisms of cholesterol oxidase from *Streptomyces hygroscopicus* and *Brevibacterium sterolicum*. *Eur. J. Biochem*. 264, 140-151.
40. Vasudevan, P.T., Zhou, T., 1996. Enzymatic assay of cholesterol by reaction rate measurements. *Biotechnol. Bioeng.* 53, 391-396.
41. Richmond, W., 1973. Preparation and properties of a cholesterol oxidase from *Nocardia* sp. and its application to the enzymatic assay of total cholesterol in serum. *Clin. Chem.* 19, 1350-1356.
42. Nishiya, Y., Harada, N., Teshima, S.I., 1997. Improvement of thermal stability of *Streptomyces* cholesterol oxidase by random mutagenesis and a structural interpretation. *Protein Eng.* 10, 231-235.
43. Witte, D.L., Barrett II, D.A., Wycoff, D.A., 1974. Evaluation of an Enzymatic Procedure for Determination of Serum Cholesterol with the Abbott ABA-100.

- Clin. Chem.. 20, 1282-1286.
44. Kovac,J., Peternai,L., Lengyel,O., 2003. Advanced light emitting diodes structures for optoelectronic applications. Thin Solid Films. 433, 22-26.
45. Yam,F.K., Hassan,Z., 2005. Innovative advances in LED technology. Microelectronics. 36, 129-137.
46. Wang,K.F., The physical foundation of semiconductor elements, Ru-Lin , Taipei, 1996.
47. Renker,D., 2004. Photosensors. Nucl. Instrum. Methods Phys. Res. A. 527, 15-20.
48. Yuh-Shyong Yang, Yuan-Yao Chang, 2004. Biochemical Sensing with Photodiode, Proceedings of the 2004 .IEEE Taipei, Taiwan. 21-23, International Conference on Networking, Senring Control.
49. Yu-Chuan Shih, Chung-Yu Wu, Yuh-Shyong Yang, 2004. The design of a novel complementary metal oxide semiconductor detection system for biochemical luminescence. Biosens. Bioelectron. 19,1185-1191.
50. Alexandra C. Pimentel, A.T. Pereira, 2007. Detection of Chemiluminescence Using an Amorphous Silicon Photodiode, IEEE Sensors Journal. 7, NO3.3.
51. Vojinović,V., Azevedo,A.M., Martins,V.C.B., Cabral,J.M.S., Gibson,T.D., Fonseca,L.P., 2004. Assay of H₂O₂ by HRP catalysed co-oxidation of phenol-4-sulphonic acid and 4-aminoantipyrine: characterization and optimization.

Journal of Molecular Catalysis B: Enzymatics. 28, 129-135.

52. Wei-Jen Hoa, Jung-Sheng Chen^b, Ming-Dou Ker ^b, Tung-Kung Wu, Chung-Yu Wu, Yuh-Shyong Yang, Yaw-Kuen Li, Chiun-Jye Yuan. 2007. Fabrication of a miniature CMOS-based optical biosensor. *Biosens. Bioelectron.*
53. DeBusschere, B.D., Kovacs, G.T., 2001. Portable cell-based biosensor system using integrated CMOS cell-cartridges. *Biosens. Bioelectron.* 16, 543–556.
54. Simpson, M.L., Sayler, G.S., Patterson, G., Nivens, D.E., 2001. An integrated CMOS microluminometer for low-level luminescence sensing in the bioluminescent bioreporter integrated circuit. *Sens. Actuators B: Chem.* 72, 134–140.
55. Yang, J.M., Bell, J., Huang, Y., Tirado, M., Thomas, D., 2002. An integrated, stacked microlaboratory for biological agent detection with DNA and immunoassays. *Biosens. Bioelectron.* 17, 605–618.
56. Huang, S.H., Shih, Y.C., Wu, C.Y., 2004. Detection of serum uric acid using the optical polymeric enzyme biochip system. *Biosens. Bioelectron.* 19, 1627–1633.
57. Golden, J.P., Ligler, F.S., 2002. A comparison of imaging methods for use in an array biosensor. *Biosens. Bioelectron.* 17, 719–725.
58. Millar, N., 1993. *Med. Device Technol.* 4, 16–21.



6. Tables

Table 1: Biomedical Detection Target.

| Target | Couple enzyme | Reaction |
|---------------------------|-------------------------------|---|
| Glucose | Glucose oxidase | $\text{Glucose} + \text{O}_2 + 2\text{H}_2\text{O} \xrightarrow{\text{Glucose Oxidase}} \text{Gluconic acid} + 2\text{H}_2\text{O}_2$ |
| Uric acid | Uricase | $\text{Uric acid} + \text{O}_2 + 2\text{H}_2\text{O} \xrightarrow{\text{Uricase}} \text{allantoin} + \text{CO}_2 + 2\text{H}_2\text{O}_2$ |
| Cholesterol | Cholesterol oxidase | $\text{Cholesterol} + \text{O}_2 \xrightarrow{\text{Cholesterol oxidase}} \text{cholesten-3-one} + \text{H}_2\text{O}_2$ |
| Lactate | Lactate oxidase | $\text{L-Lactate} + \text{O}_2 \xrightarrow{\text{Lactate oxidase}} \text{pyruvate} + \text{H}_2\text{O}_2$ |
| Phospholipids | Phospholipase/Choline oxidase | $\text{Phospholipids} + \text{H}_2\text{O} \xrightarrow{\text{Phospholipase}} \text{Fatty acids} + \text{Choline}$ |
| | | $\text{Choline} + \text{H}_2\text{O} + 2\text{O}_2 \xrightarrow{\text{Choline oxidase}} \text{betaine} + 2\text{H}_2\text{O}_2$ |
| Triglycerides / Lipase | Lipase/Glycerol oxidase | $\text{Triglycerides} + 3\text{H}_2\text{O} \xrightarrow{\text{Lipase}} \text{Fatty acids} + \text{glycerol}$ |
| | | $\text{Glycerol} + \text{O}_2 \xrightarrow{\text{Glycerol oxidase}} \text{glyceraldehyde} + \text{H}_2\text{O}_2$ |

Reference : Blum,L.J.(1997) Bio- and Chemi- Luminescent Sensors.



Table 2: Cholesterol Desirable Level in Human Body.

Adult Values:

Cholesterol:

Desirable: <200 mg/dL
Borderline: 200-240 mg/dL
Higher Risk: >**240 mg/dL**

- **HDL-Cholesterol:**

Desirable: < 40 mg/dL (if no CHD)
Higher Risk: < **40 mg/dL**

- **Triglycerides:**

Desirable: <150 mg/dL
Borderline: 150-199 mg/dL
Higher Risk: **200-499 mg/dL**

- **LDL-Cholesterol**

(measured):

Desirable if patient has CHD:
<100 mg/dL
Desirable: <130 mg/dL

- **VLDL-Cholesterol**

(calculated):

Desirable: < 30 mg/dL

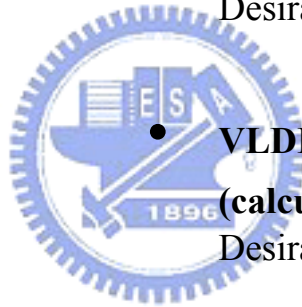


Table 3: The Comparison of the Two Generation Chips.

| First Generation CMOS | Improved CMOS Chip |
|--|--|
| <p>A 0.25 μm CMOS standard process</p> <ul style="list-style-type: none"> • 18 \times 150 photodiode array with pixel size 10 μm \times 10 μm for each photodiode. • 0.18mm \times 1.5mm • Current mirror to amplify the current measured • Resistance necessary | <p>A 0.35 μm CMOS standard process</p> <ul style="list-style-type: none"> • Enlarge Sensing Area 128 \times 128 photodiode array with pixel size 10 μm \times 10 μm for each photodiode. • (1.28mm \times 1.28mm) • (increase 6 X area) • Frequency can be adjusted • Transimpedance amplifier • Reaction volume decreases (1ml \rightarrow 500ml) |

Table 4: The optimized reaction conditions of HRP and CHOD.

| | HRP | CHOD |
|------------------------------------|---|--|
| Buffer | Used : Tris –HCl (0.1M) Phosphate buffer (0.1M) | Phosphate buffer (0.05M or 0.1M) pH = 7.0 |
| pH | Enzyme max activity : 6.0-6.5 Optimal for luminal : 8.0 Used : pH = 8.6 | Range : pH = 5-9 Optimal : CHOL+CHOD : pH= 6.5 CHO-CE (EC1.1.3.6) : pH = 7 CHO-PE (EC.1.1.3) : pH= 6.5-7.5 Used : pH = 8.6 |
| Temp | Range : 15-40 °C Optimal: 37 °C Used : 20 °C (EC.1.11.1.7 ; sigma) | Optimal : CHO-CE (EC1.1.36) : 50 °C CHO-PE (EC.1.1.3) : 45 °C Used: 25 °C (EC1.1.3.6 ; sigma) |
| Substrate (Cholesterol) | Human normal level cholesterol : 150mg/dl = 1.5mg/ml (3.88mM) dangerous level: > 250mg/dl (6.4mM) | |

Table 5: Luminescence Assay: The comparison of sensitivity, Km value, detection limits, sensing area of four instruments: Luminescence spectrometer, commercial photodiode, novel CMOS chip and early stage CMOS chip.

| Device | F4500 Fluorescence | Commercial photodiode S2387 1010R | Early Stage CMOS Chip | Novel CMOS Chip |
|-----------------|-------------------------------|--|----------------------------------|----------------------------|
| Km value | 1.8 mM | 1.7mM | 1.5mM | 1.4mM |

| Device | F4500 Fluorescence | Commercial photodiode S2387 1010R | Early Stage CMOS Chip | Novel CMOS Chip |
|-------------------------|-------------------------------|--|----------------------------------|----------------------------|
| Sensing Area | | 10mm × 10mm | 0.18mm × 1.5mm | 1.28mm × 1.28mm |
| LOD | 0.001mM | 0.01mM | 0.1mM | 0.05mM |

Table 6: The comparison of the enzyme amount required during measurement by different devices.

| Device | Commercial photodiode S2387 1010R | Amorphous Silicon Photodiode | Early Stage CMOS Chip | Novel CMOS Chip |
|----------------------|--|-------------------------------------|------------------------------|------------------------|
| Enzyme Amount | 0.16U/ml | 0.03U/ml | 0.32U/ml | 0.02U/ml |



Table 7: For GOD- HRP coupled enzyme reaction: the comparison of the enzyme amount required during measurement and the sensitivity by different devices.

| Device | Early Stage | Novel |
|----------------------|--------------------|------------------|
| | CMOS Chip | CMOS Chip |
| LOD | 0.2 mM | 0.04 mM |
| Km value | 3.5 mM | 3.2 mM |
| Enzyme Amount | 0.64 U/ml | 0.32 U/ml |



Table 8: Chromogenic Assay: The comparison of sensitivity, detection limits, sensing area of three instruments: UV-vis 3300 spectrometer, commercial photodiode, and novel CMOS chip. Under two conditions: (a.) H₂O₂ -4-AAP – Phenol HRP reaction (b.) CHOD-HRP coupled enzyme reaction.

| Device | UV- vis 3310 | Novel CMOS Chip |
|-----------------|----------------------------------|----------------------------------|
| Km value | 1.61 × 10⁻¹ mM | 1.91 × 10⁻¹ mM |
| LOD | 0.002mM | 0.005mM |

(a.) H₂O₂ -4-AAP – Phenol HRP reaction

| Device | UV- vis 3310 | Commercial photodiode S2387 1010R | Novel CMOS Chip |
|---------------------|---------------------|--|----------------------------|
| Sensing Area | | 10mm × 10mm | 1.28mm × 1.28mm |
| LOD | 0.01mM | 0.02mM | 0.1mM |

(b.) CHOD-HRP coupled enzyme reaction

Table 9: The comparison of sensitivity, saturation concentration and limit of detection of different frequency parameters with luminescence assay

| Frequency | 45Hz | 50Hz | 65Hz | 80Hz |
|--|--------|--------|-------|--------|
| Slope(Δ Initial Rate/ Δ mM) | 1.6984 | 1.1077 | 0.307 | 0.0303 |
| Saturation concentration(mM) | 1 | 1.5 | 2 | 6 |
| LOD | 0.05 | 0.05 | 0.1 | 0.6 |

Table 10: The comparison of sensitivity, saturation concentration and Km value of different frequency parameters with chromogenic assay



| Novel CMOS Chip | | | UV/vis 3310 | |
|---|----------------------------|-----------------------------|-----------------------------|-----------------------------|
| Frequency | 45Hz | 50Hz | 60Hz | |
| Km value | 6.1×10^{-2} mM | 9.78×10^{-2} mM | 8.13×10^{-1} mM | 5.36×10^{-2} mM |
| Slope(Δ Initial Rate/ Δ mM) | 0.0142 | 0.0143 | 0.0153 | 0.0266 |
| Saturation concentration(mM) | 0.2 | | | |

7. Pictures

Figure 1: The concept of a biological sensor

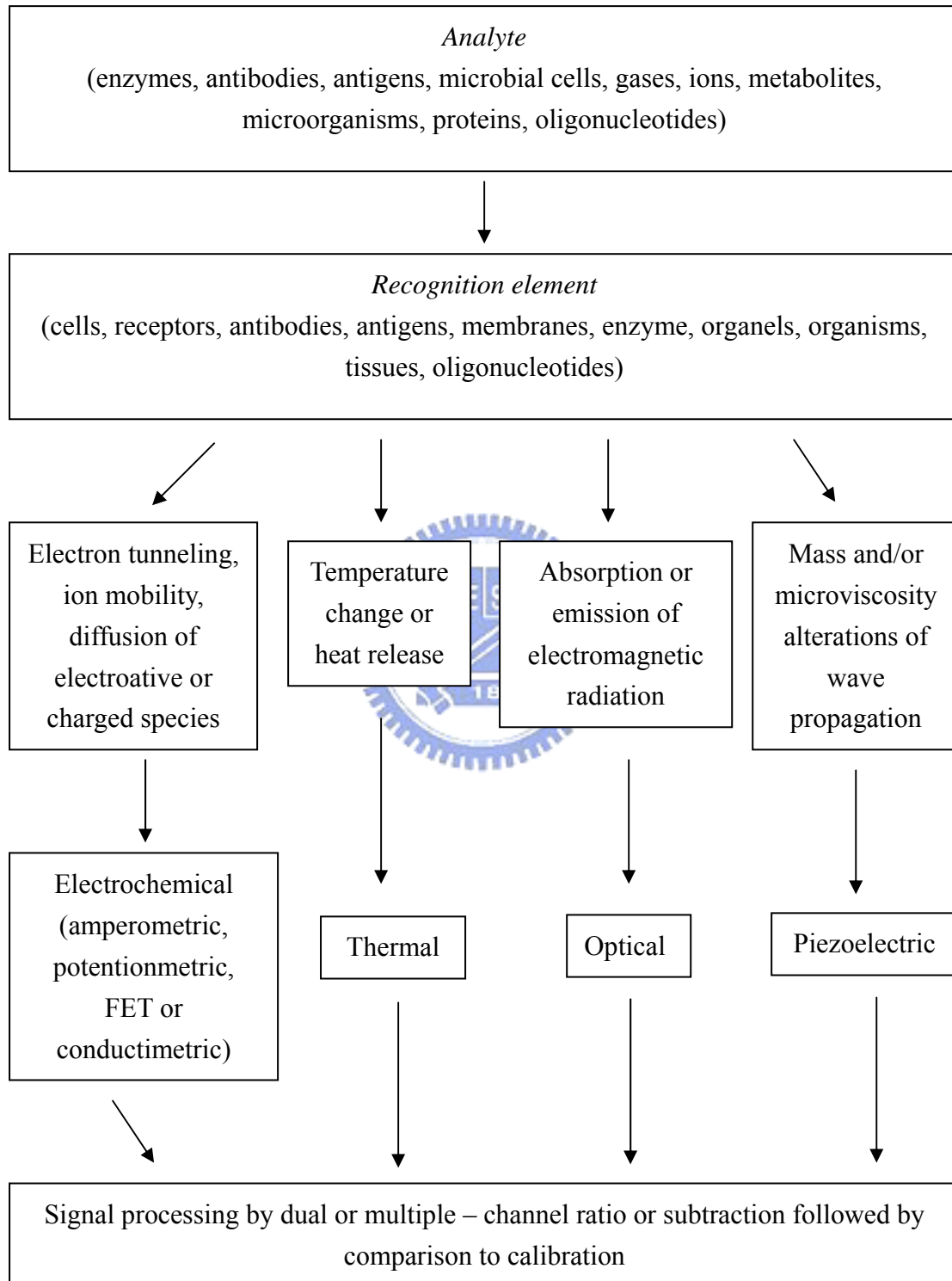


Figure 2: Optical absorption for (a) $h\nu = E_g$, (b) $h\nu > E_g$, (c) $h\nu < E_g$.

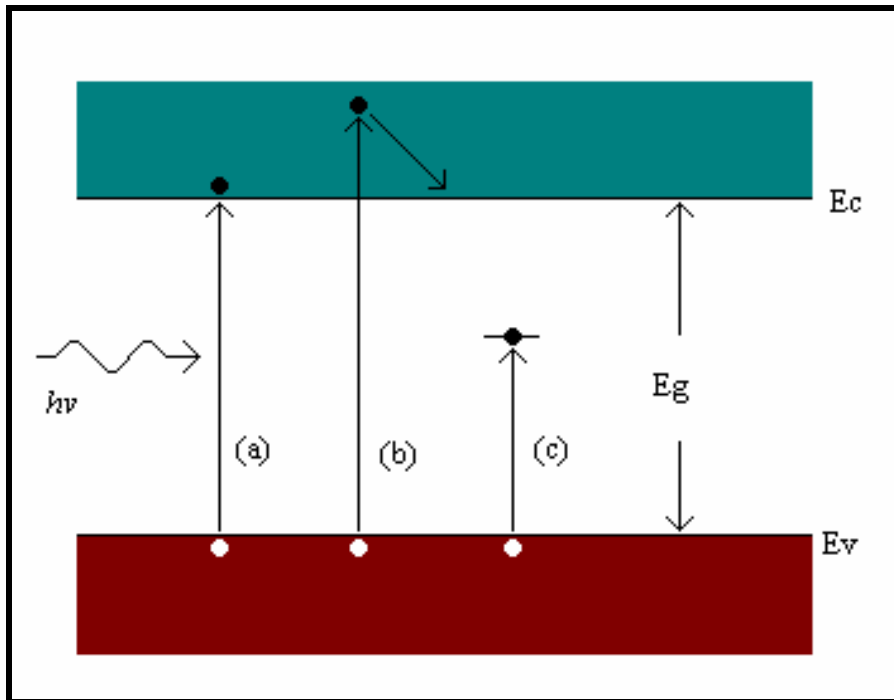


Figure 3: Absorption coefficient α versus wavelength (Sze, 1985)

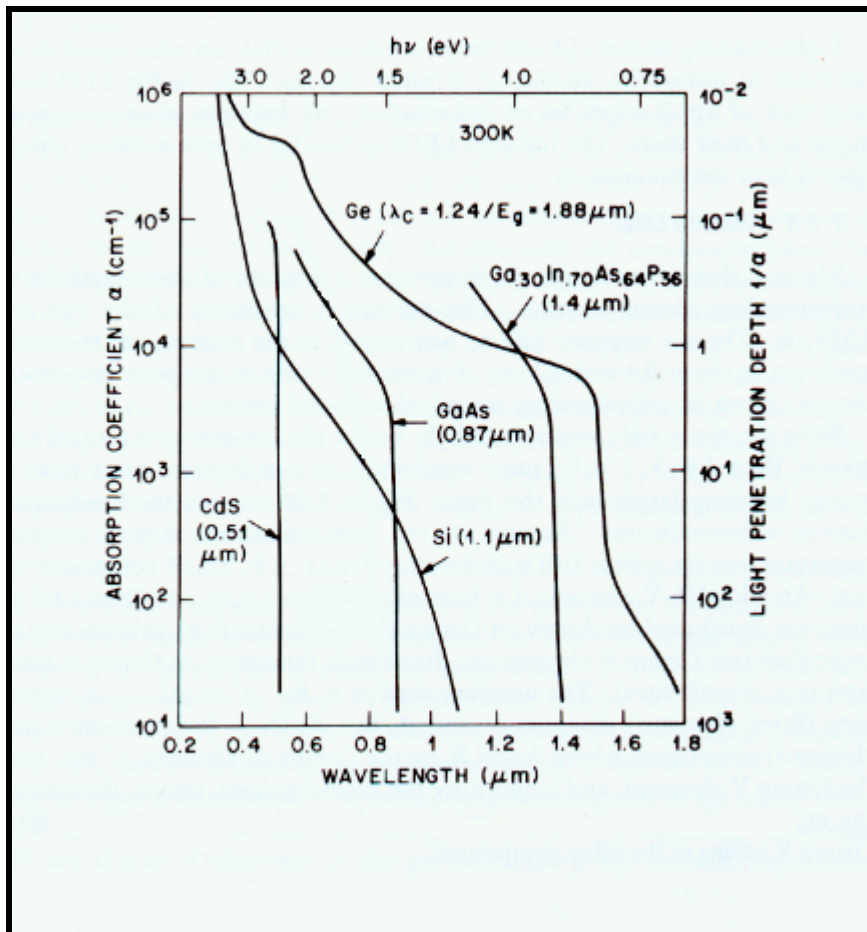


Figure 4: N+/P well photodiodes side structure view.

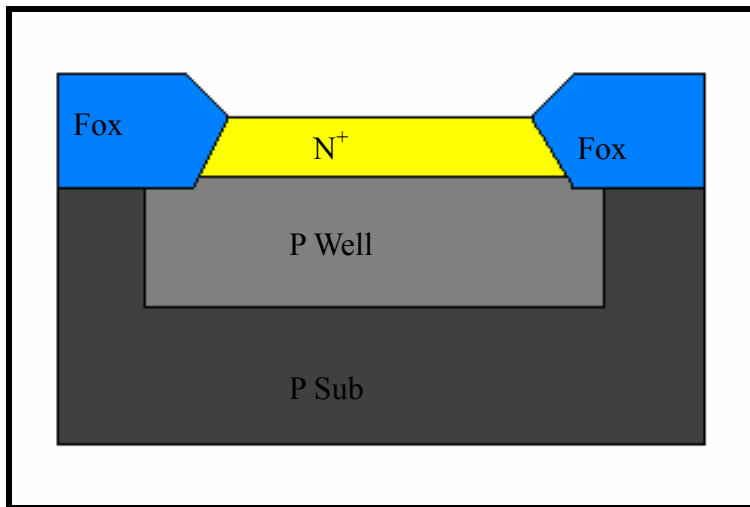


Figure 5: cholesterol conformation.

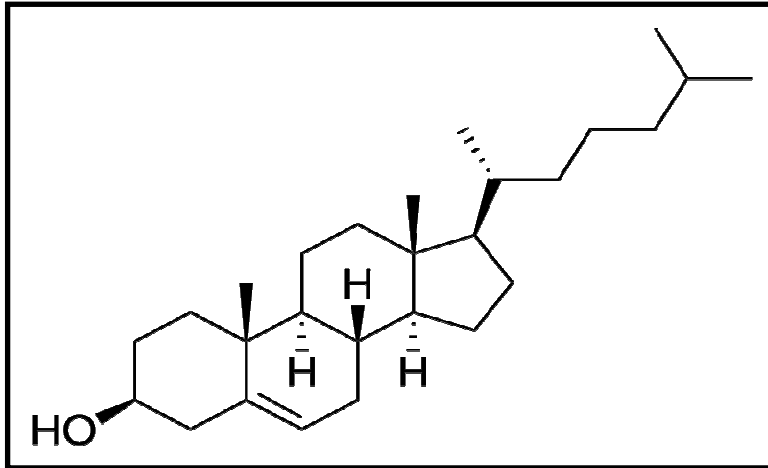


Figure 6: Roadmap of the experiment scheme.

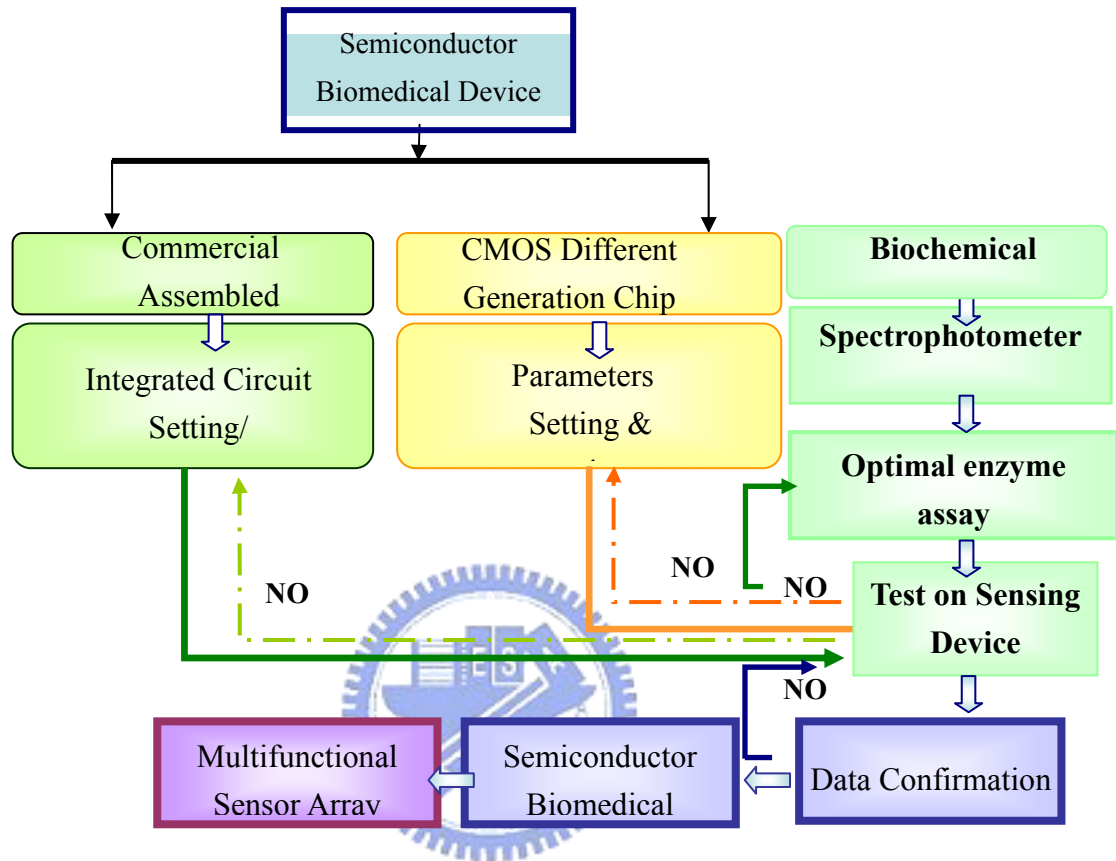


Figure 7: The component instruments connection diagram of assembled semiconductor element setup included of instruments: power supply, multimeter, GPIB card, CMOS chip, and Pulse Generator.

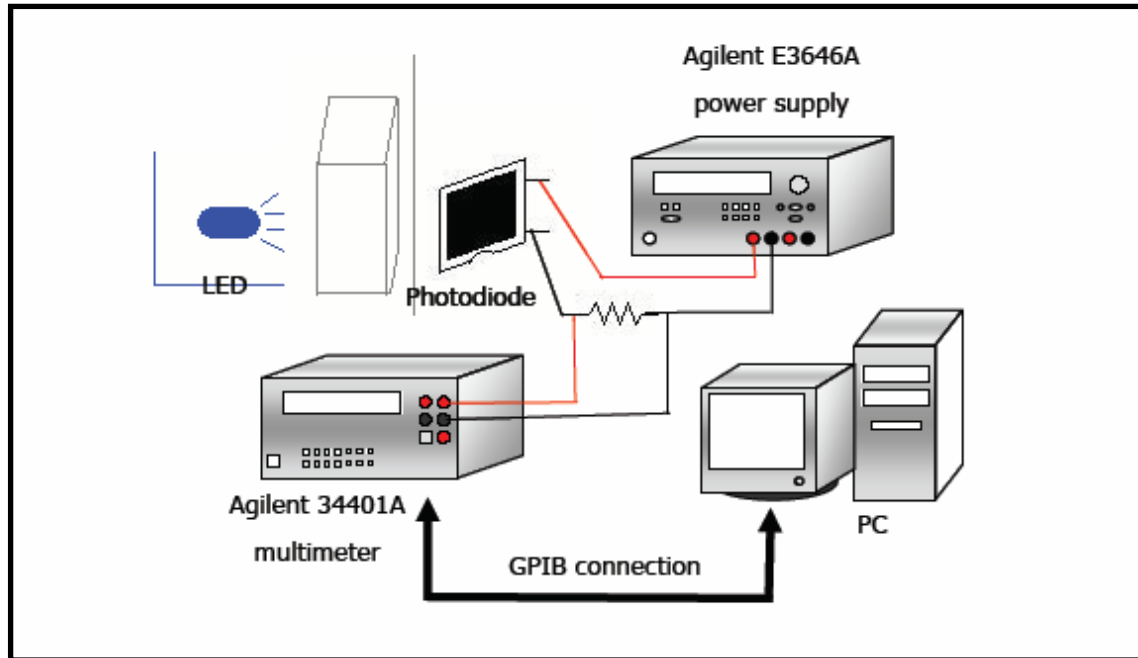
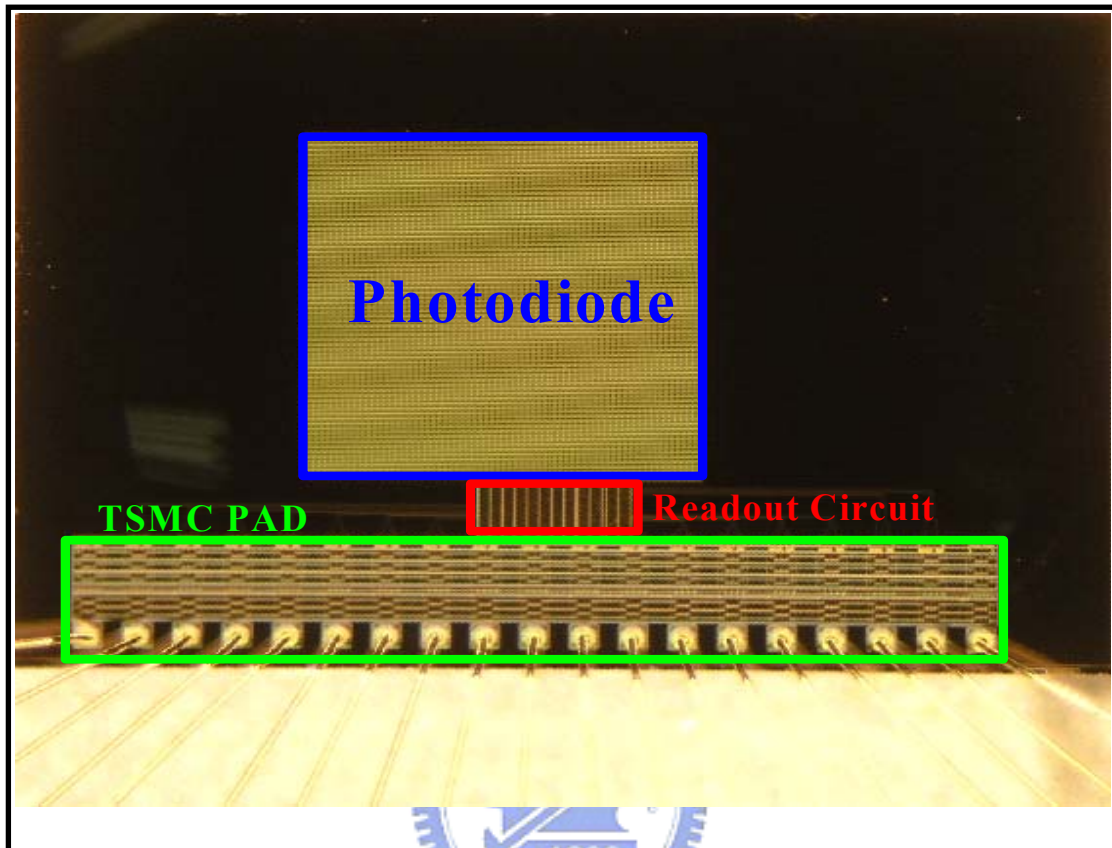


Figure 8: Die Photograph (a.) and the circuit design (b.)

(a.)



(b.)

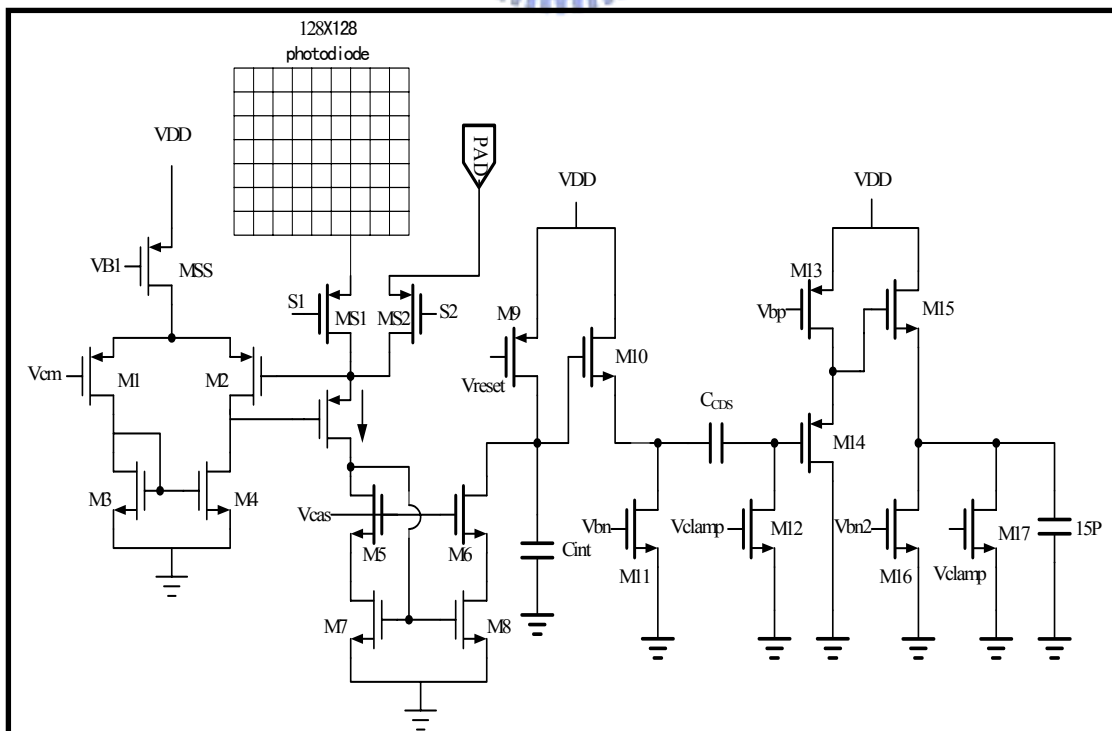


Figure 9: The optimization of the absorbance wavelength.

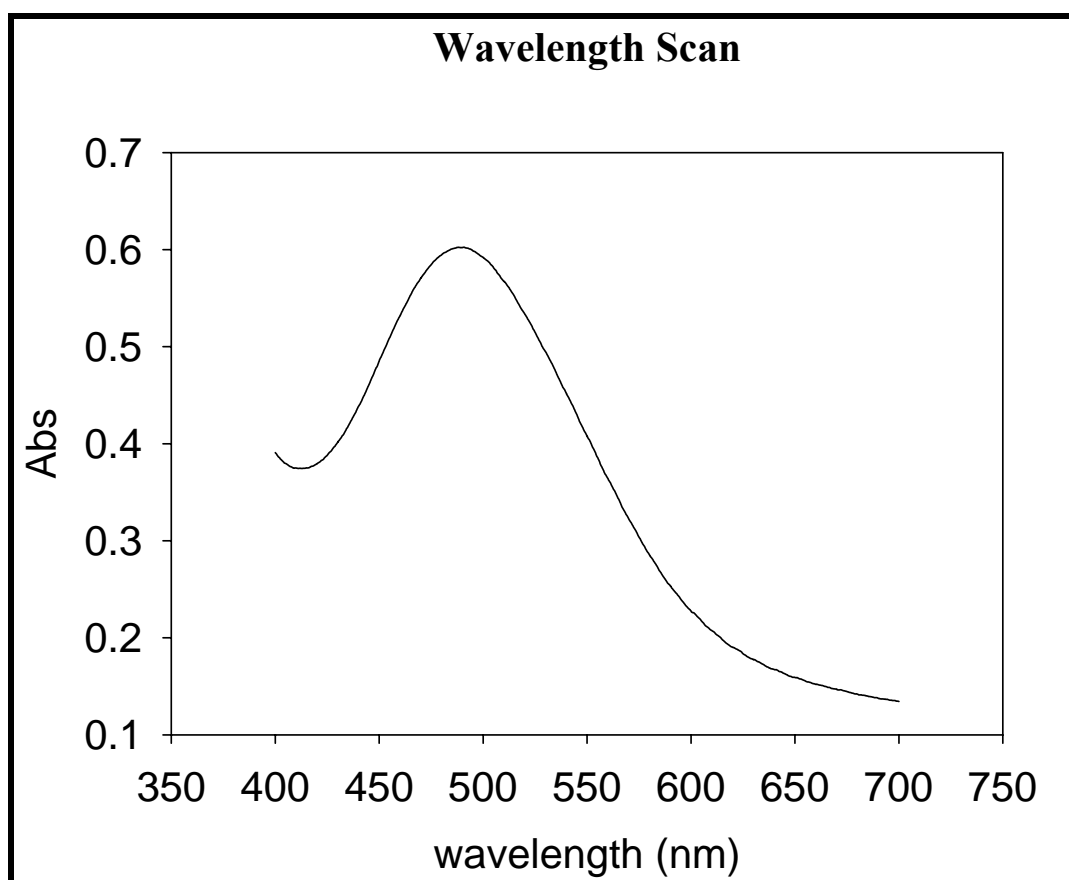


Figure10: Experimental Procedure.

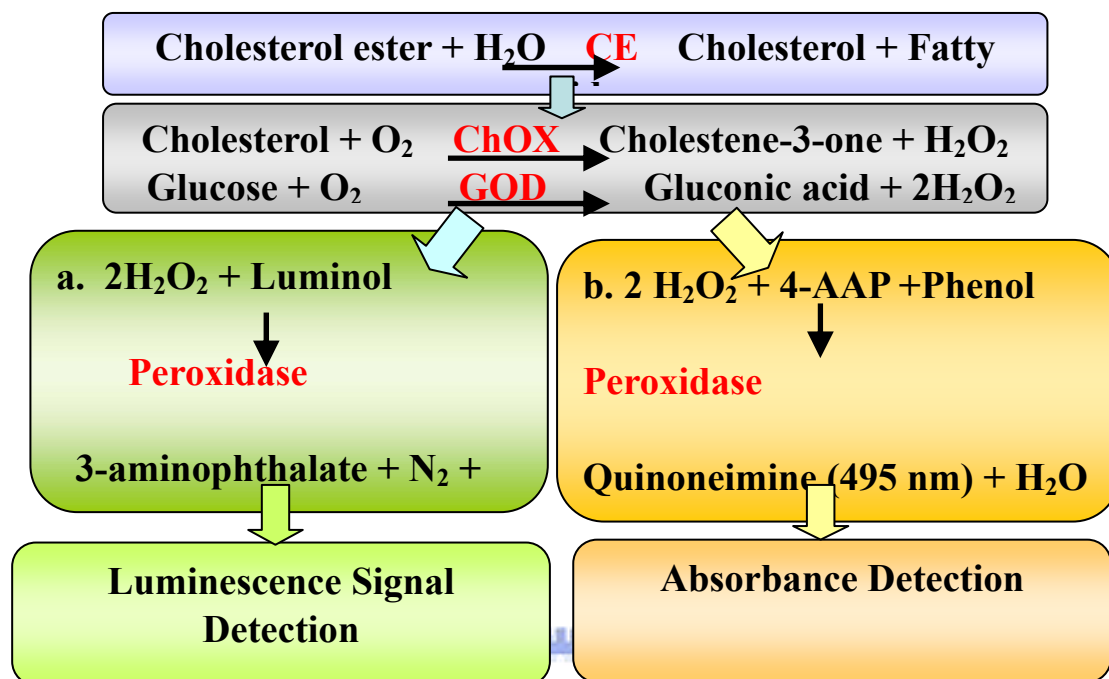


Figure 11: Environmental setup of output voltage (V_{out}) versus illuminated intensity measurement.

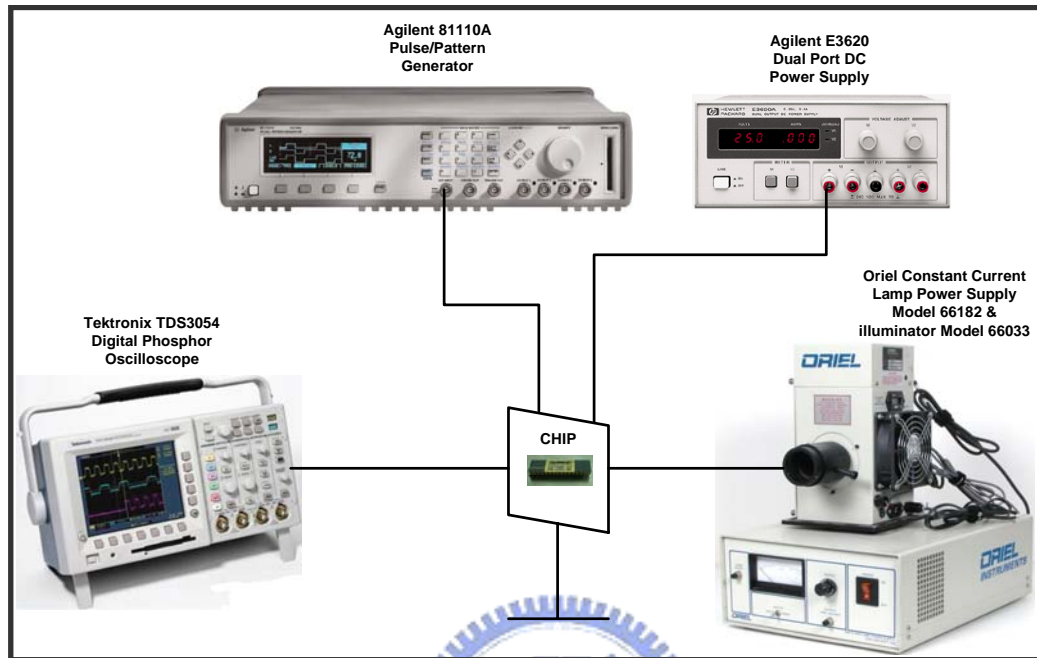


Figure 12: Frequency vs. Output Voltage Variation (Saturation/Blank ; Light/ Dark).

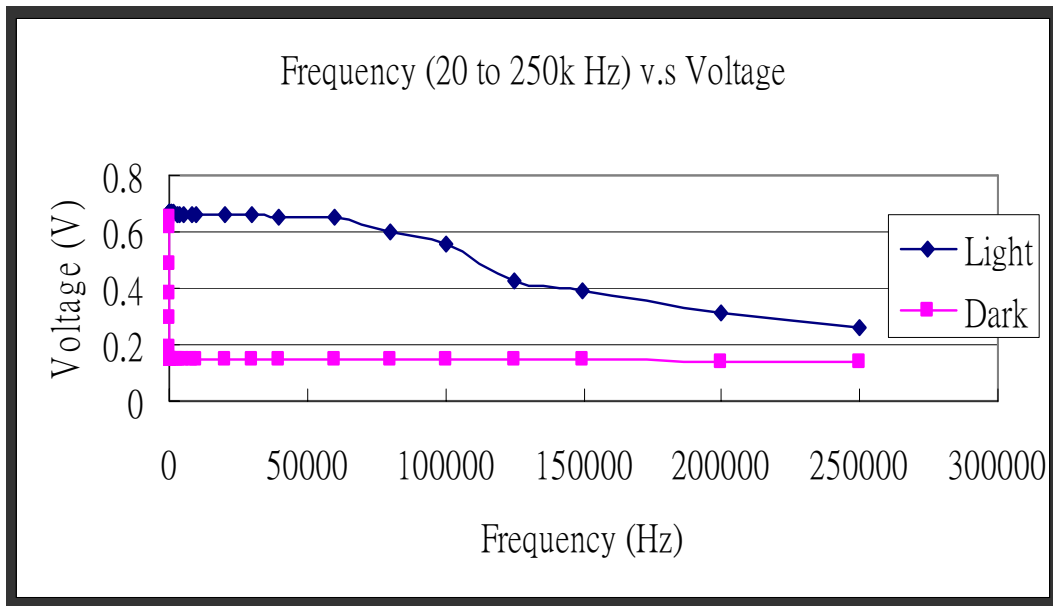
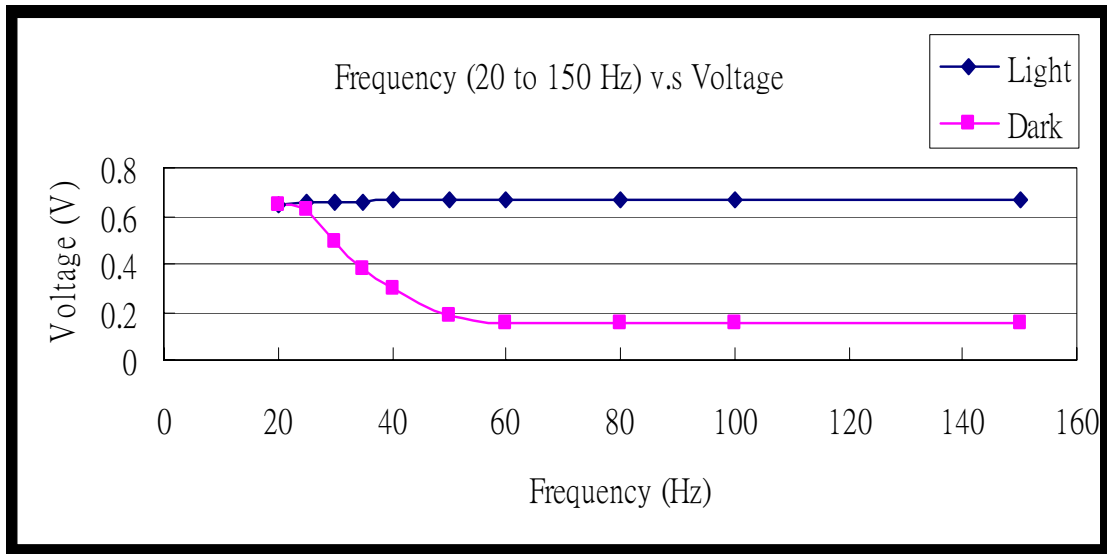


Figure 13: (a.) Frequency vs. Output Voltage Variation (20 to 150 Hz).



(b.) Frequency vs. Output Voltage Variation (40k to 250k Hz)

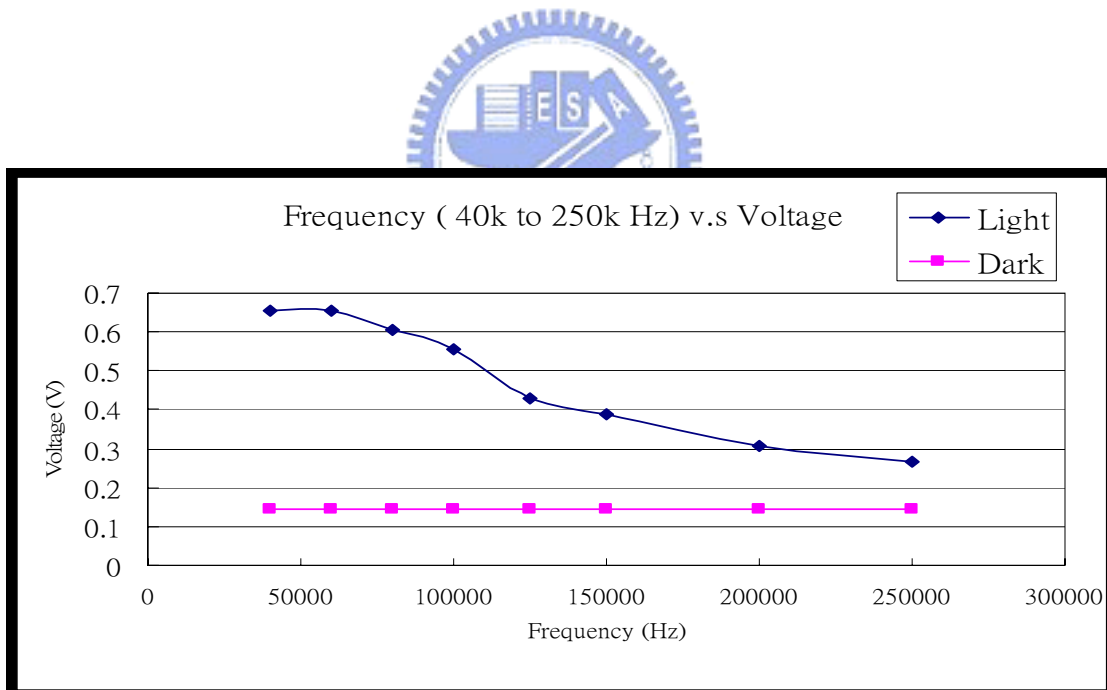


Figure 14: Measured output voltage (V_{out}) with clock frequency = 125 KHz.

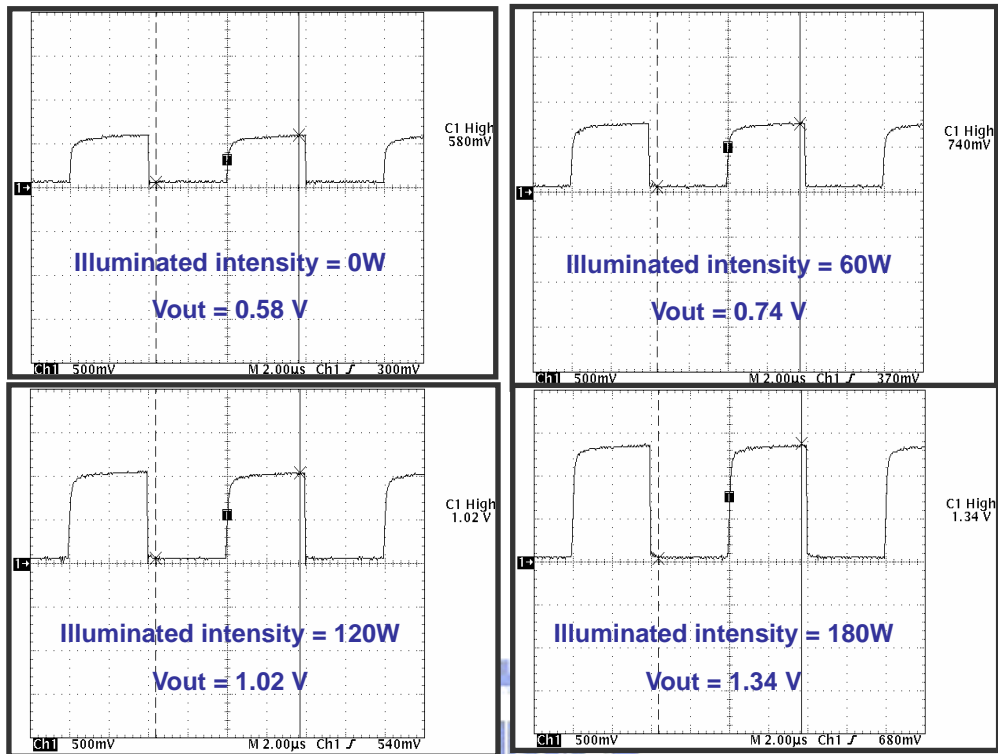


Figure 15: Measured output voltage (V_{out}) versus illuminated intensity under 125kHz.

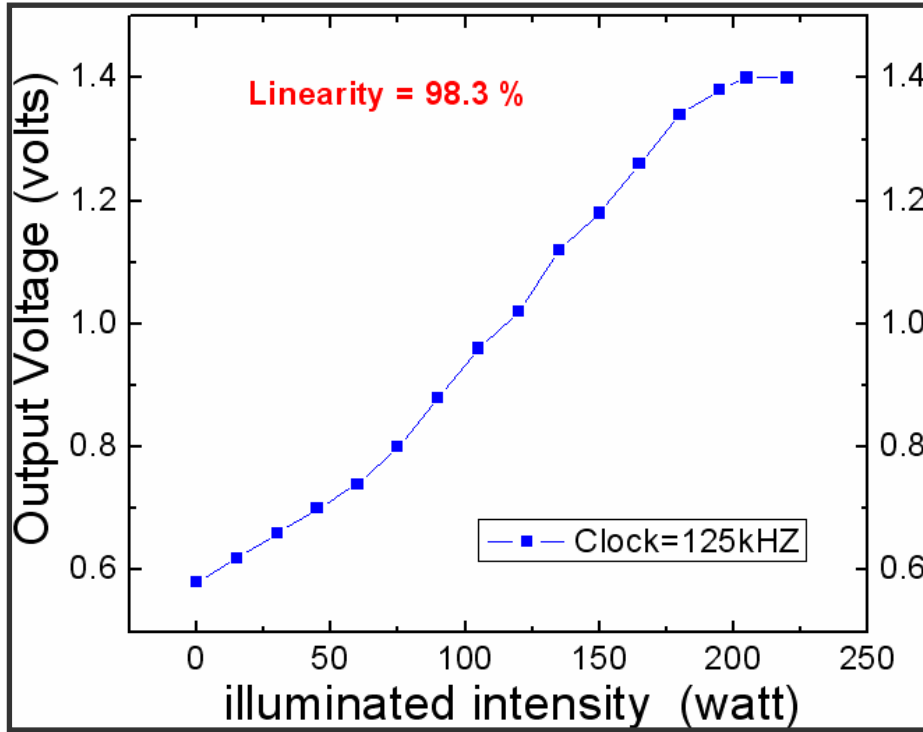


Figure 16: Measured output voltage (V_{out}) with clock frequency = 10 KHz.

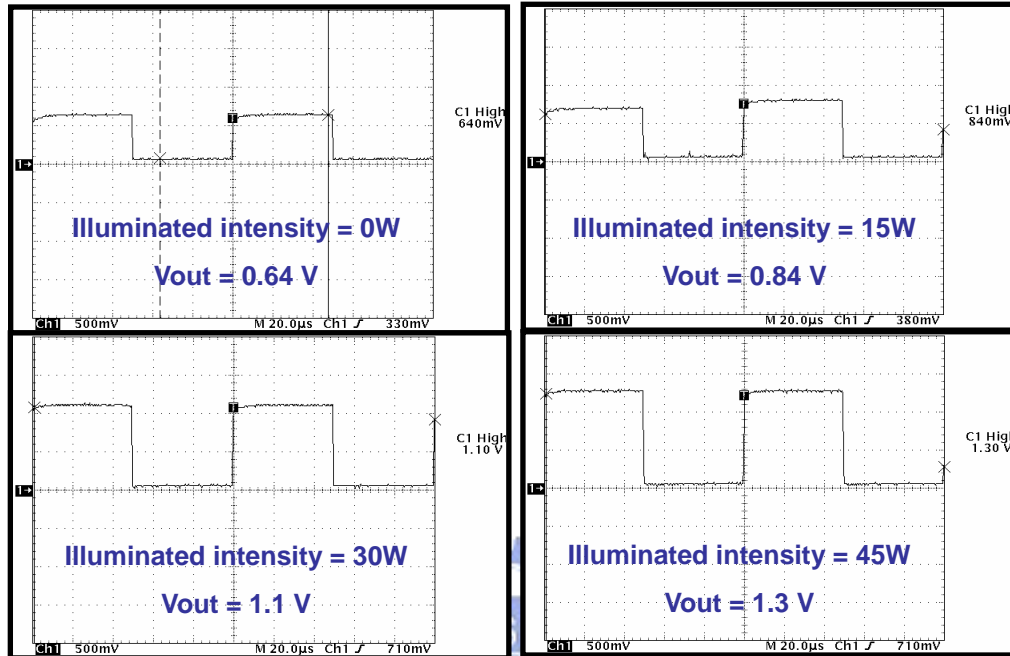


Figure 17: Measured output voltage (Vout) versus illuminated intensity under 10kHz.

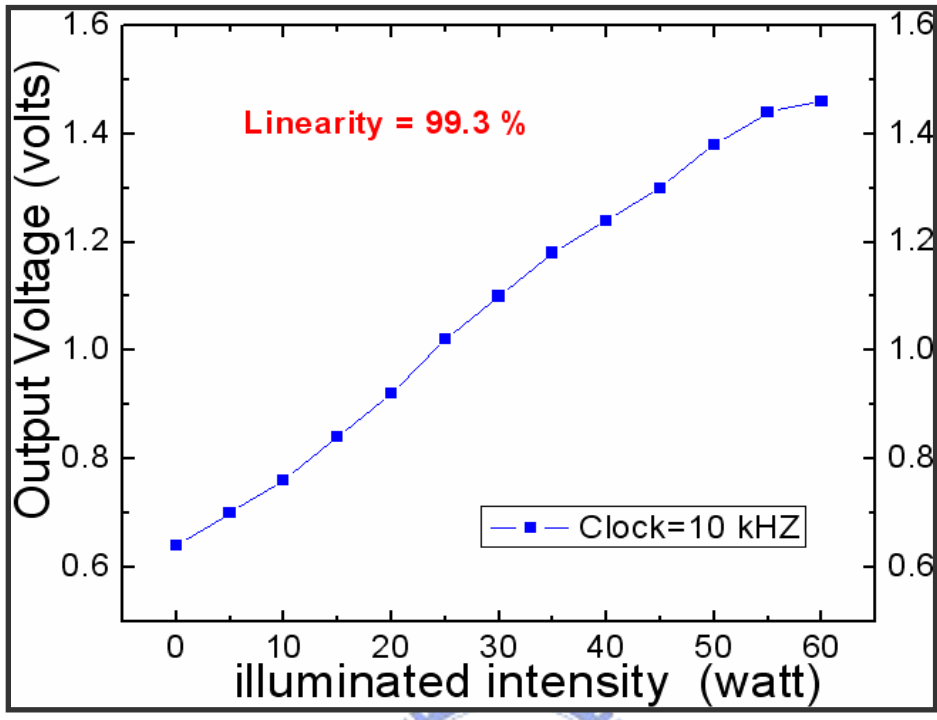


Figure18: Different Frequency versus LED supplied voltage (a.) and illuminated intensity (b.) variation.

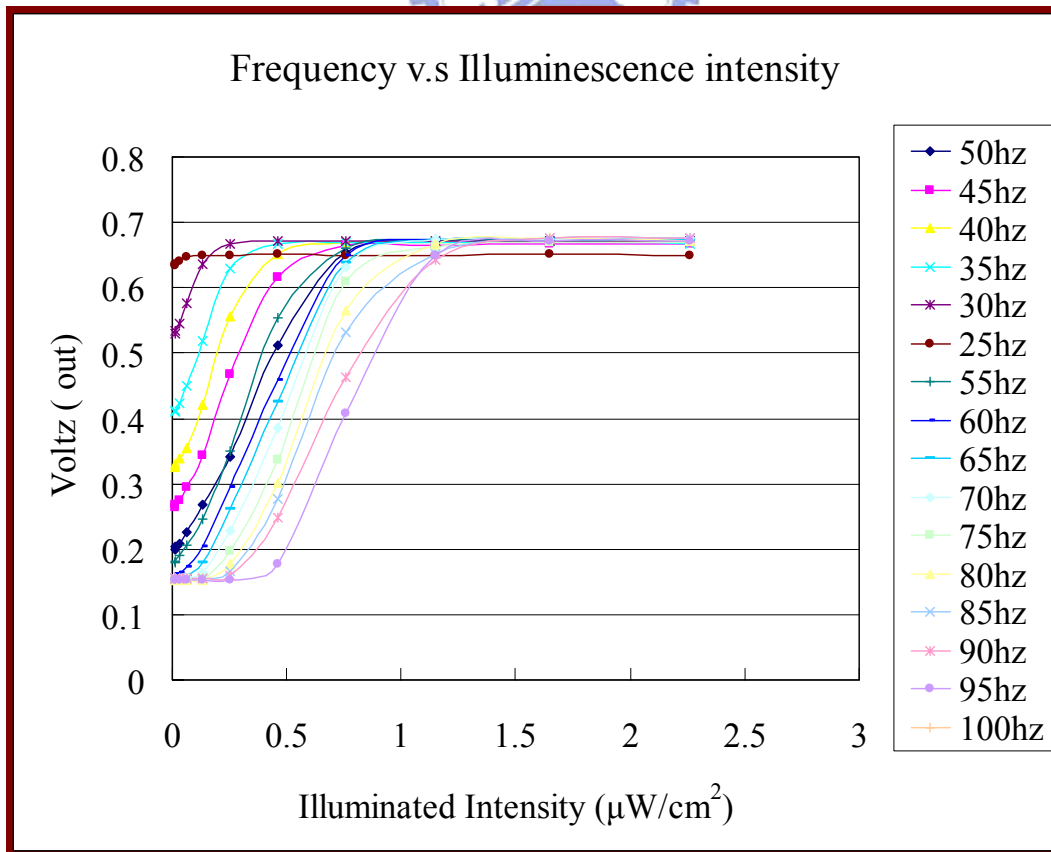
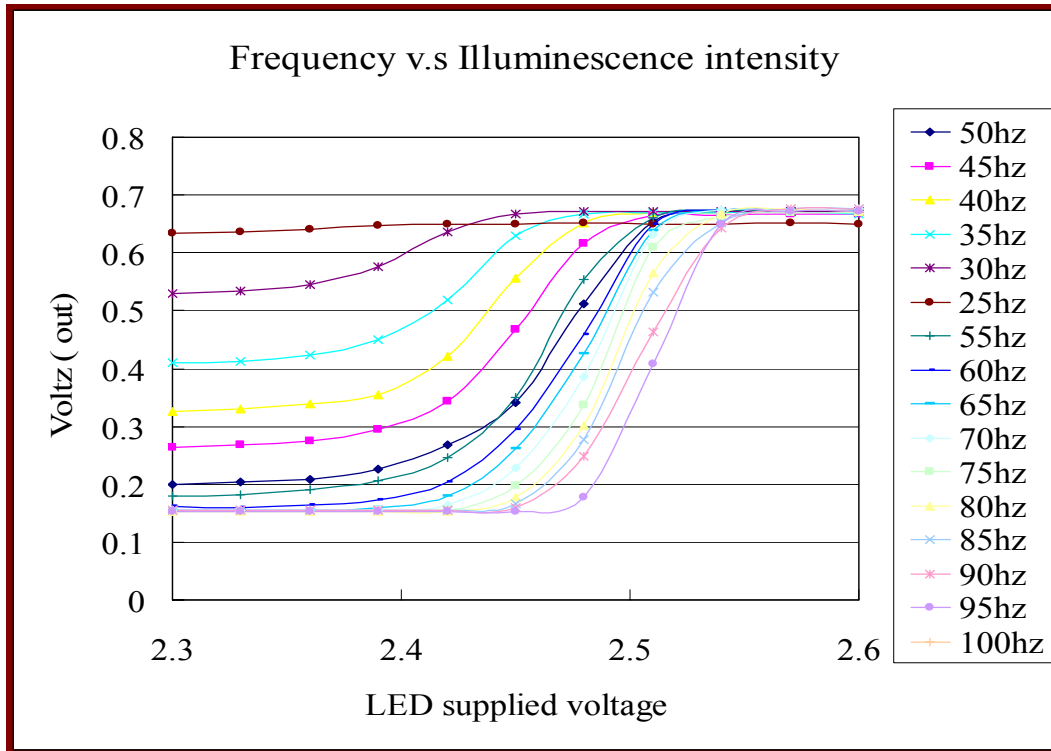


Figure19: The variation of luminal concentration in HRP-luminol- H₂O₂ system is determined by F-4500 fluorescence meter. The reaction condition is described in Experimental for standard condition for HRP-luminol- H₂O₂ system except that 0.2 unit of HRP and 0~25mM luminol is used.

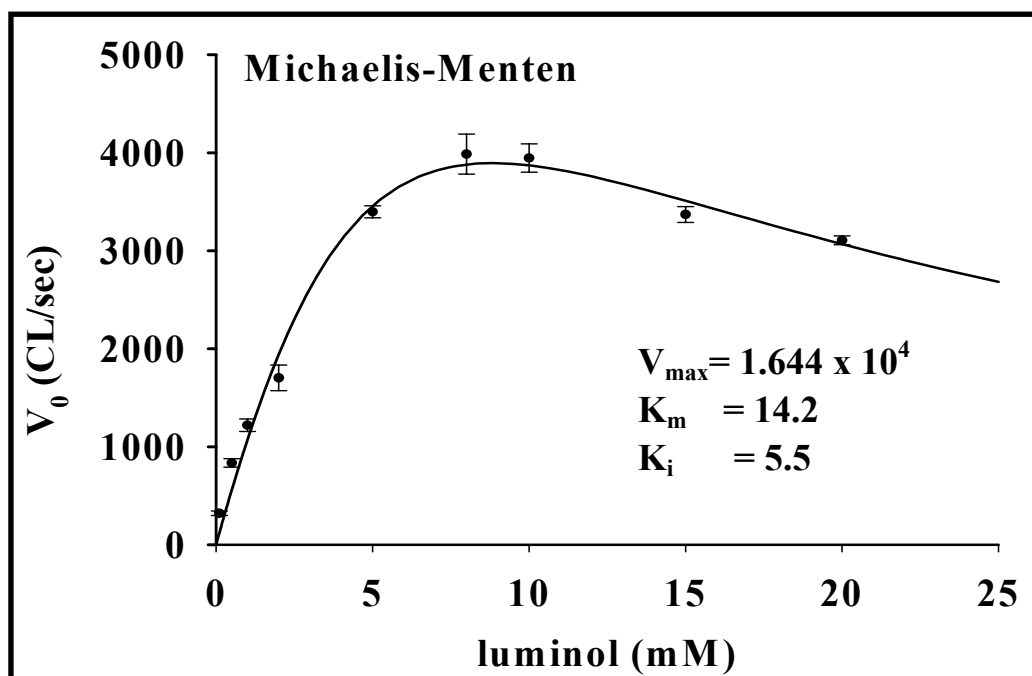


Figure20: Variation of glucose concentration in a GOD coupled HRP-luminol-H₂O₂ system determined by F-4500 fluorescence meter. The coupled reaction mixture is described in Experimental section. The glucose concentrations used are from 0.2mM to 50mM. (Reference: Ude Lu's master thsesis)

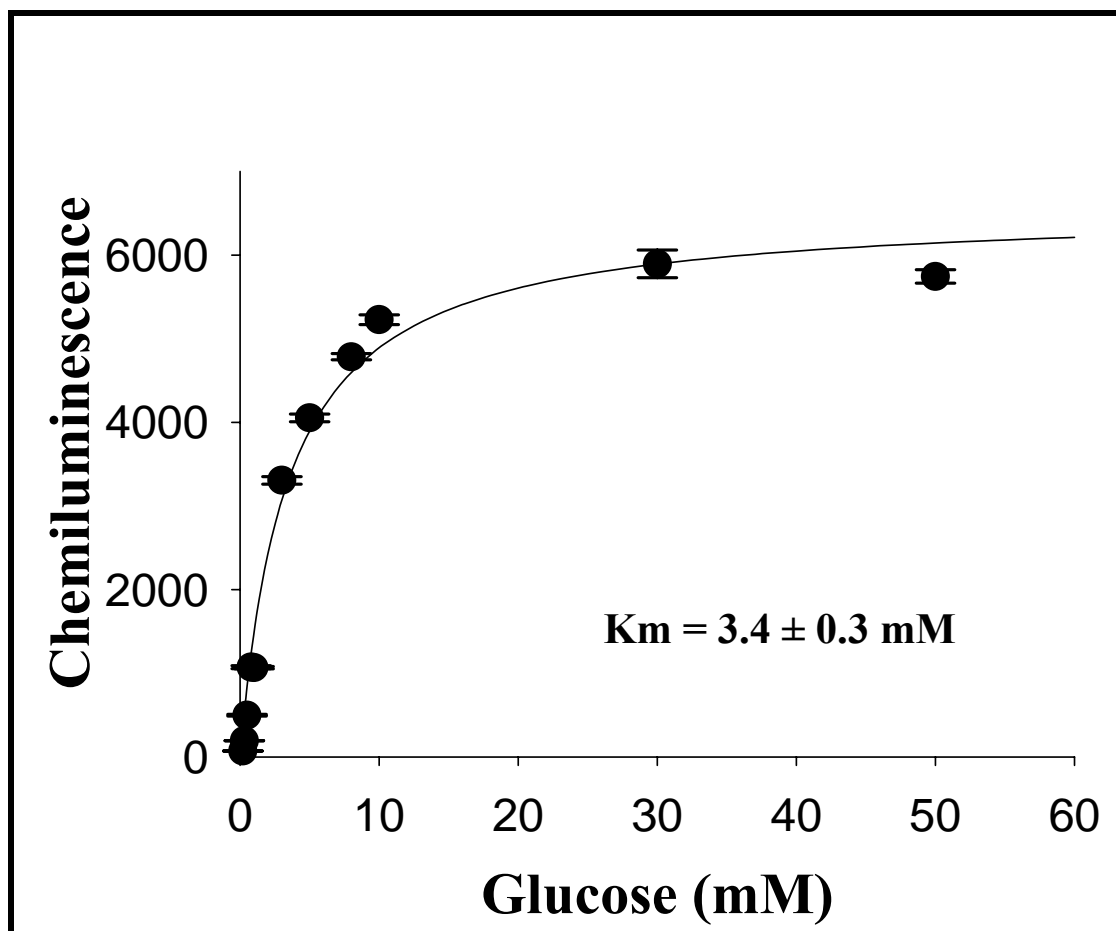


Figure 21: Variation of glucose concentration in a GOD coupled HRP-luminol-H₂O₂ system determined by our CMOS chip. The coupled reaction mixture is same as described in figure 19. The glucose concentrations used are from 0.04 mM to 60mM. (Reference: Ude Lu's master thsesis)

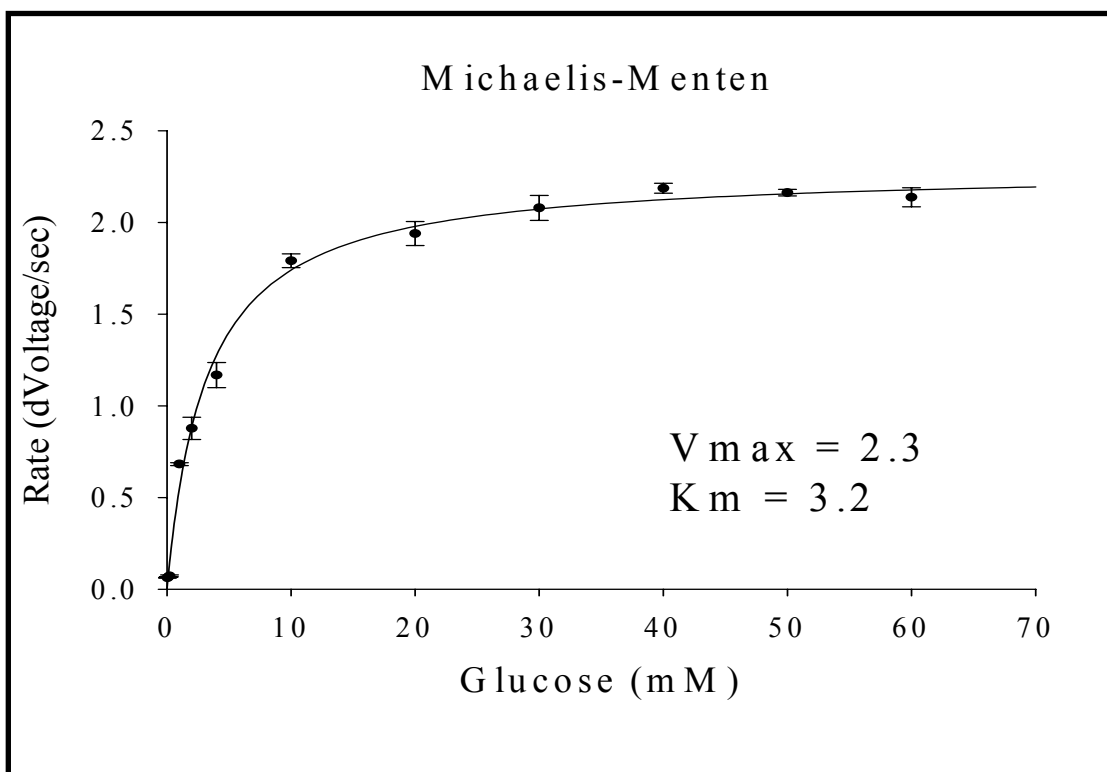


Figure 22: Michaelis-Menten kinetics graphs got from incubation test (left) and real time test (right).

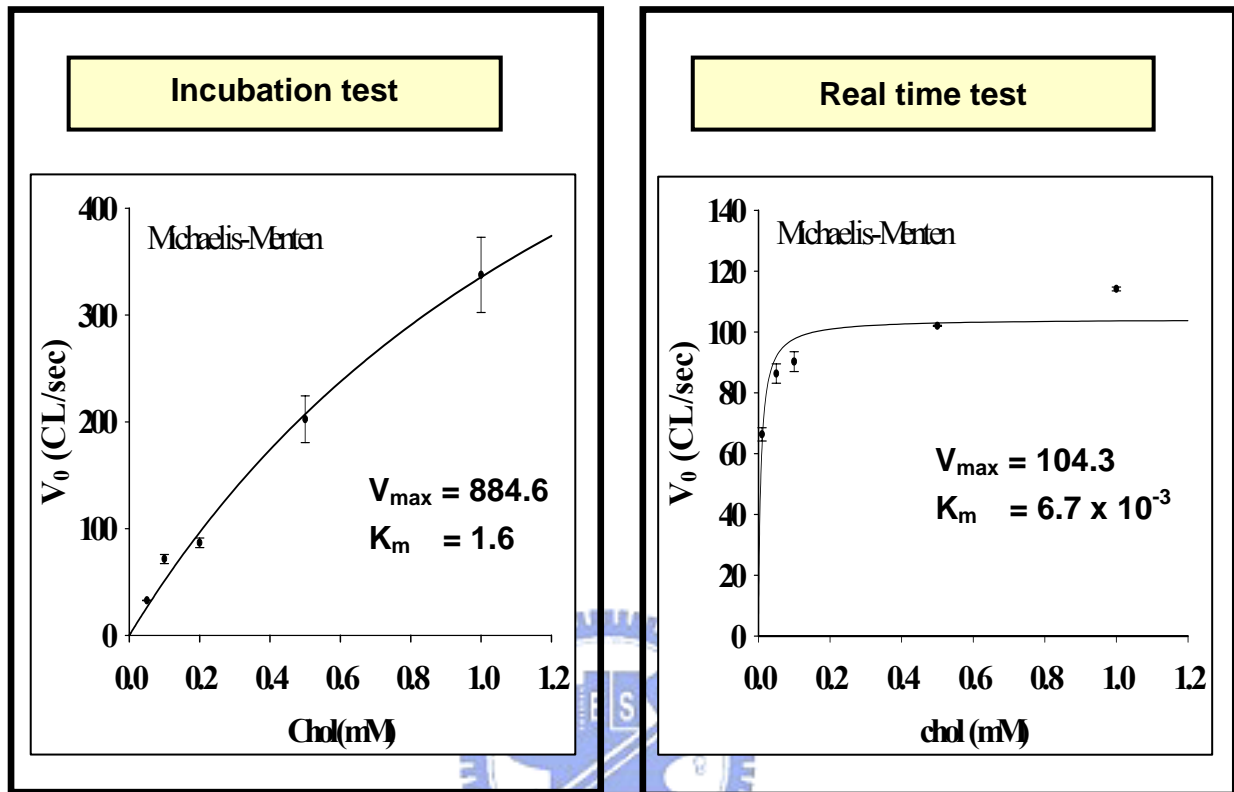


Figure 23: The Michaelis-Menten graph obtained with incubation test.

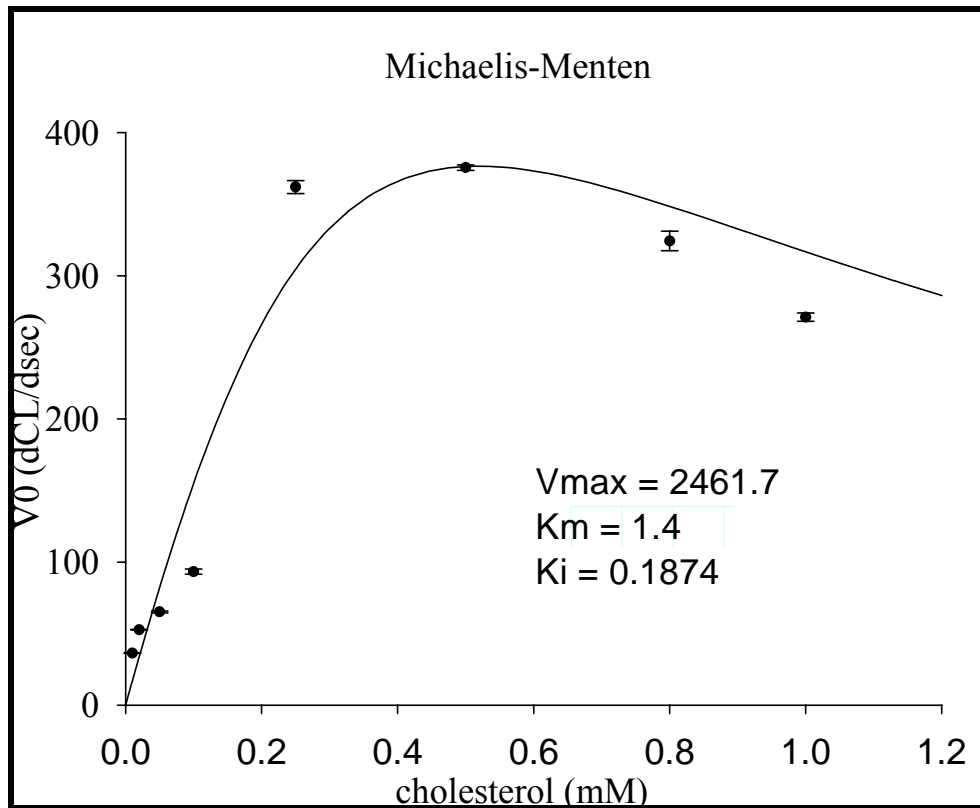
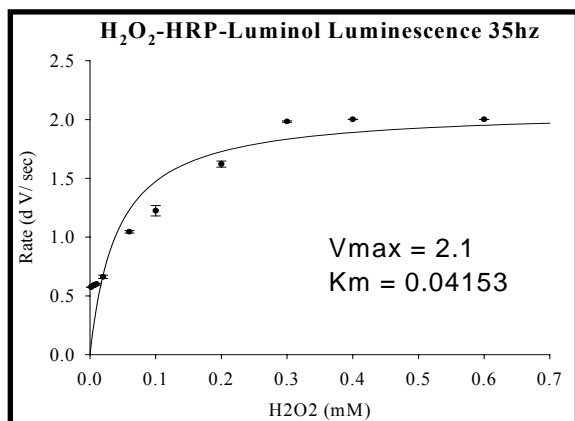
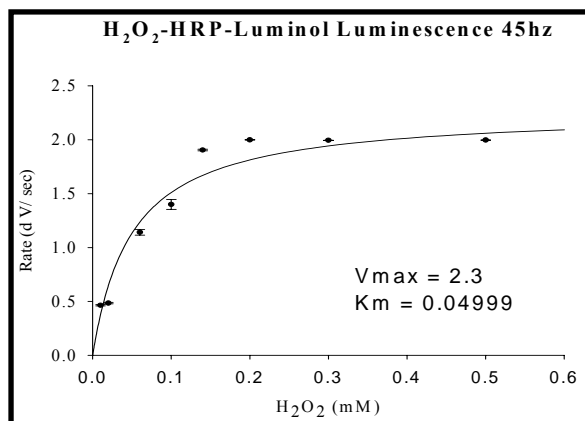


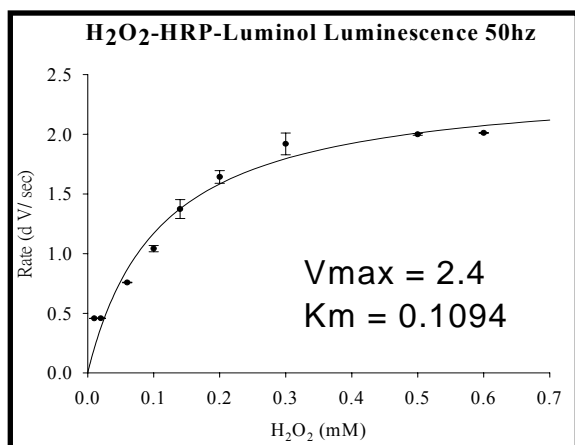
Figure 24: Frequency Adjusted in the Luminescence Reaction. Condition: HRP: 0.16 unit, Luminol: 1mM, and Tris-HCl buffer: 0.05M.



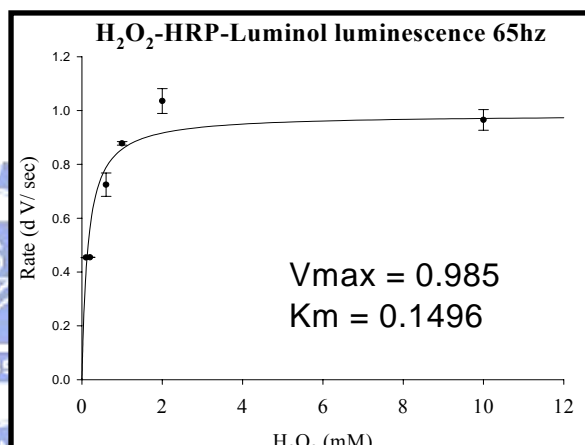
(a.) 35Hz



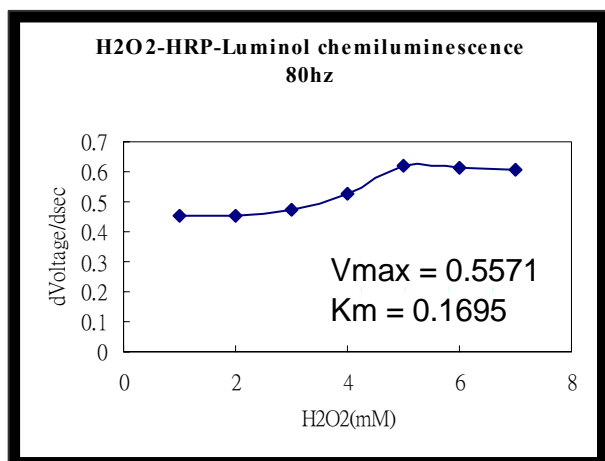
(b.) 45Hz



(c.) 50Hz



(d.) 60Hz



(e.) 80Hz

Figure 25: HRP-luminol-H₂O₂ kinetic Graph detected with F4500 luminescence spectrometer (upper graph) and the novel CMOS chip (lower graph). Condition: HRP 0.16 unit, luminol: 1mM, and Tris-HCl buffer: 0.05M.

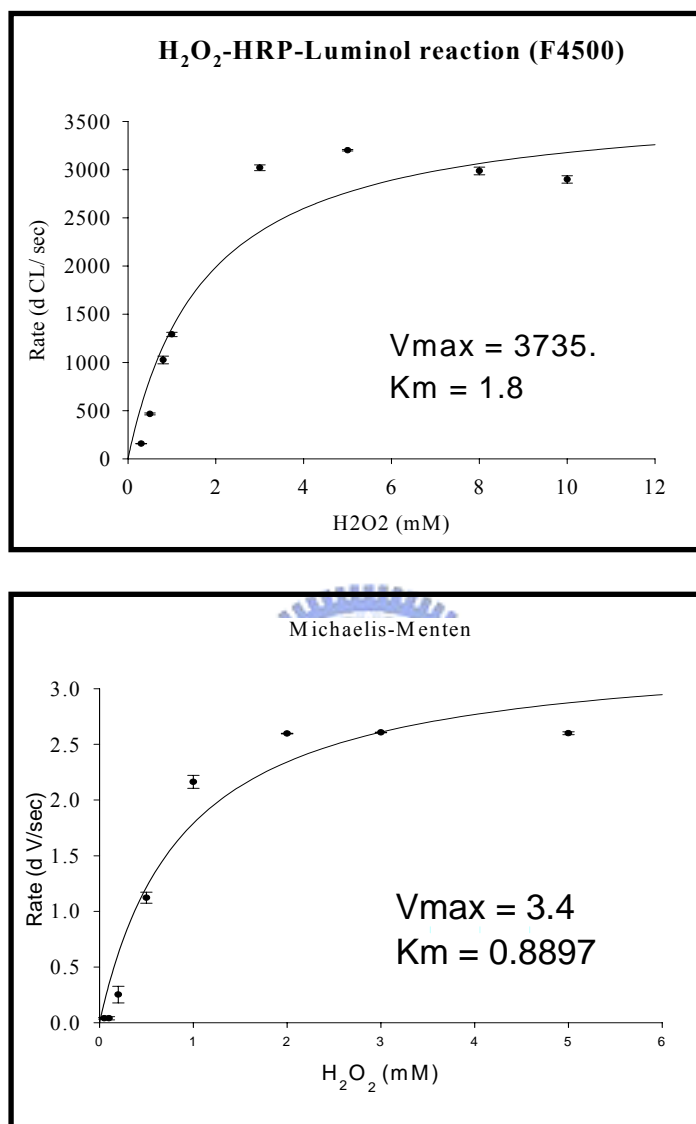


Figure 26: HRP-luminol-H₂O₂ luminescence assay kinetic graph detected by CMOS chip. Condition: HRP 0.02 unit, luminol: 1mM, and Tris-HCl buffer: 0.05M.

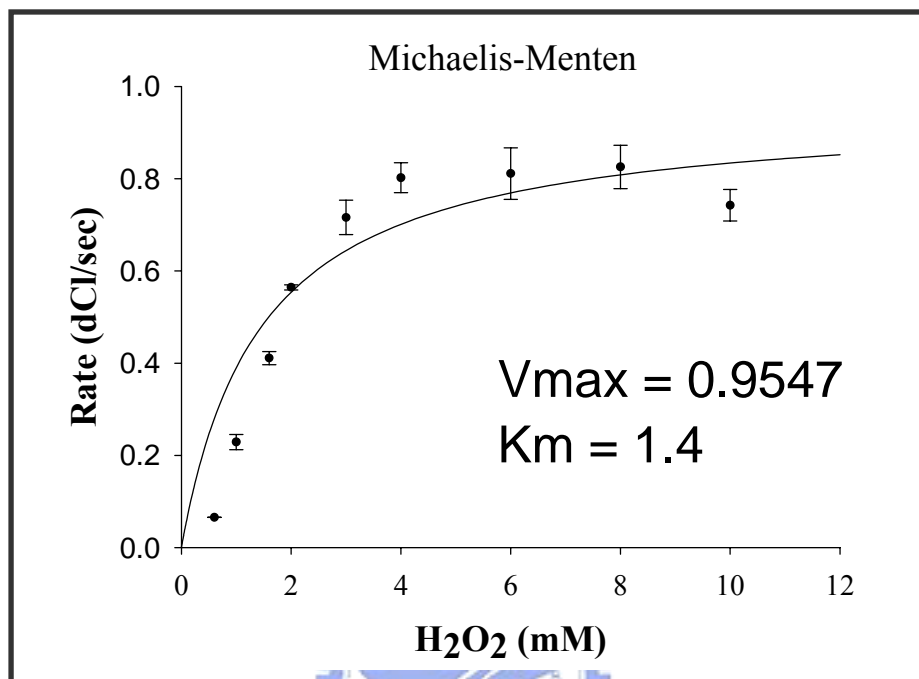
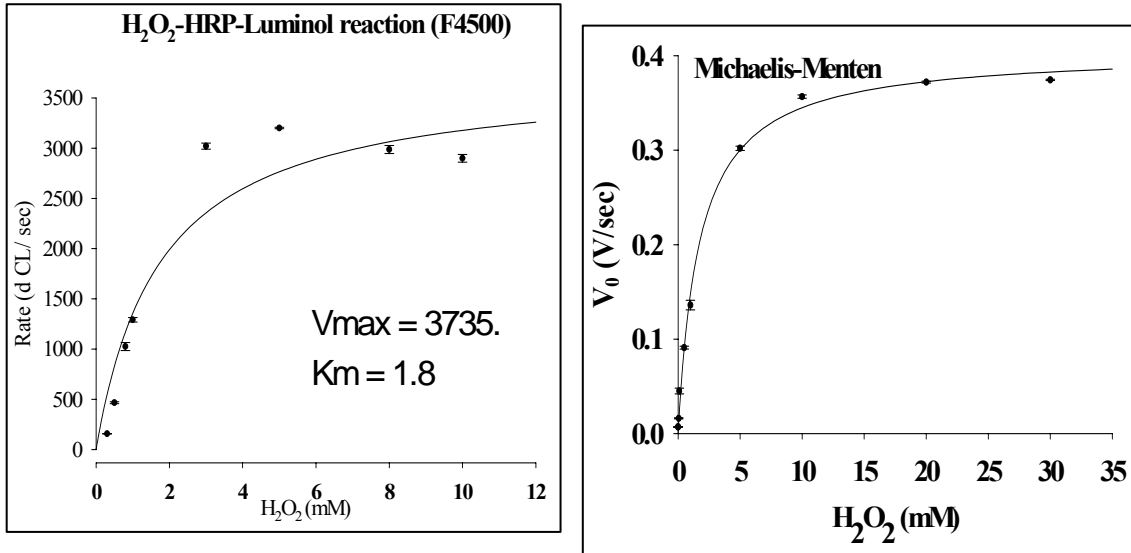
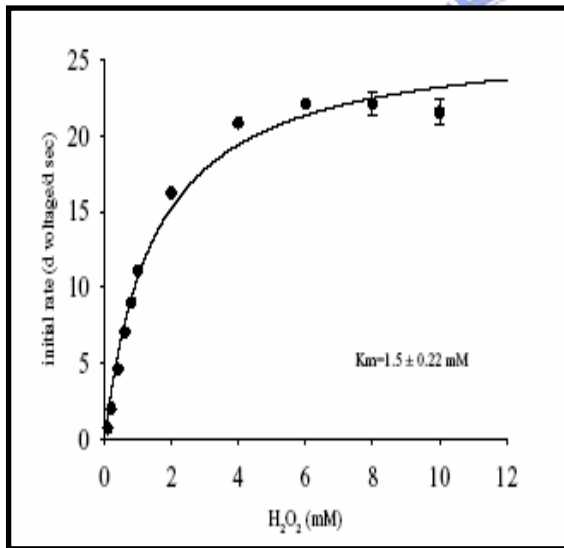


Figure 27: Variation of H_2O_2 concentration in an HRP-luminol- H_2O_2 system determined by F4500 luminescence spectrometer (a), integrated commercial photodiode system (b) and the early stage CMOS chip.



(a.) F4500 luminescence spectrometer (b.) Integrated commercial photodiode system



(c.) First Generation CMOS Chip (56)

Figure 28: Optimization of Assay Condition. The variation of pH values is observed with the condition: HRP = 0.16U, phenol =14mM, 4-AAP 0.82mM, and PBS= 7.4, 0.2M.

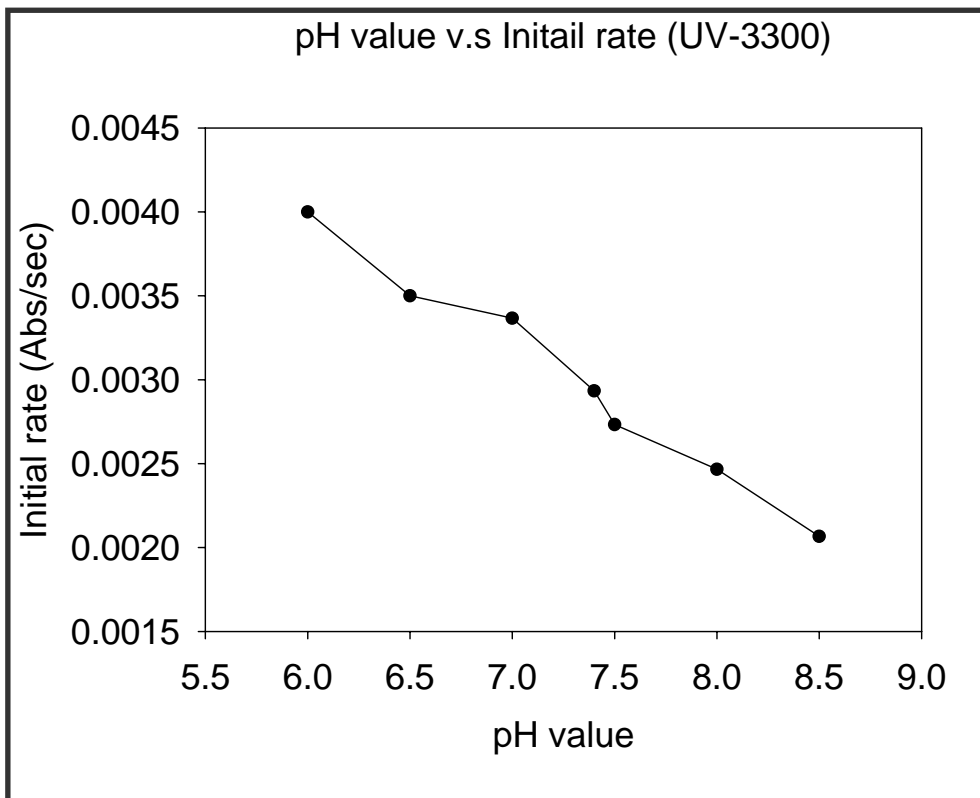


Figure 29: Temperature Optimization. The variation of initial rate with temperature is observed. Reaction condition: HRP = 0.16U, phenol =14mM, 4-AAP 0.82mM, and PBS= 7.4; 0.2M.

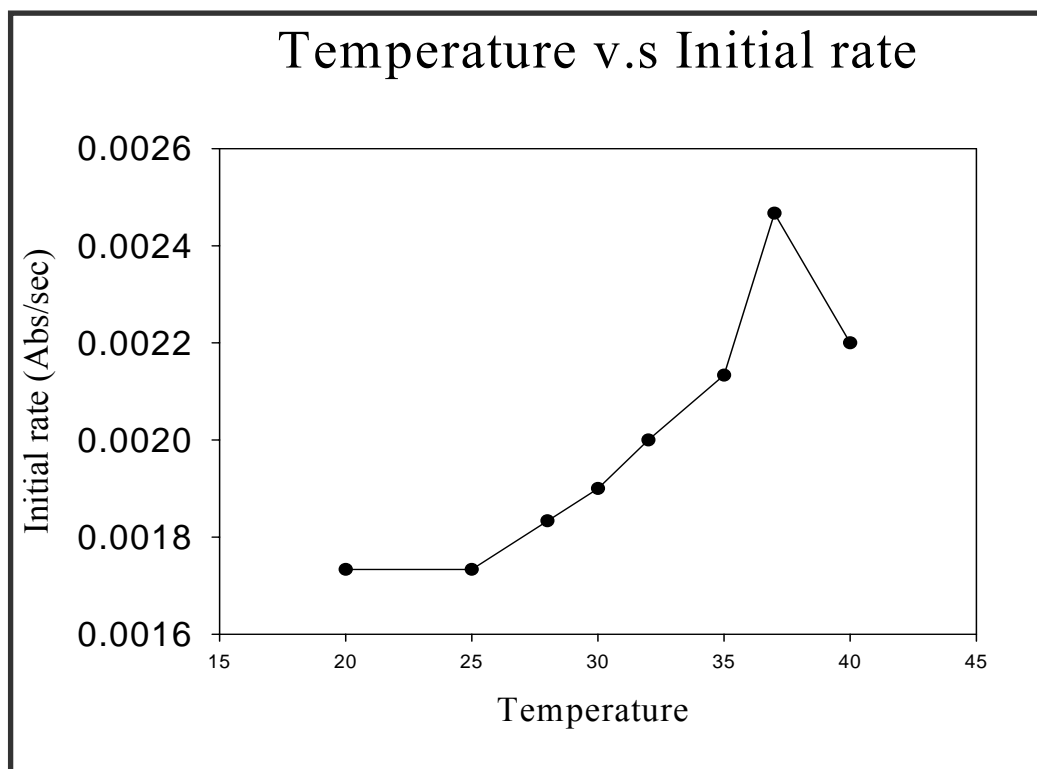


Figure 30: Incubation time optimization. The variation of initial rate with incubation time is observed. Reaction condition: HRP = 0.16U, phenol =14mM, 4-AAP 0.82mM, and PBS= 7.4; 0.2M.

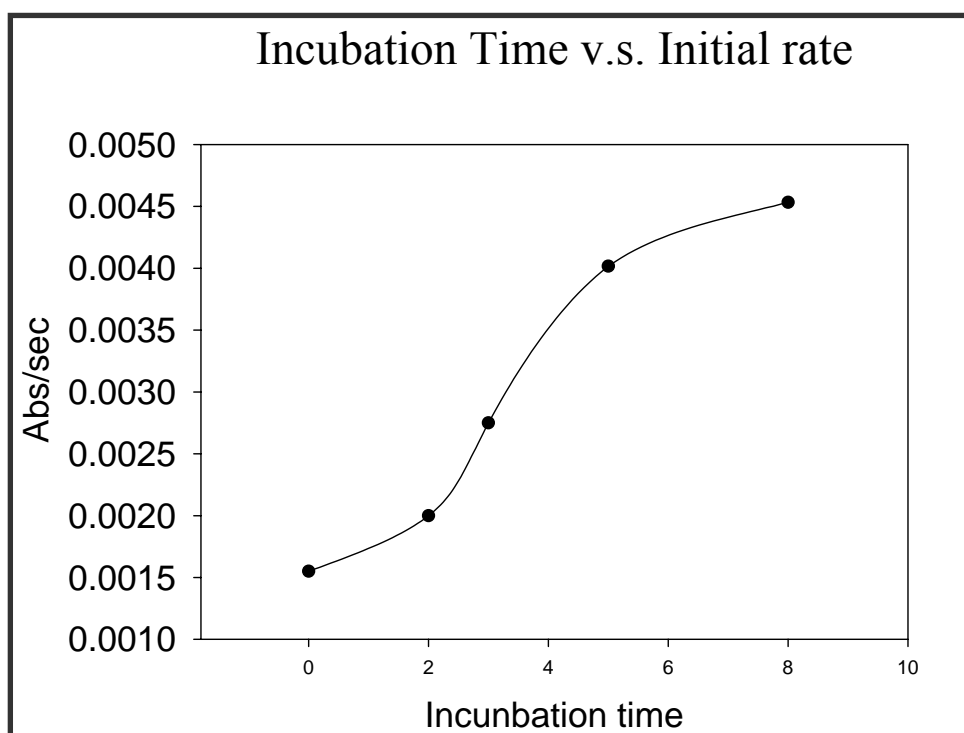


Figure 31: The linear range of HRP. The sample includes 9.6 mM 4-aminoantipyrine, 14 mM phenol, 0.2U/ml CHOD, 5 mM cholesterol, 50 mM phosphate buffer (pH 6) and 0.016 unit to 1.2 unit cholesterol oxidase at 25°C .

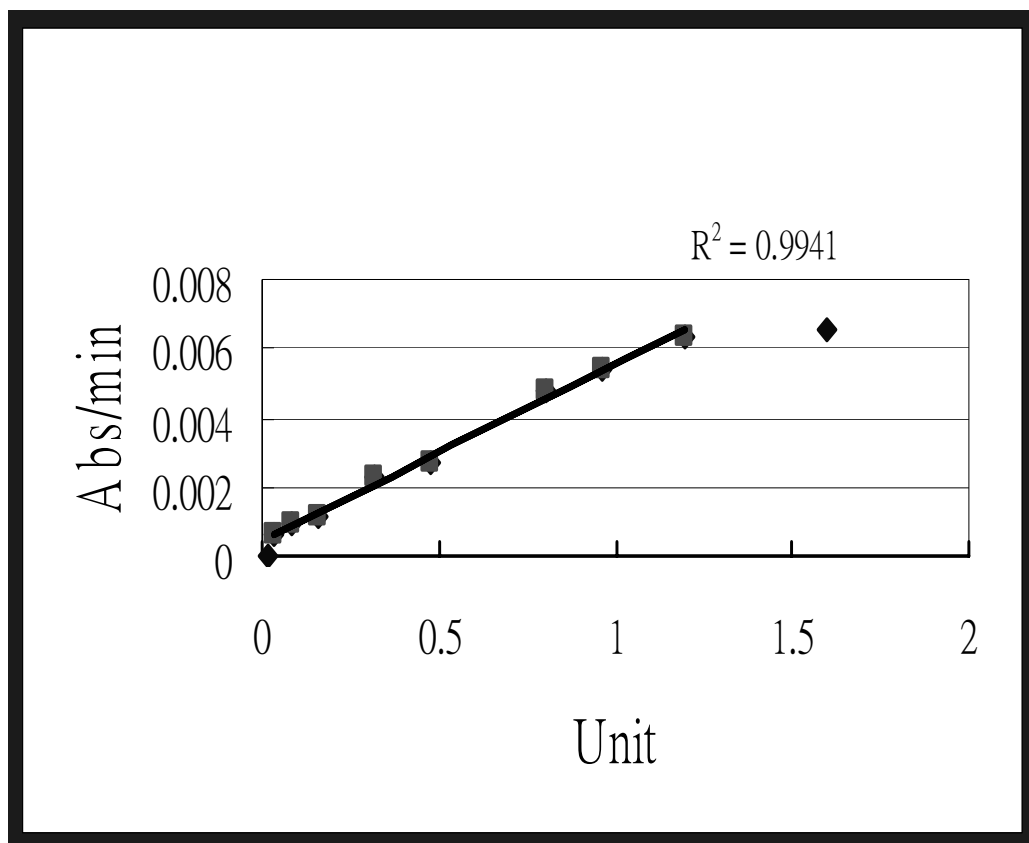


Figure 32: The linear range of cholesterol oxidase. The sample includes 9.6 mM 4-aminoantipyrine, 14 mM phenol, 0.16 U/ml HRP, 5 mM cholesterol, 50 mM phosphate buffer (pH 7.4) and 0 unit to 0.25 unit cholesterol oxidase at 25°C.

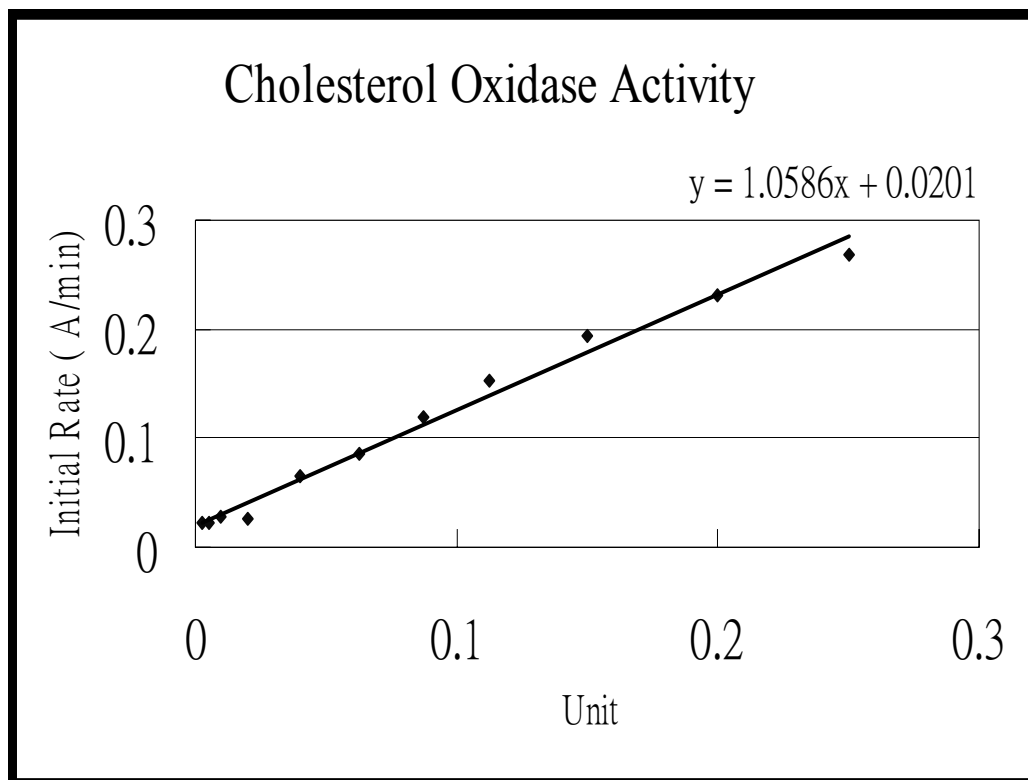


Figure 33: Phenol concentration optimization. The variation of initial rate with phenol concentration is observed. Reaction condition: HRP = 0.16U, 4-AAP 0.82mM, and PBS= 7.4, 0.2M.

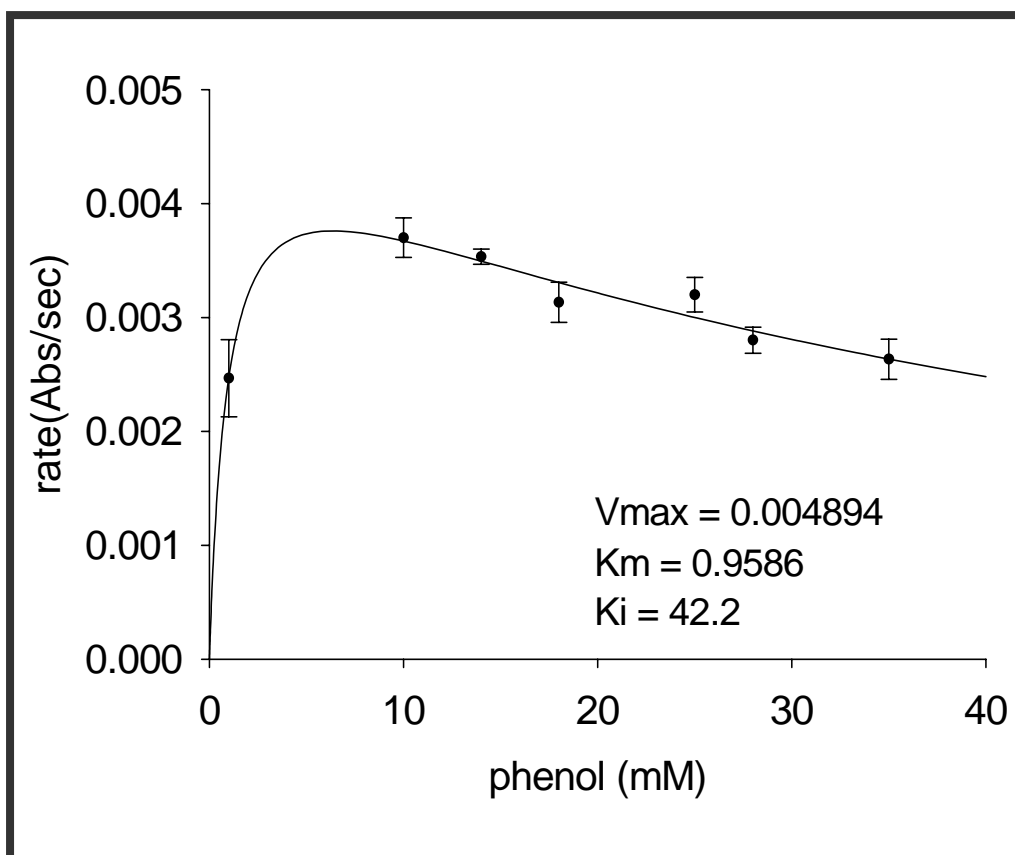


Figure 34: Aminoantipyrine concentration optimization. The variation of initial rate with 4 AAP concentration is observed. Reaction condition: HRP = 0.16U, phenol= 14mM, and PBS= 7.4, 0.2M.

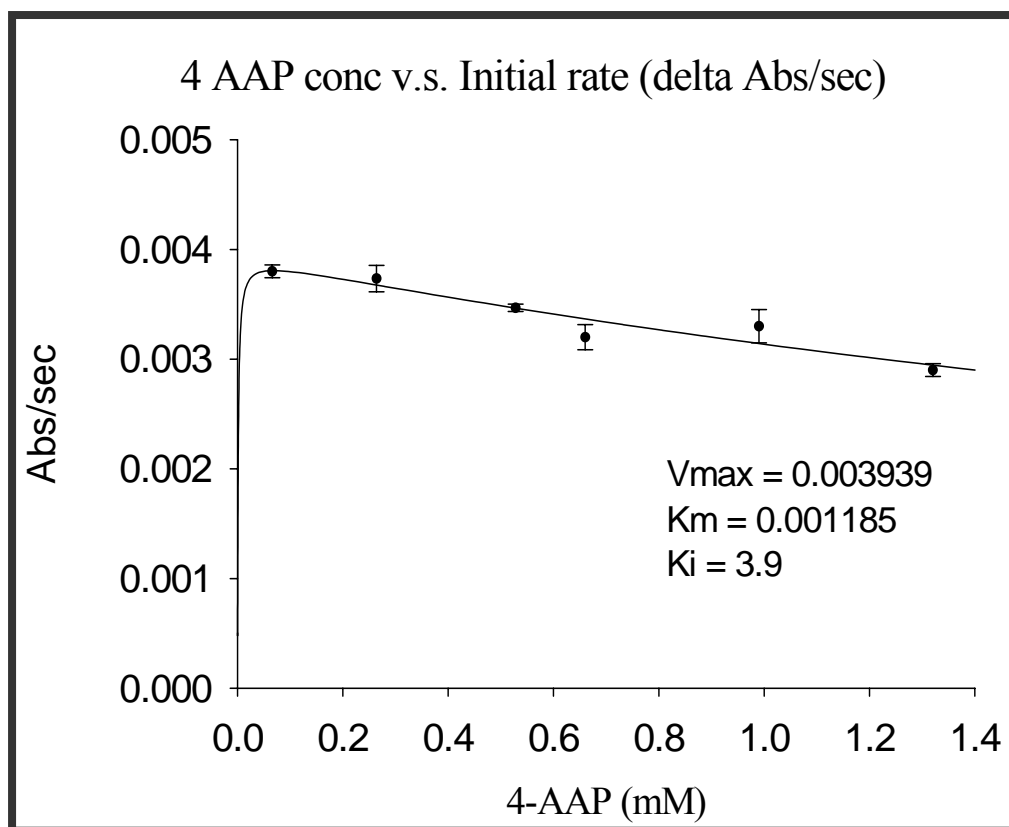
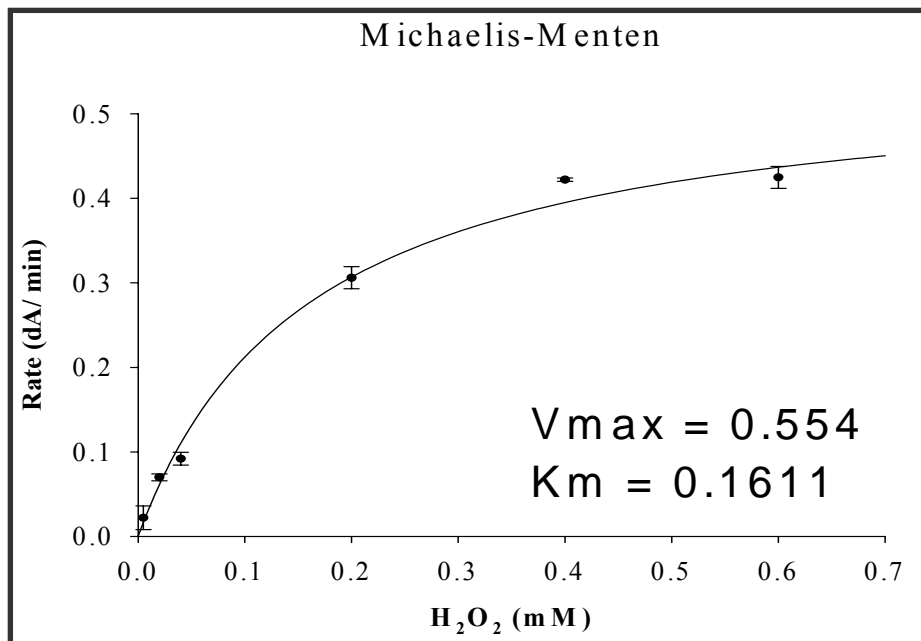
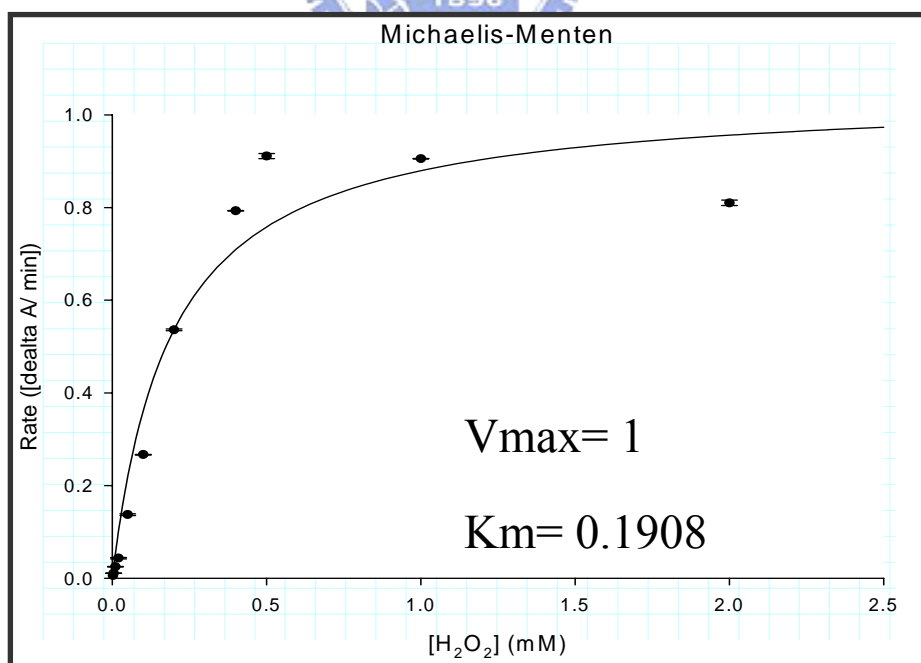


Figure 35: The variation of initial rate by varying H_2O_2 concentration via 2.5 volts supplied voltage. The measurements are detected CMOS chip (a) and UV-Vis-3300(b) as illustrations. Reaction condition: HRP = 0.16U, phenol 14mM, 4-AAP 0.82mM, and PBS buffer solution is 0.2M.

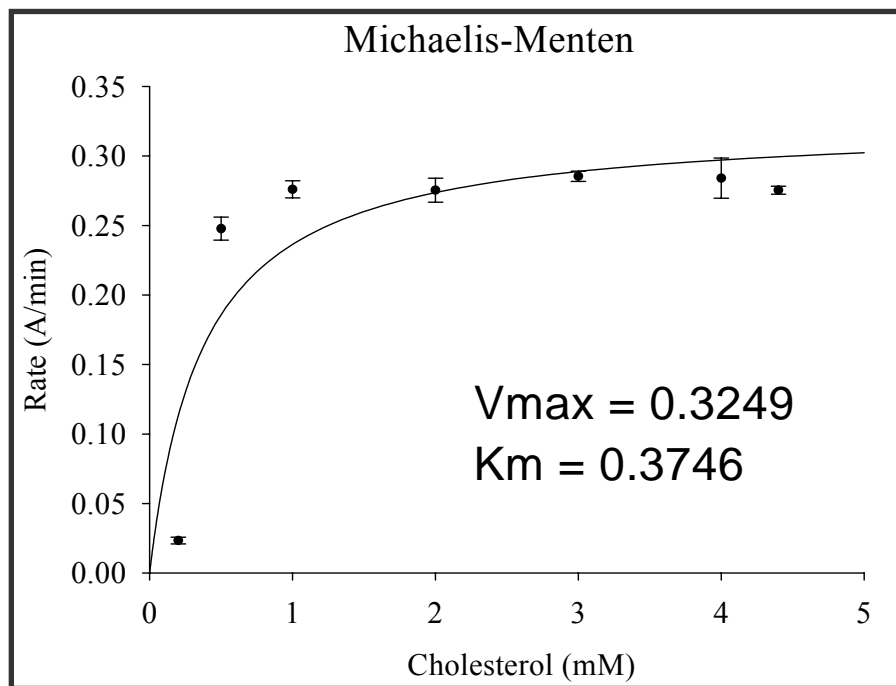


(a.) CMOS chip detection

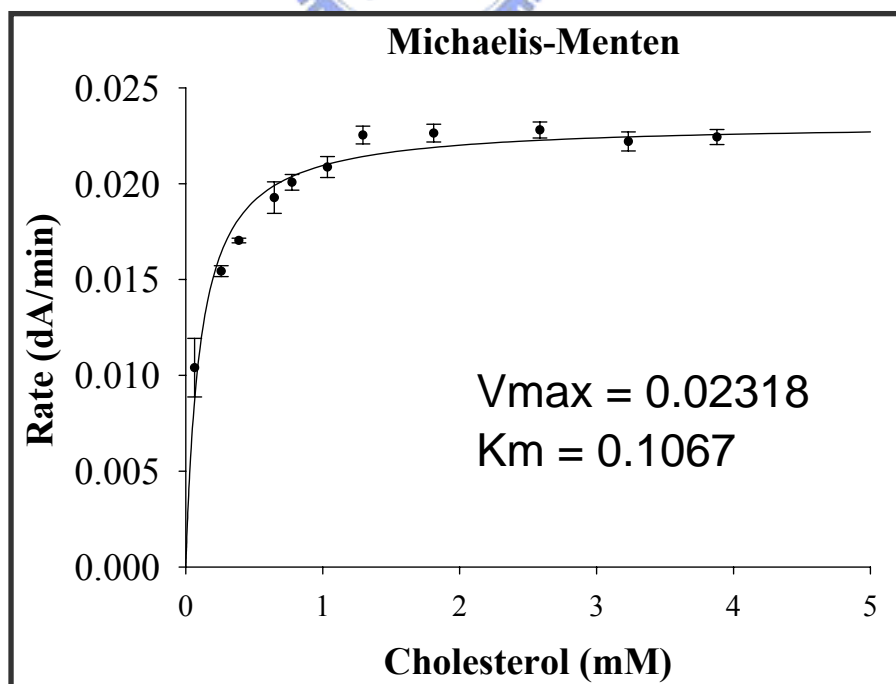


(b.) uv-vis 3300 spectrophotometer detection

Figure 36: The variation of initial rate by varying cholesterol concentration via 2.5 volts supplied voltage. The measurements are detected by CMOS chip (a) and UV-Vis-3300(b) as illustrations. Reaction condition: HRP = 0.16U, phenol 14mM, 4-AAP 0.82mM, and PBS buffer solution is 0.2M.



(a.) CMOS chip detection



(b.) uv-vis 3300 spectrophotometer detection

Figure 37: The variation of initial rate by varying cholesterol concentration via 2.48 volts supplied voltage. The measurements are detected by CMOS chip with reaction condition: HRP = 0.16U, phenol 14mM, 4-AAP 0.82mM, and PBS buffer solution is 0.2M. Incubation time is 0 minute before detection.

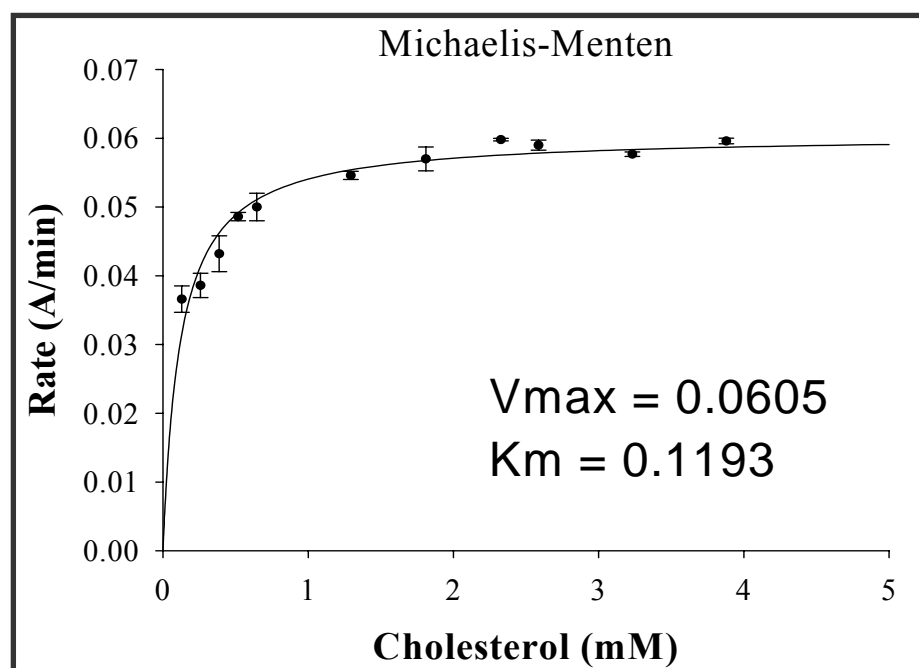
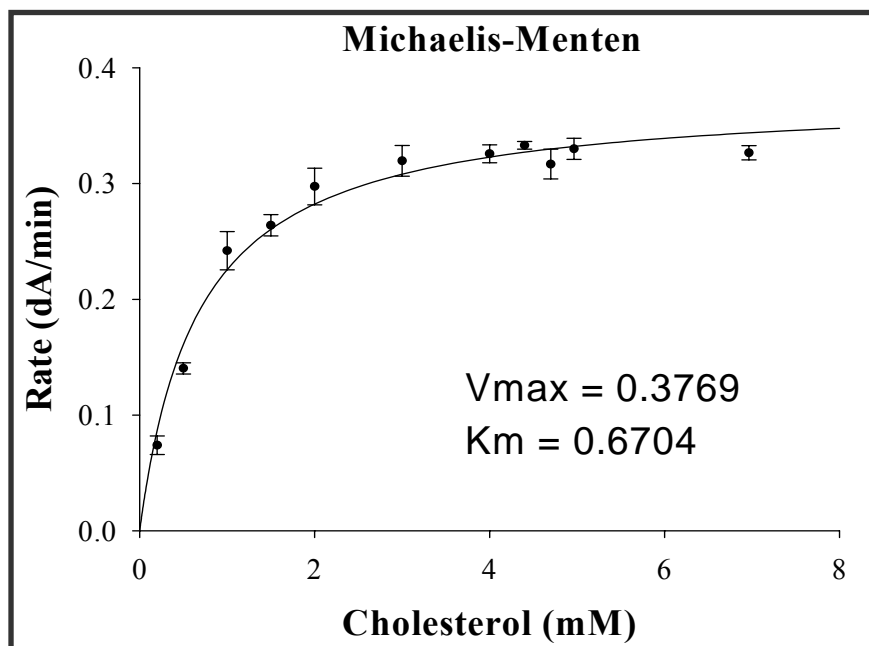
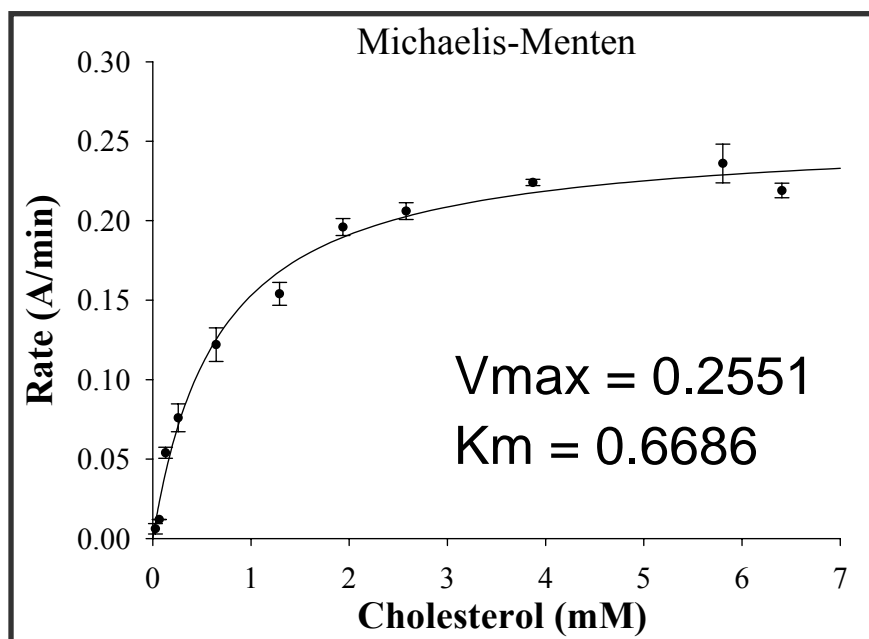


Figure 38: The variation of initial rate by varying cholesterol concentration via 2.48 volts supplied voltage. The measurements are detected by CMOS chip (a) and UV-Vis-3300(b) as illustrations with reaction condition: HRP = 0.16U, phenol 14mM, 4-AAP 0.82mM, and PBS buffer solution is 0.2M. Incubation time is 3 minutes before detection.



(a.) CMOS chip detection



(b.) uv-vis 3300 spectrophotometer detection

Figure 39: Glucose test with colorimetric assay

GOD-HRP colorimetric assay detect by uv/vis 3310 (a.) and GOD-HRP colorimetric assay detect by CMOS chip in 45 Hz (b.), 50 Hz (c.) and 60 Hz (d.).

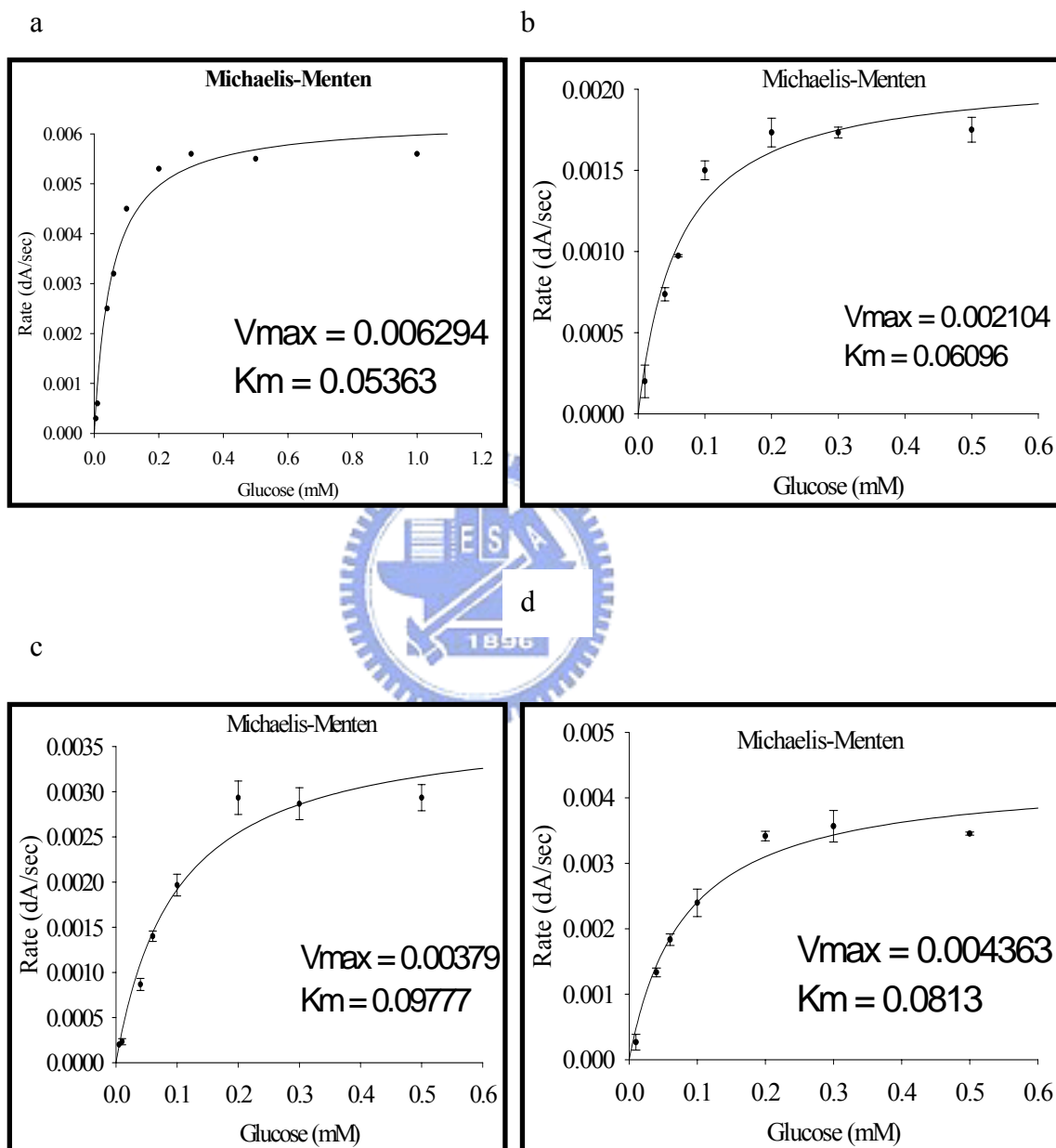
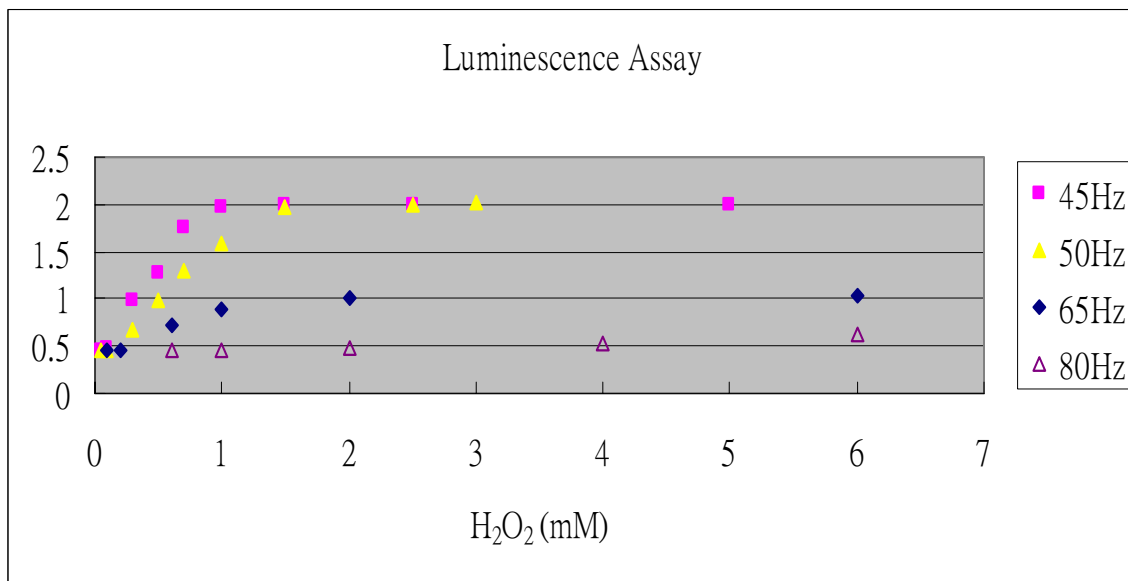


Figure 40: Sensitivity variation with different frequency parameter

(a.) Luminescence Assay



(b.) Chromogenic Assay

